Pergamon

Progress in Oceanography 51 (2001) 125–214

Progress in Oceanography

www.elsevier.com/locate/pocean

On the origin of the warm inflow to the Nordic Seas

Michael S. McCartney *, Cecilie Mauritzen

Physical Oceanography Department, Woods Hole Oceanographic Institution, Woods Hole, MA 02543, USA

Abstract

Warm and saline waters enter the Nordic Seas from the south as part of the warm-to-cold water transformation of the thermohaline circulation of the northern North Atlantic. One explanation for the origin of the Nordic Seas Inflow is a "shallow source hypothesis" under which the Inflow waters are a modification of upper ocean subtropical waters. Warm waters from the subtropical gyre are carried to the eastern North Atlantic by the North Atlantic Current and branch northwards, joined by poleward upper thermocline flow along the upper continental slope, to provide the Nordic Seas Inflow. Along this pathway the upper water column is progressively cooled and freshened by winter convection, the subpolar mode water transformation process, and this sets the Inflow characteristics.

A "deep source hypothesis" provides an alternative explanation for the characteristics of the Nordic Seas Inflow and the pathway delivering the waters to the Inflow. Under this hypothesis Inflow waters originate from the core of the Mediterranean Overflow Waters in the Gulf of Cadiz carried northward at mid-depth by the eastern boundary undercurrent in the subtropics, continuing into the subpolar gyre along the eastern boundary, and rising from depths near 1200 m in the Rockall Trough to less than 600 m to cross the Wyville-Thomson Ridge into the Faroe-Shetland Channel and thence to the Nordic Seas. The deep source hypothesis focus is on lower thermocline source waters beneath the sill depth for the Nordic Seas Inflow, in contrast to the shallow source hypothesis focus of transformation of upper thermocline waters above the sill depth.

On the basis of regional water mass distributions, geostrophic shear, and direct current measurements, we reject the deep source hypothesis in favor of the shallow source hypothesis. Rather than a flow of deep Mediterranean Overflow Water along the eastern boundary rising from depth to feed the Nordic Seas, the Inflow is supplied directly by transformed North Atlantic Current waters from the same depth range as the Inflow. Mediterranean Overflow Water is a constituent of the Inflow, but only through its contribution to defining the temperature-salinity relationship of the interior of the subtropical gyre from which the North Atlantic Current draws its water, rather than by direct northward advection of Mediterranean Outflow Water via the eastern boundary undercurrent crossing from the subtropics into the subpolar domain. Instead, the eastern boundary undercurrent wholly expels its transport of Mediterranean Overflow Water into the eastern edge of the subtropical gyre, creating the mid-depth westward extending subtropical salinity plume.

For the lower thermocline isopycnal range of the core of the Mediterranean Overflow Water, measurements show that at the Wyville-Thomson Ridge the flow is southward and descending (rather than northward and rising), representing cold spillover from the Faroese Channels entraining warm upper ocean waters as the spillover plume descends and warms into the northern Rockall Trough. No evidence is found in Rockall Trough northward of 54°N (Porcupine Bank) for direct advection of Mediterranean Overflow Waters via an eastern boundary undercurrent extension, and the very dilute Mediterranean Overflow Waters in the Trough reflect the interaction of the Wyville-Thomson Ridge plume

* To whom correspondence should be addressed.
E-mail address: mmccartney@whoi.edu (M.S. McCartney).

PII: S0079-6611(01)00084-2

descending into the Trough from the North, and lower thermocline waters delivered to the Trough from the south.

Contents

1. Hypotheses for the origin of warm waters entering the Nordic Seas

Warm Atlantic waters are altered in the Nordic and North Polar Seas to the cold dense source waters for the Nordic Seas Overflows of the Greenland-Scotland Ridge and the cold fresh source waters for the Arctic Outflows through the Canadian Archipelago and in the East Greenland Current. These outflows sum (Dickson & Brown, 1994; Mauritzen, 1996) to about 9 Sv (1 Sv = 10^6 m^3s^{-1}) and a rough estimate of the required northward flow of warm waters, the "Nordic Seas Inflow", is about 1 Sv less than this, reflecting the net transpolar flow from the North Pacific to the North Atlantic (Coachman & Aagaard, 1988; Wijffels, Schmitt, Bryden & Stigebrandt, 1992). The bulk of that inflow occurs between Iceland and Scotland, with only about 1 Sv between Greenland and Iceland. There are two hypotheses for the origin of this Nordic Seas Inflow: A "deep source hypothesis", (Reid, 1979, hereafter R79) and a "shallow source hypothesis" traced to origins in Nansen's work early in the twentieth century (Nansen, 1912), which we will develop in detail in this paper. According to the deep source hypothesis, there is a flow along the eastern boundary that carries Mediterranean Overflow Water (hereafter MOW) from its strongest signal near 1200m in the Gulf of Cadiz directly northward and upward to pass through the shallow Faroe-Shetland Channel into the Norwegian Sea, thereby contributing substantially and directly to the transport and high salinity of the Norwegian Current. According to the shallow source hypothesis, part of the North Atlantic Current's eastward transport of warm and saline thermocline waters at mid-basin turns northward in the eastern basin to supply the Nordic Seas Inflow (hereafter "Inflow"), with MOW being a dilute and indirect influence on the Inflow.

We emphasize that while there are two potential issues involving MOW in the Inflow, only one of these is in dispute. Not in dispute in these two hypotheses is that MOW is a constituent of the Inflow. More generally MOW is one of several distinct water sources whose blending determines the basin scale water mass distribution of the North Atlantic (e.g. Worthington, 1976). Other sources are the relatively fresh waters of the South Atlantic and the subpolar gyre, and the relatively saline near surface waters of the subtropical gyre, and effects of the air-sea fluxes of heat and fresh water. The pioneering studies by Helland-Hansen and Nansen (1926), Jacobsen (1929), Wüst (1935), Iselin (1936), and Montgomery (1938) in particular have discussed the formation of the subtropical gyre's North Atlantic Central Water by the balancing of the saline influences with the fresher influences of the South Atlantic and the subpolar gyre waters. Most recent literature frames the blending in terms of isopycnal advection and mixing. The North Atlantic Central Water dominates the thermocline of the Gulf Stream and North Atlantic Current, and thus the shallow source hypothesis implicitly includes an MOW influence on the salinity of the near surface waters of the Norwegian Current.

What is different between these two hypotheses is the advective origin for the Nordic Seas Inflow: by what pathways do warm saline waters arrive at the Inflow? Indisputably, warm water flows from the Rockall Plateau area into the Faroe-Shetland Channel. Upstream from there the hypotheses diverge: from what depth range and from what pathways does the Nordic Seas Inflow receive water? In Fig. 1 we present two sets of schematics of the circulation for two layers, 0–800 m, and 800–1600 m. In the initial development of the deep source hypothesis (R79) the primary focus was on property distributions, but with a baroclinic shear map included and some reference to earlier discussion of the shear in Reid (1978, hereafter R78). How the deep source hypothesis is reflected in detail in horizontal circulation is found in a later treatment (Reid, 1994, hereafter R94), where additional property maps for DS isopycnals and lighter and heavier surfaces were shown and a complete set of circulation maps were given in the form of steric height maps adjusted with a barotropic element to reflect absolute circulation. In Fig. 1((a),(b)) is a simplified schematic representation of the circulation corresponding to the deep source hypothesis, based on figures and dis-

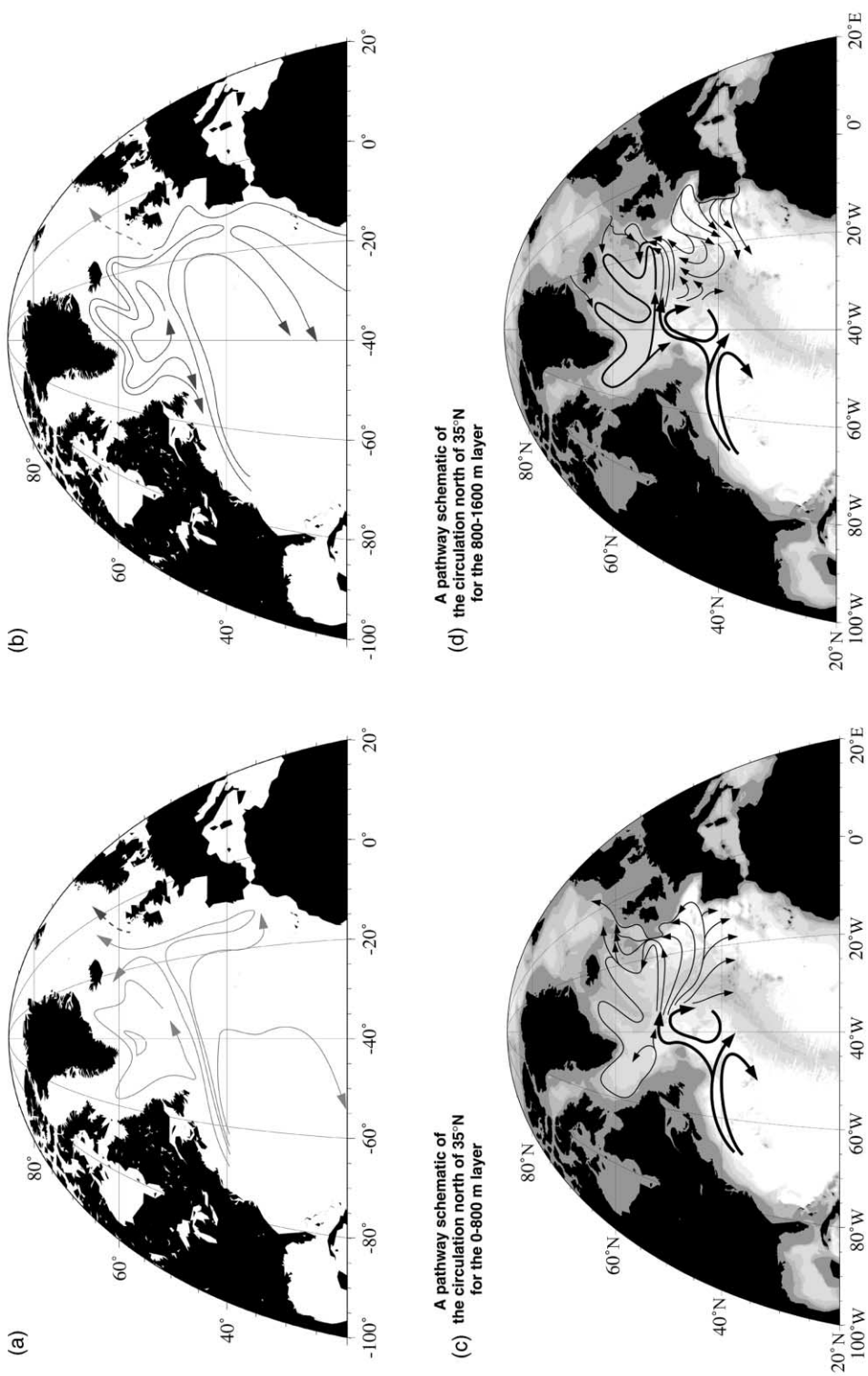

Fig. 1. Circulation schematics for the deep source hypothesis and the shallow source hypothesis. (a) Schematic of the upper (0–800 m) circulation according to Reid's deep source hypothesis. (b) Schematic of the mid-depth (800–1600 m) circulation according to Reid's deep source hypothesis. (c) Schematic of the upper (0–800 m) circulation according to the shallow source hypothesis. (d) Schematic of the mid-depth (800–1600 m) circulation according to the shallow source hypothesis. (e) Upper ocean circulation (<2000 db) relative to a 2000 db reference level (Pollard et al., 1996). (f) Upper ocean circulation (<800 m) from a constrained inverse (Paillet & Mercier, 1997).

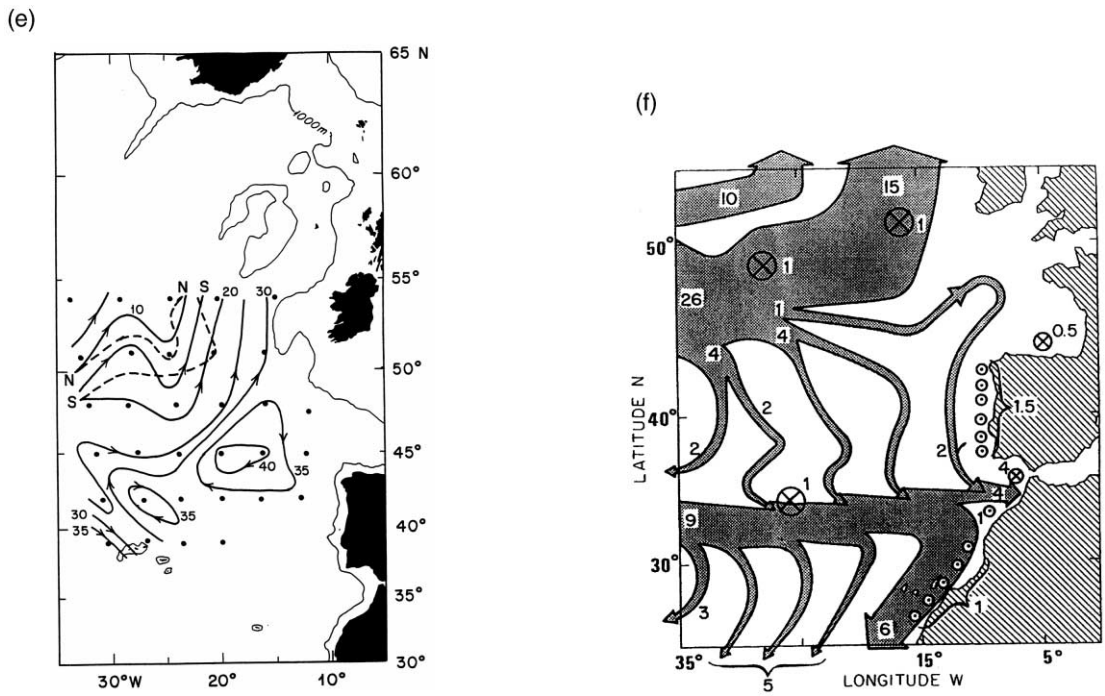

Fig. 1. (*continued*)

cussion in these three primary references, R78, R79, and R94). In Fig. 1((c) and (d)) the circulation corresponding to the shallow source hypothesis is schematically illustrated, based on data and interpretations from a variety of sources. Below we discuss the basis for these schematics as well as their implications.

We feel that there is ample evidence against the deep source hypothesis, and that it can be set aside. Perhaps many readers already have, for many papers of recent years at least implicitly deal with the Nordic Seas Inflow in the shallow source hypothesis framework. But invoking of the deep source hypothesis persists. Sometimes this is because of writers not making the distinction referred to above between MOW influences on North Atlantic water masses and MOW flow pathways. Other papers are quite explicitly arguing for the deep source hypothesis being operative. Johnson (1997a,b, 1998) has the deep source hypothesis as a cornerstone of his call for a controlling dam at the Strait of Gibraltar. He forecasts that salinity increase within the Mediterranean will drive increased MOW outflow intensity, and that the increased salinity flux will be rapidly communicated to the Nordic Seas by the eastern boundary undercurrent pathway of the deep source hypothesis. He contends that this will soon trigger a glaciation. There are other issues with his imminent glaciation scenario that are outside the scope of our paper (see, e.g., Marotzke, Adcroft & Johnson, 1997; Rahmstorf, 1998a,b). But the hypothetical undercurrent pathway is the enabler of rapid and relatively undiluted MOW influence on the Nordic Seas in Johnson's scenario, by its bypassing of the vast interior volume of the North Atlantic. The damping effect that large volume would have on Outflow fluctuations is short-circuited by the rapid communication along the undercurrent pipeline. Another recent study by Iorga and Lozier (1999a,b) presents two internally consistent representations of the flow on MOW isopycnals in the mid-latitude eastern North Atlantic, and uses a weighted sum of the two fields to represent the absolute flow on the isopycnals, with the weights chosen so as to give an undercurrent penetrating to high latitudes. While recent modeling literature (New, Barnard, Herrmann & Molines, 2001) is consistent with the shallow source hypothesis and inconsistent with the deep source

hypothesis, we feel that it is important to address the North Atlantic measurements as thoroughly as possible with respect to the two hypotheses, in hopes of being definitive as to the observational evidence.

2. The deep source hypothesis

A hypothesized poleward-flowing eastern boundary undercurrent has been deduced (R78, R79) using maps of salinity and other properties, including geostrophic shear, with principal focus (R79) on a density surface intersecting the core of the MOW in the Gulf of Cadiz. Some of these maps are reproduced here as Fig. 2((a)–(e)). The following is a summary of aspects of regional distributions suggestive of the deep source hypothesis, using the R79 interpretative framework emphasizing isopycnal flow along property tongues.

- While the axis of the MOW salinity tongue projects westward near 35°N, the isohalines of the northern side of the tongue bulge northward towards the Nordic Seas near the eastern boundary.
- The depths of MOW isopycnals descend from mid-basin to the eastern boundary, and the associated mid-depth geostrophic shear relative to a deeper reference surface indicates northward MOW flow in the eastern basin north of 40°N.
- Elevated silicate and lowered oxygen protrude northward from the MOW tongue in the eastern subtropical gyre into the eastern subpolar gyre and the Faroe-Shetland Channel.
- This MOW core density surface, near 1100–1200m in the Gulf of Cadiz, along the MOW tongue, and in Rockall Trough, is found in the Norwegian Current at 200m, uninterrupted by the ridges separating the Norwegian Sea from the subpolar gyre.

The formulation of the deep source hypothesis began with these maps, suggesting (R79, p. 1206):

> "...the possibility that the Mediterranean outflow waters, moving northward as an eastern boundary undercurrent, may rise near the surface and cross the Iceland-Scotland Ridge and contribute substantially to the warm and very saline waters of the Norwegian Current".

The next step of development of the deep source hypothesis involved a composite section along the path of the hypothesized eastern boundary flow (R79 Figs. 7–10 and 12). Fig. 3 shows a similarly placed section we have constructed from recent CTD stations; the locations of this and subsequently illustrated sections and stations are shown in Fig. 4. Northward from the Gulf of Cadiz along the eastern boundary the MOW core isopycnal remains fairly deep until just south of the Wyville-Thomson Ridge at the northern end of the Rockall Trough where a steep rise into the Faroe-Shetland Channel occurs. Under the deep source hypothesis, accompanying the rise of the surface is rising isopycnal flow that allows the deep MOW to "contribute substantially" (R79, p. 1199) to the Norwegian Current, including the Current's characteristic weak salinity maximum, weak oxygen minimum, warmth, and elevated silicate. While the temperature, salinity, and oxygen data alone did "not preclude the possibility that it is only the upper waters" (R79, p. 1220) that are Norwegian Current source waters (that is, the shallow source hypothesis in our terminology), silicate data were interpreted as conclusive (R79, p. 1220):

> "The silica pattern, however, requires the deeper Atlantic waters as a source for the higher values entering the Norwegian Sea. While a contribution of some characteristics from the upper layers through mixing with the deeper waters cannot be excluded, the contribution from the denser waters with their higher silica, is necessary".

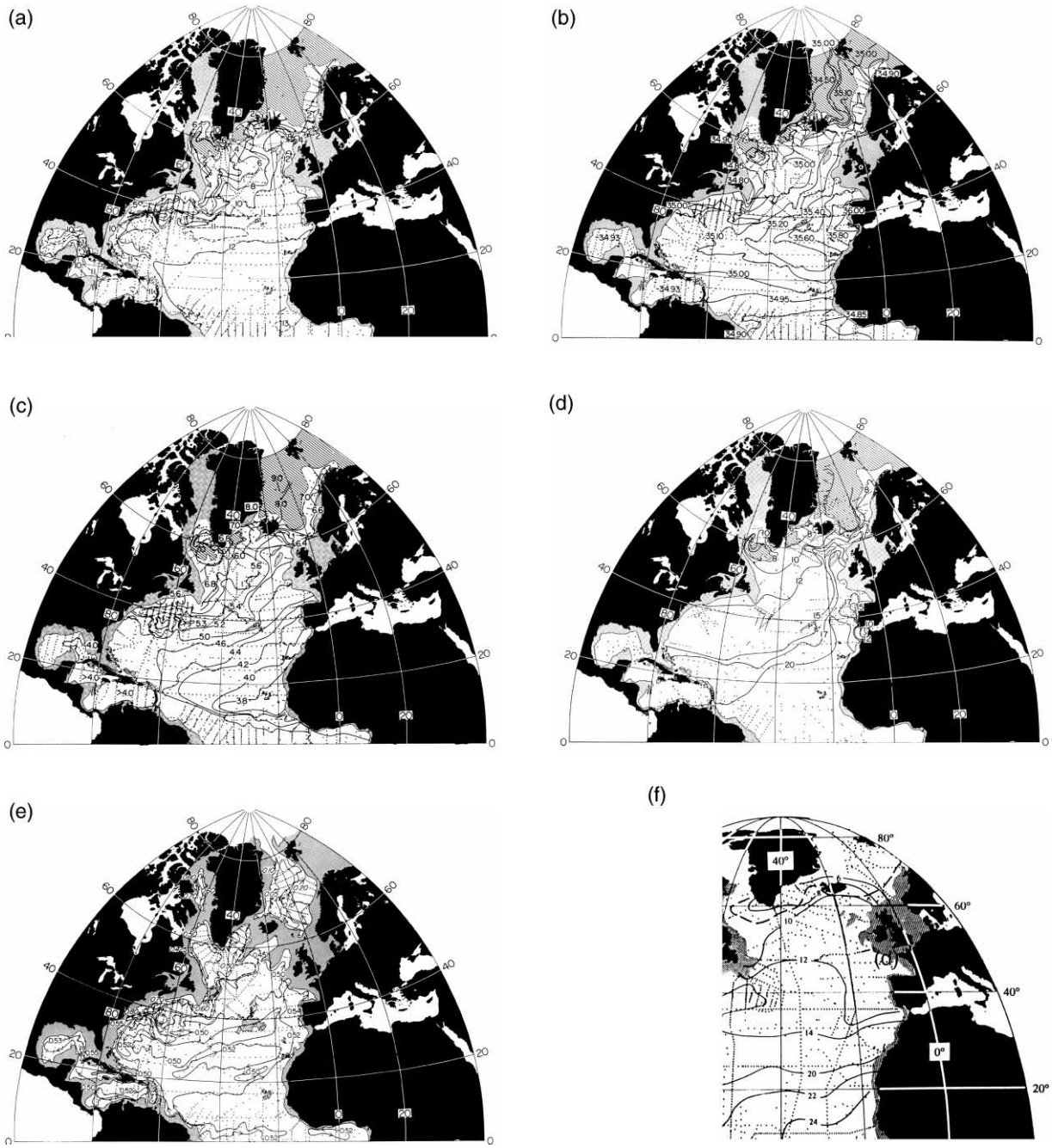

Fig. 2. MOW distributions, old equation of state σ_1 = 32.274, [about $\sigma_1 \approx$ 32.24 in EOS80] (Reid, 1979, panels a–d.) (a) depth [100 m contour interval] of σ_1 = 32.274 (Reid, 1979; old equation of state, about $\sigma_1 \approx$ 32.24 in EOS80), (b) salinity on σ_1 = 32.274 (Reid, 1979; old equation of state, about $\sigma_1 \approx$ 32.24 in EOS80), (c) oxygen [ml/l] on σ_1 = 32.274 (Reid, 1979; old equation of state, about $\sigma_1 \approx$ 32.24 in EOS80), (d) silicate [μg-at.l^{-1}] on σ_1 = 32.274 (Reid, 1979; old equation of state, about $\sigma_1 \approx$ 32.24 in EOS80), (e) 1000/2000 steric height [dynamic meters] (Reid, 1979), (f) silicate [μmol kg^{-1}] on σ_1 = 32.2 (Reid, 1994).

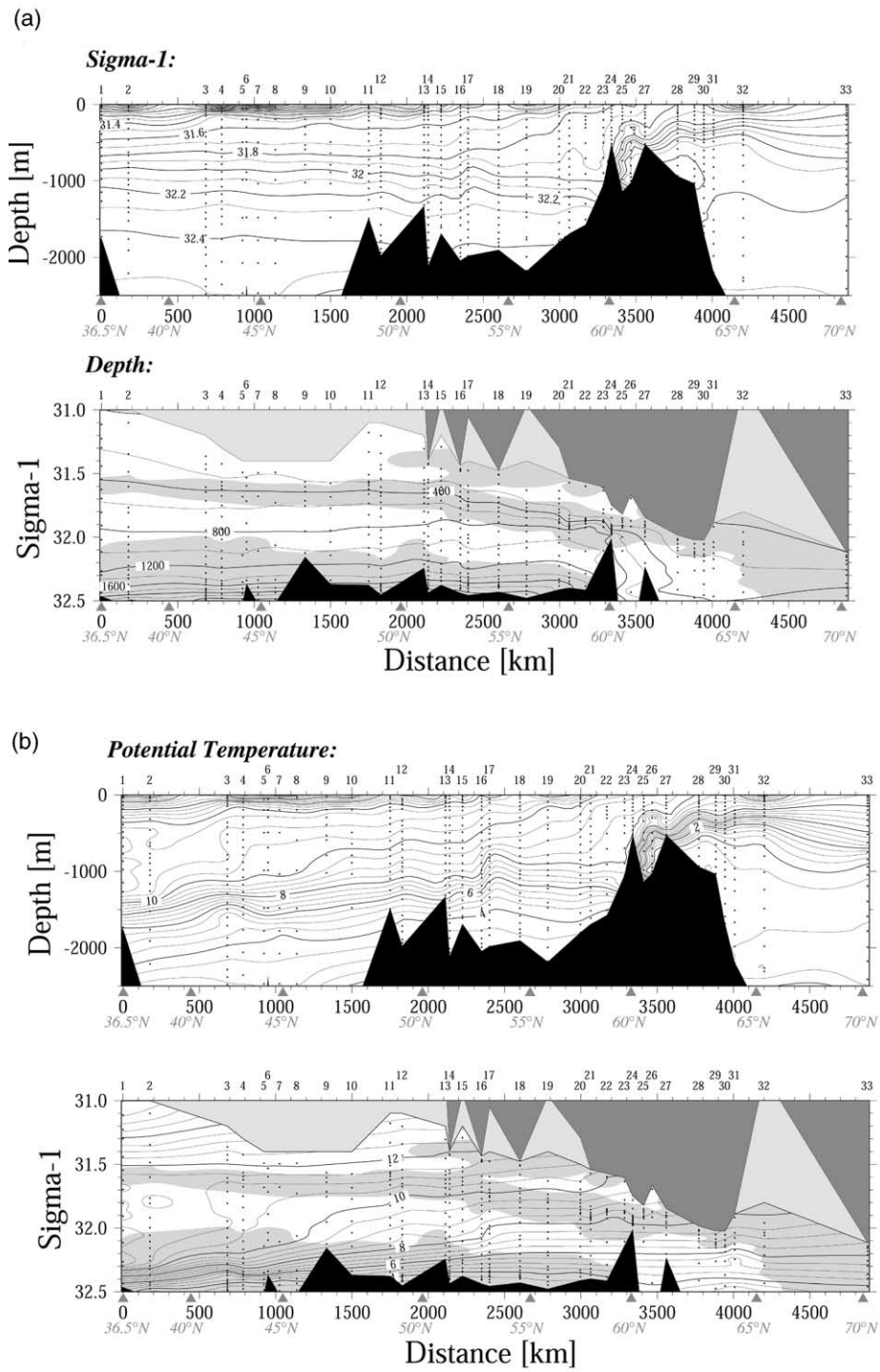

Fig. 3. Property distributions along a quasi-meridional section near the eastern boundary, as a function of depth, upper panels, and of potential density referenced to 1000 db, lower panels. Shading shows low potential vorticity. Panels (a)–(f) for newly composited data (see Fig. 4(a) for location) and panel (g) from Reid, 1979. (a) depth (m) and potential density parameter referenced to 1000 db reference pressure, (b) salinity, (c) potential temperature [°C], (d) oxygen [ml/l], (e) silicate [μmol kg^{-1}], (f) potential vorticity) [10^{-12} $m^{-1}sec^{-1}$], (g) silicate [μg-at. l^{-1}] (Reid, 1979).

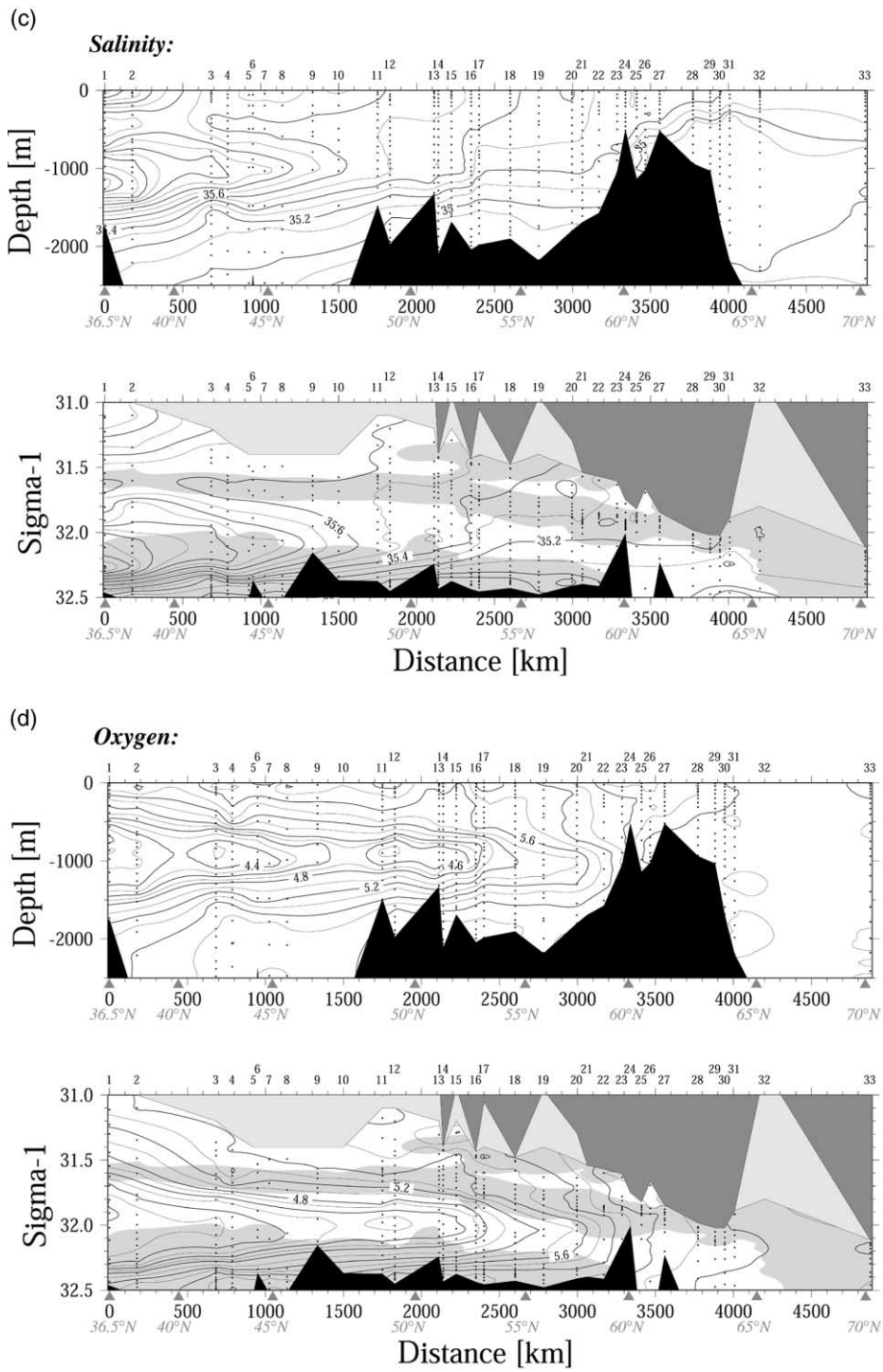

Fig. 3. (*continued*)

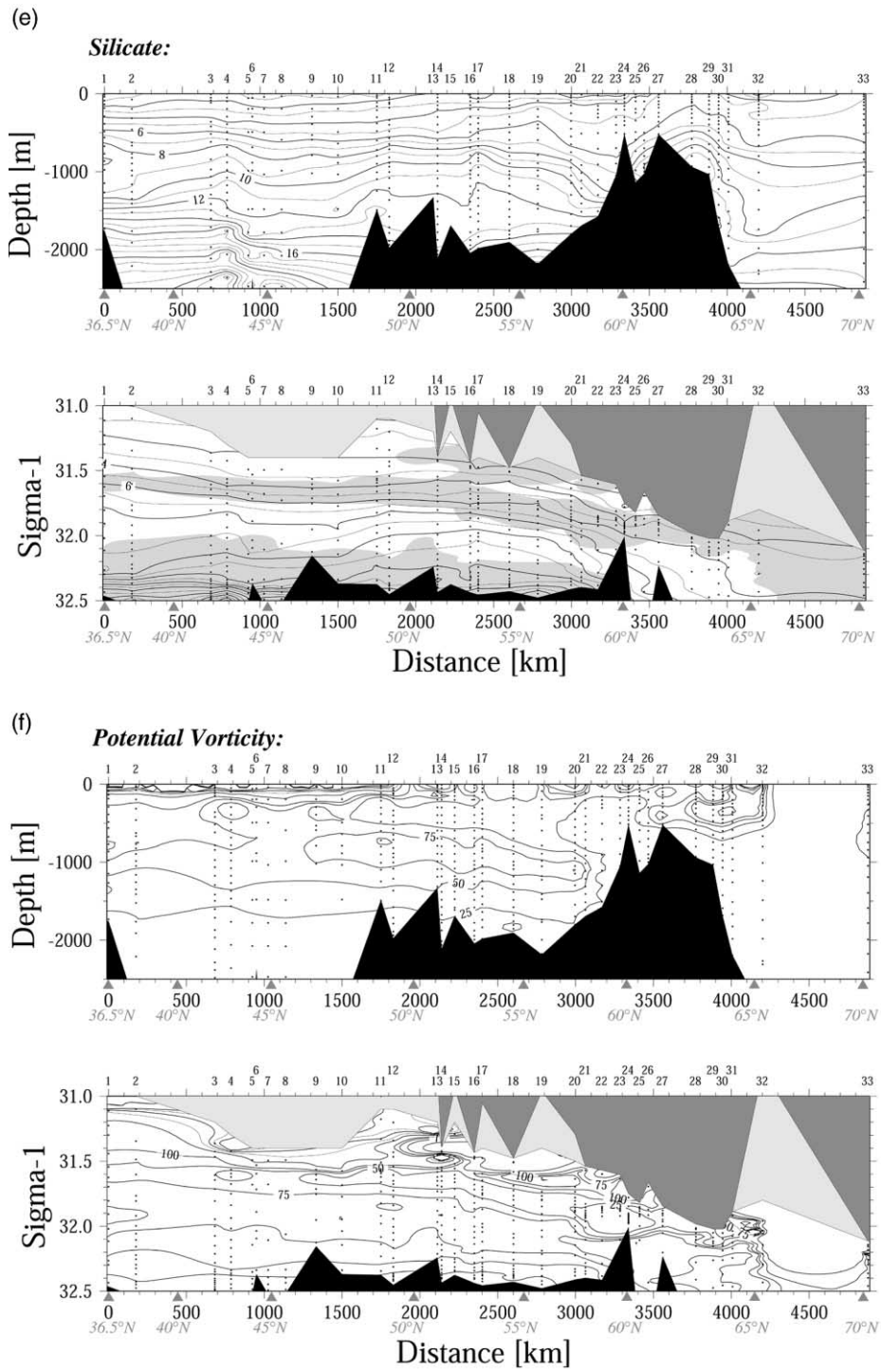

Fig. 3. (*continued*)

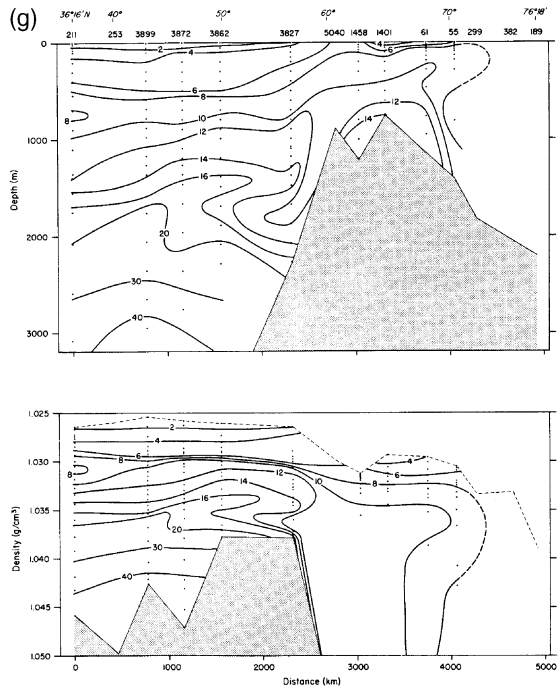

Fig. 3. (*continued*)

These silica data were described as providing "a more convincing argument" that MOW provides a "major component" to the waters flow into the Nordic Seas (R79, p. 1199). A conclusion that follows from the deep source hypothesis is that it is the deep salinity maximum waters of the MOW in the eastern boundary undercurrent that are viewed as "a source of the saline waters of the Norwegian Current" and that "contribute importantly" (R79, p.1219) "to maintain the high salinity of the Norwegian Sea" (R79, p.1220).

The last stage of development of the deep source hypothesis is found in R94, where a set of estimated absolute circulation maps for various isobars illustrates how the eastern boundary current is embedded in the basin scale circulation. Those charts show the familiar large-scale subtropical anticyclonic gyre and the subpolar cyclonic gyre, but there is additional structure in the eastern domain described this way (R94, p.7):

> "The flow of the northern cyclonic gyre is eastward near 50°N and turns northward near the eastern boundary, but below a few hundred meters part of it first loops southward near 20°W toward the Iberian Peninsula and then northward along the eastern boundary".

This looping flow is present on all the R94 circulation maps down to 3500db including the isobaric surfaces 0, 250, 500, 800, 1000, 1500, 2000, 2500, 3000, and 3500db, and the isopycnal surface $\sigma_{1.5}$ = 34.64 (σ_1 = 32.364, just below the DS isopycnal layer as we will define it below).

In summary, the deep source hypothesis involves an eastern boundary undercurrent with declining MOW intensity following the flow. The isopycnal flow along this hypothetical pathway arrives at depth in the Rockall Trough, rises steeply across the Wyville-Thomson Ridge, and continues on through the Faroe-Shetland Channel to contribute substantially to the Norwegian Current upon exiting (northeastward) the Channel. This is indicated in Fig. 1((a),(b)) by the dashed contour shared by both schematics, representing

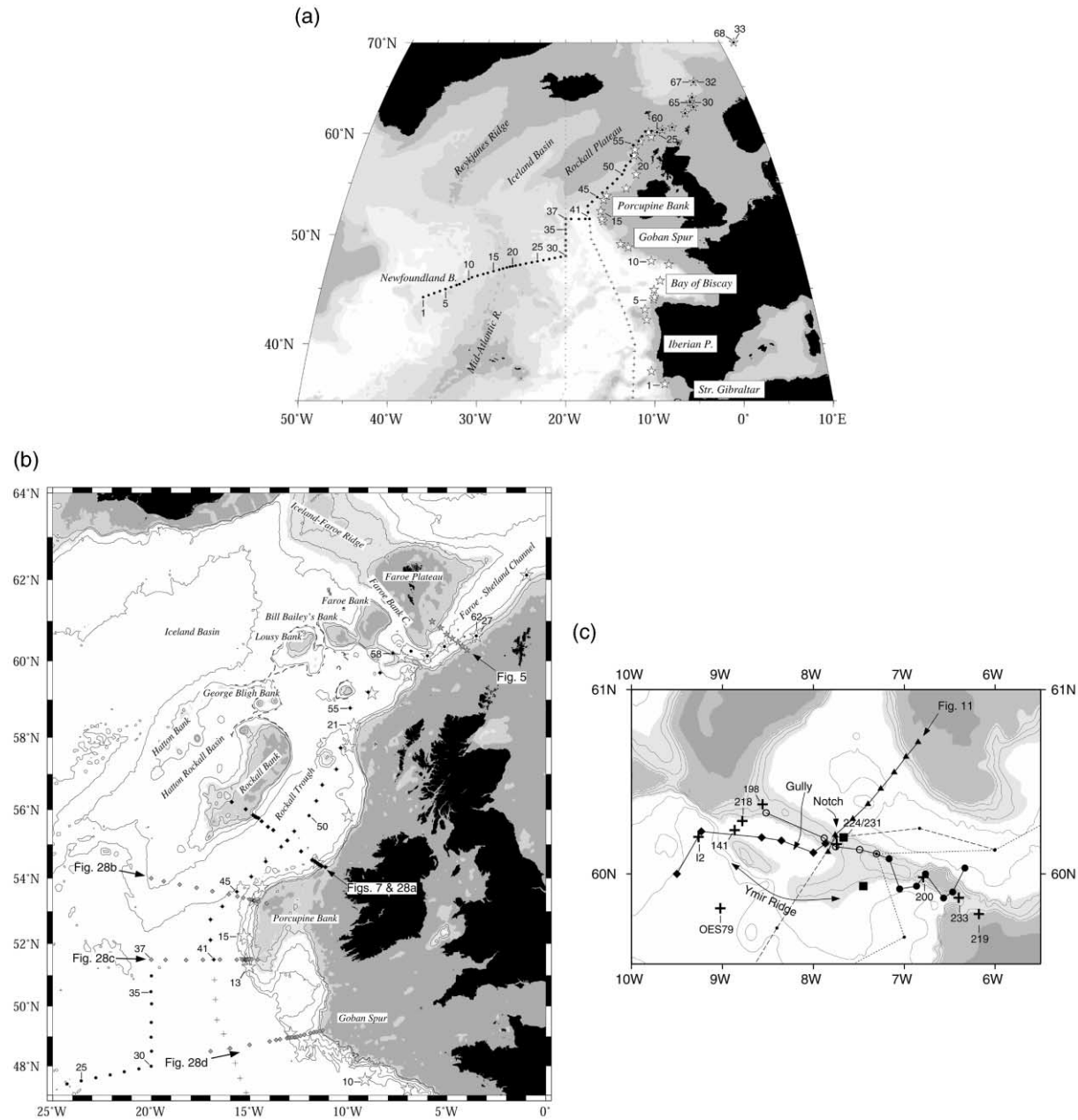

Fig. 4. (a) Section and station locations, place names, and bathymetry. White stars: Fig. 3; black circles: Fig. 20; gray diamonds: Fig. 29 (*Oceanus* 1988); crosses: Fig. 29 (Bord Est), (b) As Fig. 4(a), but expanded scale details for the Rockall Plateau complex, the Faroe Bank Channel, and the Faroe-Shetland Channel. 1100-m isobath is stippled. 400 m and 600 m are shaded. White stars: Fig. 3; black circles: Fig. 20; crosses: Fig. 25 (Bord Est); black diamonds: Fig. 7; gray diamonds: Fig. 28; gray stars: Fig. 5, (c) As Fig. 4(a), but details of the region of Norwegian Sea Deep Water spill-over of the Wyville-Thomson Ridge. Black triangles: Fig. 11; large circles: Fig. 8; small circles/dotted line: Fig. 3; black diamonds: Fig. 12; crosses: mooring locations; small circles/dashed line: Fig. 23; black squares: Tait 1937 stations.

the eastern boundary undercurrent rising from the deep layer to the shallow layer. While the deep source hypothesis has many facets, a cornerstone of the hypothesis is the silicate data.

3. Critique of the deep source hypothesis

3.1. Definition of the deep source isopycnal layer

We will hereafter refer to the nominal isopycnal range of the deep source hypothesis σ_1 = 32.0–32.3 as the Deep Source isopycnals (DS isopycnals). These isopycnals are in the lower thermocline in the eastern subtropical gyre, for example between 900 and 1500 m in the Gulf of Cadiz and in the Rockall Trough — in the latter region they roughly span 8–5°C. The density surface of Fig. 2 (old equation of state σ_1 = 32.274, about $\sigma_1 \approx 32.24$ in EOS80) lies within the lower third of this layer. While σ_1 = 32.0 lies in the lower part of the North Atlantic Central Water above the MOW core, maps of that surface's salinity (e.g. Tsuchiya, 1989) exhibit the MOW tongue type of salinity distribution, as do even lighter surfaces (e.g. σ_1 = 31.938, R94; σ_1 = 31.90 [$\sigma_{0.5}$ = 29.7], Iorga & Lozier, 1999b; σ_1 = 31.85, Lozier, Owens & Curry, 1995; σ_1 = 31.70 [$\sigma_{0.5}$ = 29.5], Iorga & Lozier, 1999a,b). Mauritzen, Morel and Paillet (2001) address the mixing origins of this part of the MOW tongue, indicating a diapycnal flux of salt, a detrainment, from the MOW core upward through the lower thermocline in the outflow regime of the Gulf of Cadiz as the initiation of the elevated salinity of the Central Water of the lower thermocline.

An essential aspect of the difference between the deep source and shallow source hypotheses is visible in Fig. 3. The DS isopycnals in the Rockall Trough segment of the section lie beneath a thick weakly stratified "warm pool", $\sigma_1 \leq 32.0$, whose properties and characteristic weak stratification reflect the regional penetration of winter convection to about 800m (McCartney & Talley, 1982; Meincke, 1986). Under the deep source hypothesis the hypothetical rising flow along the DS isopycnals must contend with that warm pool layer, by truncating the warm pool thickness in order to rise to the 600m depth of the Wyville-Thomson Ridge crest, and/or by diverting the horizontal flow within that warm pool, which otherwise would flow northward across the Ridge. In the shallow source hypothesis it is the direct horizontal flow of that warm pool itself that is the immediate origin for the Inflow. Any slope to the DS isopycnals principally represents geostrophic shear between the deep water and the warm pool water. Additionally, the isopycnal slope can reflect in some areas a southward descending plume spilling over the WyvilleWyville-ThomsonThomson Ridge crest (see Section 3.3). There can also be horizontal flow through sloping isopycnals, associated with buoyancy forcing driven water mass transformation following the flow (e.g. Luyten, Stommel & Wunsch, 1985 (see Section 4)). Within Rockall Trough this occurs, for example, for the σ_1 = 31.8 and 31.9 surfaces (Fig. 3(a)). For the present purpose, the DS isopycnals as defined include the surface focused upon in R79, $\sigma_1 \approx 32.24$, and an upper surface σ_1 = 32.0 chosen so as to lie immediately beneath the Rockall Trough maximum winter convection density immediately south of the Wyville-Thomson Ridge, to cleanly separate the waters involving direct transformation by air-sea buoyancy fluxes from the lower thermocline waters isolated from such ventilation. We return to the characteristics, origins, and downstream evolution of that warm pool in Section 4 after first discussing in this section some difficulties we find with the deep source hypothesis.

3.2. Silicate data and the deep source hypothesis

The most compelling observations in R79 suggesting the deep source hypothesis are the silicate contours on the MOW density surface (Fig. 2(d)) defining a northward extrusion of higher silicate waters, the 17 and 15μg-at.l^{-1} contours, from south of 40°N to the Rockall Plateau area. From there a silica tongue, the 12, 10 and 8μg-at.l^{-1} contours, projects through the Faroe-Shetland Channel and thence along the Norweg-

ian Current. Upper ocean silicate values in Rockall Trough are lower than this tongue's concentration (R79's Fig. 13), and the deep source hypothesis attributes the Norwegian Current silicate tongue to the influence of the high silicate mapped on the DS density surface to the south in Rockall Trough (Fig. 2(d)). That interpretation is reinforced by the eastern boundary section (Fig. 3(g)), where a diapycnal bulging of silicate contours is found at Discovery II stations 3827, 3862, 3872, and 3899 (43–57°N).

Our inspection of regional silicate data leads us to conclude that these silicate data are spurious, both within Rockall Trough and in the Norwegian Current. At-sea spectrophotometer-based silicate determinations from the 1950s and 1960s are known to have large errors. Metcalf (1969) in an early usage of silicate for deep-water studies, indicated accuracy "under good conditions is probably something of the order of ±10%". Heath (1974) stated that "comparison of supposedly identical deep-sea profiles determined by different vessels suggests that errors of 10–20% are common and 50% not unusual", In the present circumstances, with the low concentrations involved, in addition to these multiplicative factors, there may be bias errors from the accuracy of blank determinations and the possibility of samples having been frozen before processing. Considerable technical improvement has ensued since the IGY, with, for example, the requirements of the WOCE program, ±3%, being more than realized with the preparation of standards with accuracy and precision approaching 0.1% (Gordon, Jennings, Ross & Kress, 1993). Because of the central role of silicate in the deep source hypothesis, we next detail the problematic silicate data.

3.2.1. Silicate data in the Norwegian Current

The silicate aspect of the deep source hypothesis hinges on the particular stations used (R79) in the Norwegian Current that attribute elevated silicate values to the Current, namely USSR data from the research vessels *Sevastopol* (in 1958) in the Faroe-Shetland Channel and, further north, *Knipovich* (in 1969). With our advantage of a larger database of modern high-quality measurements, we do not find support for these elevated Norwegian Current silicate values either in our composite section (Fig. 3(e)), or in other modern data. We focus here on the *Sevastopol* data as they were from the more important location, at the transition between Rockall Trough and the Norwegian Current, hence they define the Inflow characteristics in Faroe-Shetland Channel. Fig. 5 shows property distributions for a 1987 section across

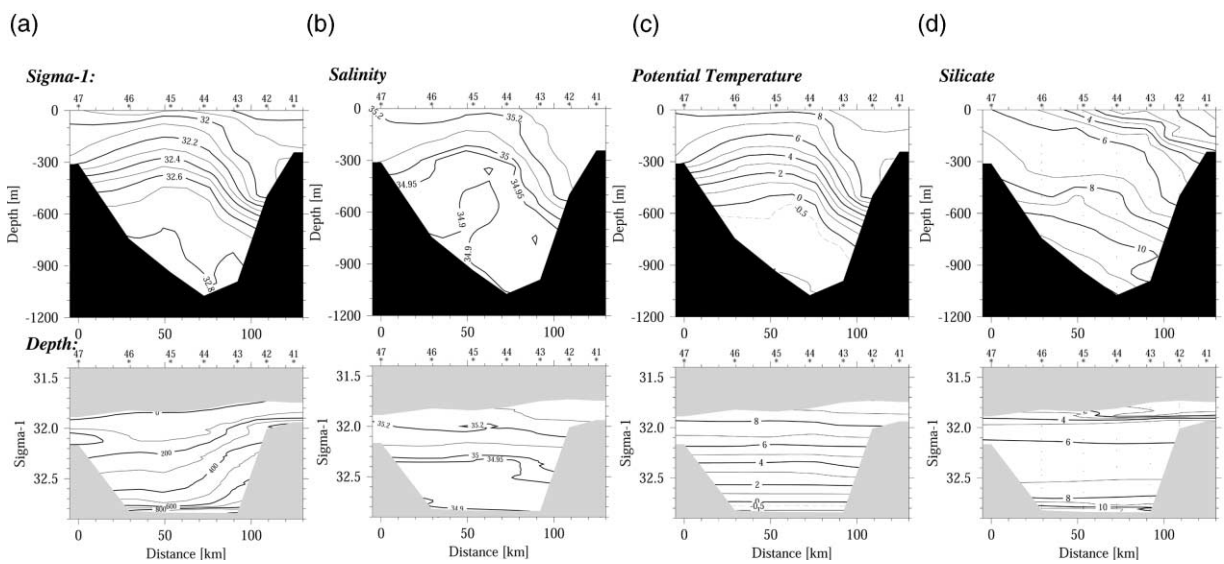

Fig. 5. Property distributions for a 1987 section across the Faroe-Shetland Channel — the beginning of the Norwegian Current (location Fig. 4(b)). (a) depth (m) and potential density parameter referenced to 1000 db reference pressure, (b) salinity, (c) potential temperature [°C], (d) silicate [μmol kg^{-1}]. Distance runs west to east.

the Faroe-Shetland Channel, the immediate source waters of the warm saline core on the Norwegian Current. This section, which is typical of the many existing sections across the Channel, shows the properties that an Inflow hypothesis must explain. The Inflow source has to supply water warmer than 7–8°C and more saline than about 35.2, but with silicate less than ~ 6μmol kg^{-1}, rather than greater than ~7–8μg-at. l^{-1} as indicated by the R79 MOW core density map (Fig. 2(d)), and eastern boundary section (Fig. 3(g)). Silicate increases with depth across the transition layer between the warm Inflow water and the outflowing cold Norwegian Sea Deep Water, being 5–7μmol kg^{-1} in the DS isopycnal layer density range and >10μmol kg^{-1} in the Deep Water.

We suspect that the *Sevastopol* data from 1958 were in error being slightly on the high side; not a surprise for data in that time frame, which were some of the earliest at-sea silicate determinations. A skeptic might ask whether perhaps silicate actually was higher in 1958. We cannot answer that definitively, for there are no reliable data of that vintage, but we doubt it, because later data show no evidence suggestive of that large a natural variability. The *Sevastopol* stations in the Faroe-Shetland Channel in 1958 are compared with selected later cruises in the 1970s, 1980s, and 1990s in Fig. 6. The data were from a download of all available stations with silicate in this region in the NODC Ocean Profile Database. We selected the years indicated as ones with major expeditions to the region and eliminated from the plot stations with silicates reported only as integer values as a first cut edit. One of two cruises in 1982 which, although defining a tight scatter, the data were about 5μmol l^{-1} lower than for the other 1982 cruise's data and the other years' data; this sort of oddball cruise file is a common problem in large data collections. The year-to-year and cruise-to-cruise scatter is somewhat larger than the "width" of any given cruise; this could either indicate residue accuracy issues (standardization errors including blanks) or real seasonal or interannual variability, since the impact of winter convection on the warmer waters varies. But the data from later cruises (1982, 1986, 1987 and 1992), probably all based on continuous flow analyzers, have a composite width at a given temperature of only 2μmol 1^{-1}, suggesting that the natural variability is of that size or less. The scatter reinforces the characterization of the silicate of the Inflow given above. The *Sevastopol* data appear biased high compared to the bulk of the data and, additionally, exhibit considerable intra-cruise scatter, suggestive of sampling and methodology artifacts occurred during that expedition.

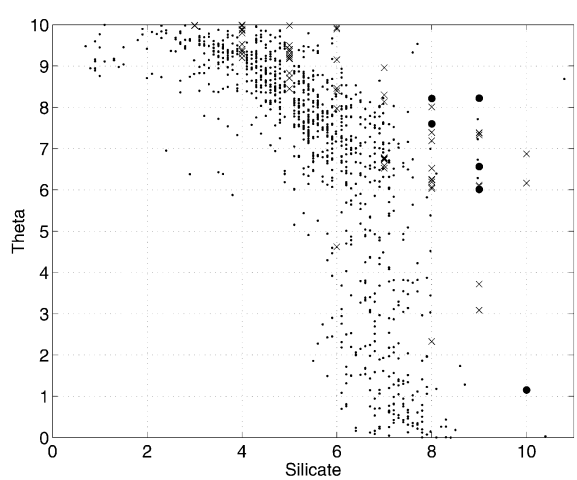

Fig. 6. Comparison of 1958 Sevastopol silicate data, ×'s including the pair of stations used in R79, filled circles, to selected Faroe-Shetland Channel cruises in 1967, 1973, 1975, 1976, 1982, 1987, and 1992, small dots [μmol l^{-1}].

3.2.2. Silicate data in the Rockall Trough

We also find that the 1958 *Discovery* II data utilized to characterize the deep MOW in the Rockall Trough on both the R79 vertical silicate section (Fig. 3(g)) and the R79 MOW core isopycnal silicate map (Fig. 2(d)) are high in comparison to modern data (previously noted by McCartney, 1992). More recent maps (R94), e.g. Fig. 2(f) for σ_1 = 32.2, do not use these particular early data. Fig. 7 shows property distributions for a section across the Rockall Trough near 55°N in 1996, well south of the Wyville-Thomson Ridge. Deep silicate values are not nearly as high as indicated on the earlier R79 MOW isopycnal silicate map (Fig. 2(d)). Rather than exceeding 15 or 17μg-at.l^{-1}, DS isopycnals in Rockall Trough have silicate around 10 to 12μmol kg^{-1}, and warm pool water at and above the sill depth of the Wyville-Thomson Ridge have silicates less than ~7μmol kg^{-1}, similar to the corrected silicate values for the Inflow at Faroe-Shetland Channel (Figs. 5 and 6).

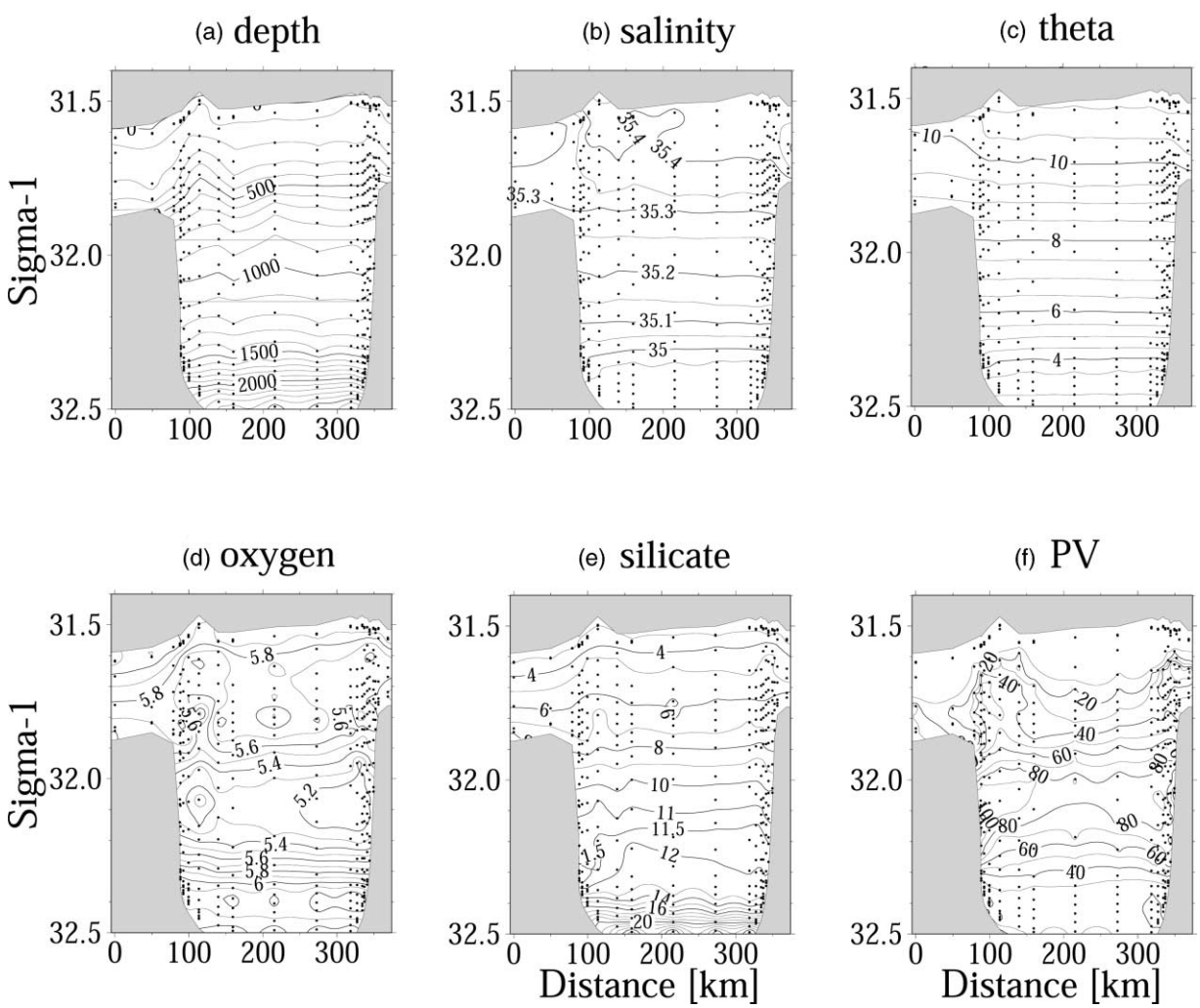

Fig. 7. Property distributions for a 1996 section across the Rockall Trough (location Fig. 4(b)). (a) depth (m) and potential density parameter referenced to 1000 db reference pressure, (b) salinity, (c) potential temperature [°C], (d) oxygen [ml/l], (e) silicate [μmol kg^{-1}], (f) potential vorticity [10^{-12} $m^{-1}sec^{-1}$].

Further evidence of the continuity of the warm pool waters across the Wyville-Thomson Ridge, and lack of evidence for elevated silicate values indicative of a rising flow from depth of DS isopycnal waters, is provided by a hydrographic section along that Ridge's crest (Fig. 8) a section made during the same expedition as that of Fig. 5, discussed in Saunders (1990). In the sill section silicates for the warm pool layer are $<5\mu$mol kg^{-1}. Silicates for the DS isopycnal layers range between 5 and 6μmol kg^{-1}, distinctly lower than the 9 to 12μmol kg^{-1} in the DS isopycnal layer at depth in the Rockall Trough at 55°N (Fig. 7(e)), but similar to the values in the DS isopycnal layer in the Faroe-Shetland Channel (Fig. 5(d)). The isolated occurrence of denser water at the notch in the Ridge sill (station 77 in Fig. 7) reflects the spillover of the Ridge by cold dense Norwegian Sea Deep Water (NSDW), with silicates exceeding 9μmol kg^{-1} at the bottom of the notch. This is consistent with the NSDW characteristic near 600–700m in the Faroe-Shetland Channel (Fig. 5). We will call this focal point of the spillover the "Overflow Notch" when we discuss conditions near the Wyville-Thomson Ridge in more detail.

To document further that the *Discovery II* data that provided the evidence for elevated silicate concentrations in the Rockall Plateau area of Fig. 2(d) are spurious, we offer Fig. 9. The four *Discovery II* stations that defined the upwards diapycnal bulging of silicate contours in the R79 eastern boundary section (Fig. 3(g)) are compared to nearby stations from the TTO NAS program in 1982 and the WOCE ACCE program in 1996. The temperature-salinity relations (not shown) at the stations being compared showed no salinity anomalies in 1958 relative to more recent data, and therefore there is no reason to expect differences in the silicate data. The 1958 data do show lower oxygen levels than the recent data, because of a known standardization error, which amounts to about 5% for pre-1959 cruises using the Woods Hole methodology (see Worthington, 1976, p 54). Correction for that error results in the 1958 oxygen data being similar to the later data. Thus there is no indication in the 1958 *Discovery* II data for a climate change signal that would explain the higher observed silicate, thus we conclude that the 1958 data are biased high because of some standardization error. The standardization error may involve an intracruise standard drift or shifts between standard batches, as the early stations in the *Discovery* II cruise, panels (a) & (b), exhibit the high bias, while the later stations in the cruise, panels (c) & (d) do not.

3.2.3. The impact of elimination of spurious silicate data

The elimination of the spurious silicate data has large impact on the underpinnings of the deep source hypothesis. The striking northward bulge of *elevated* silicate along the eastern boundary into Rockall Trough in the R79 DS isopycnal map (Fig. 2(d)), e.g. see the 10, 12, 15 and 17μg-at. l^{-1} contours, has been superseded in the R94 map Fig. 2(f) (σ_1 = 32.20, see also R94's Fig. 11(f), silicate on the σ_1 = 31.938 surface), by silicate concentrations being *diminished* near the eastern boundary relative to the interior at a given latitude, e.g. the 12μmol kg^{-1} contour, and silicate steeply declines through the Faroe-Shetland Channel. This newer map of silicate is structurally similar to that in Tsuchiya (1989) for a lighter DS isopycnal (the σ_1 = 32.00 surface, typically 300m shallower than the σ_1 = 32.20 surface of Fig. 2(f)). Tsuchiya's interpretation is that the mid-basin northeastward bulging of silicate contours reflects the advection pathway of the North Atlantic Current, and ultimately reflects higher silica influence from the Antarctic Intermediate Water that is supplied to the Florida Current and Gulf Stream from the South Atlantic. Tsuchiya, Talley and McCartney (1992) assign a similar interpretation to a silicate maximum layer immediately south of the Rockall Plateau in their 20°W section, silicates $>11\mu$g-at.l^{-1}, density about σ_1 = 32.2. The suggestive upward and diapycnal bulge of silicate contours in the R79 eastern boundary section (Fig. 3(g)) has no counterpart in the eastern boundary section using more modern data (Fig. 3(e)). Northward along the eastern boundary at $\sigma_1 \leq 31.8$ low silicate contours progressively cross to heavier densities, while for $\sigma_1 > 31.8$ a slight elevation of silicate, ~1μmol kg^{-1}, or less, occurs near Porcupine Bank reflecting the arrival to the eastern boundary of Tsuchiya's weakly enhanced silicate in the North Atlantic Current. This has little influence northward along the eastern boundary; Fig. 3(e) shows lower silicate of the warm pool waters predominantly in the northern Rockall Trough, rather than elevated silicate.

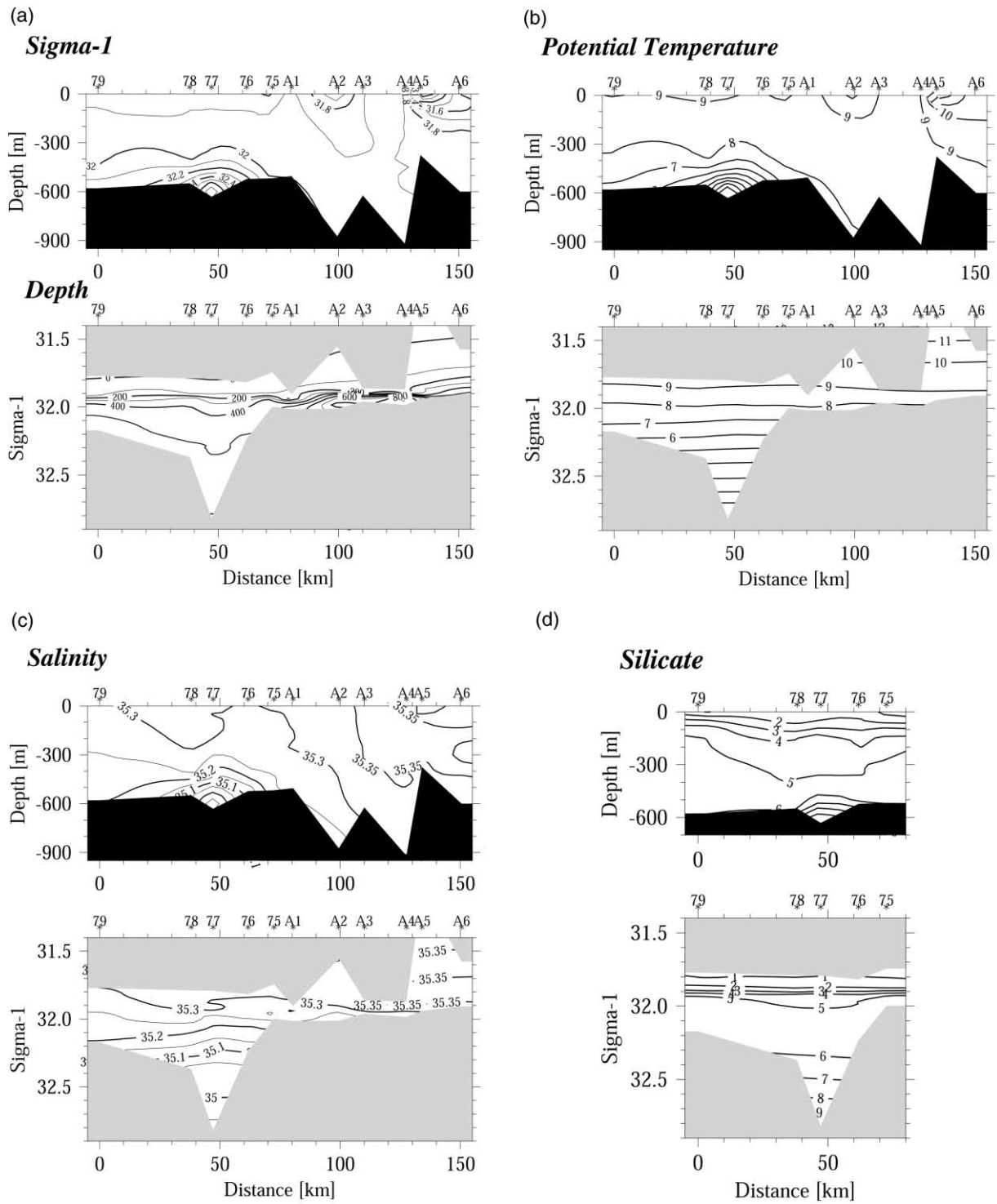
(a)
Sigma-1
Depth
Depth [m]
Sigma-1
Distance [km]
(b)
Potential Temperature
Depth [m]
Sigma-1
Distance [km]
(c)
Salinity
Depth [m]
Sigma-1
Distance [km]
(d)
Silicate
Depth [m]
Sigma-1
Distance [km]
79 78 77 76 75 A1 A2 A3 A4 A5 A6

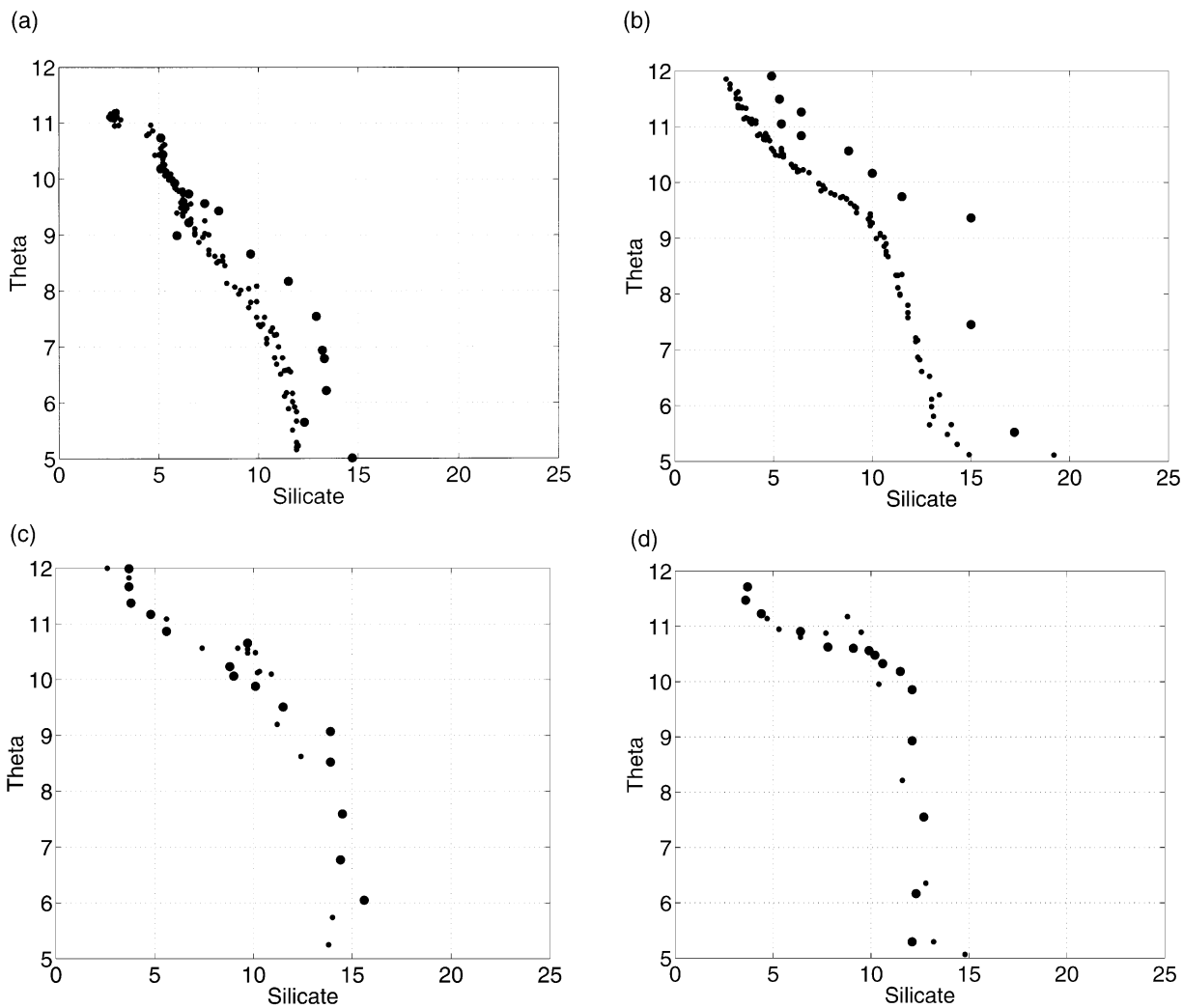

Fig. 9. Comparison of silicate data for four Discovery II stations in 1958 to later stations near the same locations. (a) Discovery II station 3827 (large filled circles) compared to WOCE ACCE program stations (dots) in 1996, (b) Discovery II station 3862 (large filled circles) compared to WOCE ACCE program stations (dots) in 1996, (c) Discovery II station 3872 (large filled circles) compared to TTO-TAS station program station 115 (dots) in 1982, (d) Discovery II station 3899 (large filled circles) compared to TTO-TAS station program station 114 (dots) in 1982.

Thus we reject the “more convincing argument” that “the contribution from the denser waters, with their high silica, is necessary” to explain the characteristics of the Inflow. We find no evidence indicative of upwelling of high silica influence in the Rockall Trough, nor do we find eastern intensification of high silica, which if it existed might be interpreted as requiring northward advection along the eastern boundary from the subtropical gyre through the Rockall Trough to the Norwegian Sea. Instead we find that the silica

Fig. 8. Property distributions for a 1987 section (Saunders & Gould, 1988; Saunders, 1990) along the crest of the Wyville-Thomson Ridge (location Fig. 4(b) and c). (a) depth (m) and potential density parameter referenced to 1000 db reference pressure, (c) potential temperature [°C], (c) salinity, (d) silicate [μmol kg^{-1}].

values of the warm pool of the Inflow (Fig. 5) are similar to the upper warm pool waters over the Wyville-Thomson Ridge (Fig. 8) and in the Rockall Trough (Fig. 7).

3.3. The depth of the DS isopycnal layer along the eastern boundary in Rockall Trough

From a circulation point of view, the cornerstone of the deep source hypothesis is that the eastern boundary current, carrying MOW, rises northward to cross the Iceland-Scotland Ridge and "contributes substantially" to the Norwegian Current. We examine in turn three natural questions that arise in the context of this requirement. Firstly in this subsection, does the DS isopycnal layer along the eastern boundary of the Rockall Trough rise northwards? In Section 3.4, is the DS isopycnal continuous across the Wyville-Thomson Ridge that separates the Rockall Trough from the Faroe-Shetland Channel? In Section 3.5, what is the nature of the flow in the DS isopycnal layer near the Wyville-Thomson Ridge?

The DS isopycnal layer as represented in our eastern boundary section (Fig. 3(a)) does not rise northwards along the eastern boundary in Rockall Trough. At stations 13–17, over the continental slope near Porcupine Bank, at the mouth of the Rockall Trough, the DS isopycnal layer is about 500m thick with its upper isopycnal σ_1 = 32.0 between 850 and 1000 m. Stations 18 to 22 indicate the layer remains at depth, with some indication that its upper isopycnal descends slightly northwards. At Station 23, only about 15 km south of the eastern end of the Wyville-Thomson Ridge, most of the DS layer is grounded out on the shoaling topography of the Ridge. The top of the DS isopycnal layer, σ_1 = 32.0, is still not grounded, and remains deep at 1000m, deeper that the entire span of the crest of the Ridge. At this station the warm pool waters occupy a depth range shallower than the crest (500–700m) of the Ridge immediately to the north, while the DS isopycnals remain below sill depth.

We have used a relatively small number of stations in the Rockall Trough segment of our eastern boundary section (Fig. 3), because we require the stations used to include silicate determinations to facilitate comparison to the original R79 section. We examined many additional stations southward in the Rockall Trough in case there might be stations that contradict this indication of the DS isopycnal layer always remaining deep near the eastern boundary of Rockall Trough, and we summarize the evidence in the following paragraphs.

In the section across the Trough at ~55°N (Fig. 7) the DS isopycnal layer is deep at the eastern boundary, spanning the depth range of about 950 to 1400m. There are many sections available near this location that confirm the robustness of the conclusion that the layer is always deep at and south of 55°N. Additionally note that the DS layer is deep all the way across the Rockall Trough (Fig. 7), so there is no indication of an offshore regime where the DS layer is shoaling northward instead of along the eastern boundary. We conclude that at the mouth of the Rockall Trough the DS isopycnal layer is uniformly deep and well below the depth of the crest of the Wyville-Thomson Ridge.

Ellett and Martin (1973) described 10 repeat sections (1963–1965) across the Rockall Trough intersecting the 1000m isobath of the continental slope near 56.2°N. These sections were located about 460km south of the Wyville-Thomson Ridge. The warm pool of the upper ocean Rockall Trough is very thick, and the DS isopycnals remain deep in all occupations and at all cross-Trough positions. Fig. 10(a) shows a representative station from their data set, a site in 1500 m water-depth over the continental slope about 30km west of the continental shelf break at 56.3°N. Using 5.0–7.5°C as nominal limits for the DS isopycnal layer, the top of the layer lies near 1000m.

Ellett (1978), (see also Ellett, Edwards & Bowers, 1986) reported on average conditions for 19 crossings (1975–1978) of the Trough a bit farther north, about 360 km south of the Wyville-Thomson Ridge (Fig. 4), with a section intersecting the continental slope near 57.1°N. Fig. 10(b) shows the mean and standard deviation for data from a repeated station from this set, in 1500m water depth about 15km west of the shelf break at 57.1°N. The upper ocean warm pool is thick, and the DS isopycnals are very deep. The mean depth of 7.5°C is about 990m, and its shallowest occurrence in the 19 stations was at about 600m.

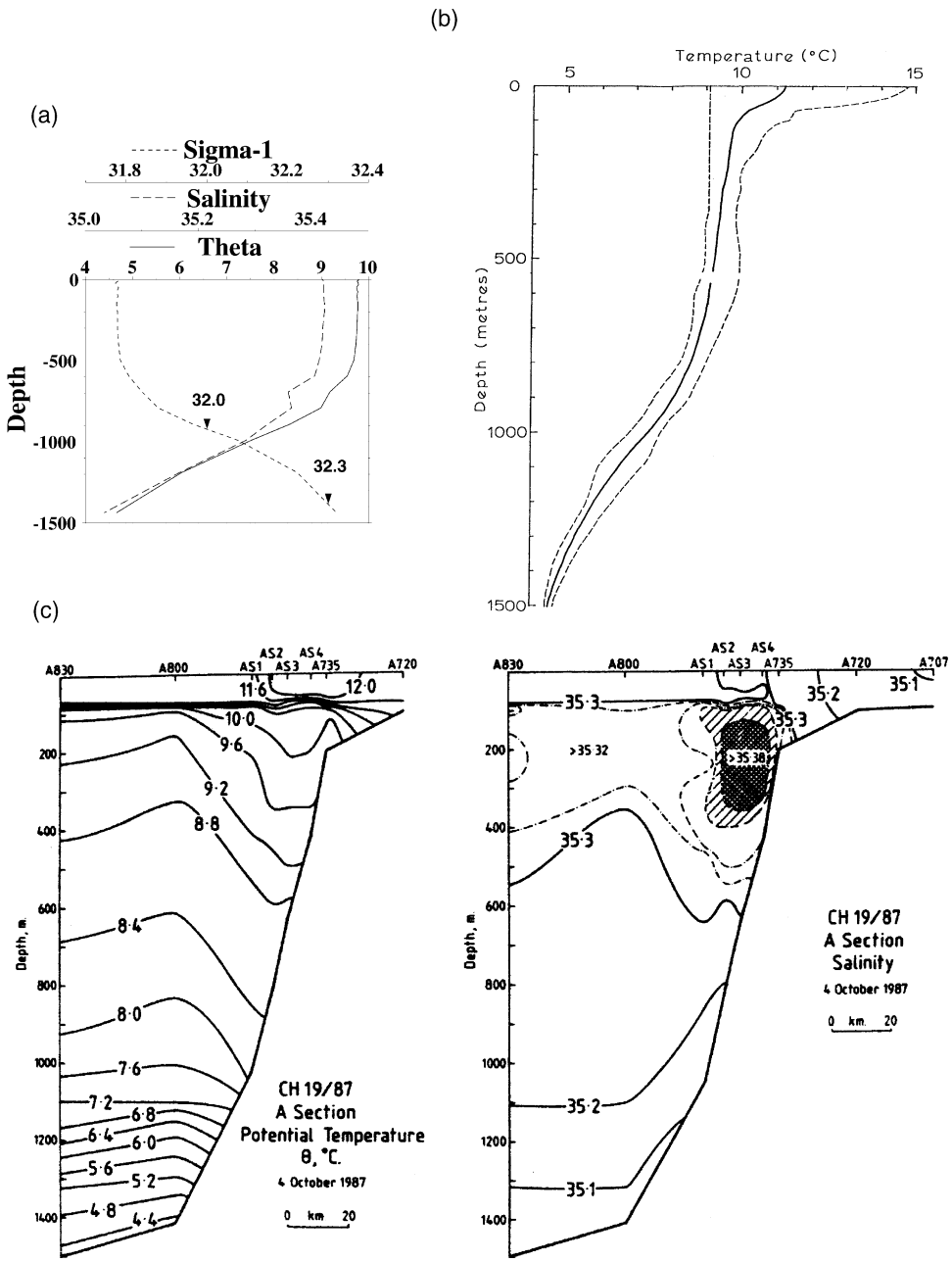

Fig. 10. Miscellaneous stations and sections illustrating that the DS isopycnal layer remains deep in the northeastern Rockall Trough, immediately south of the intersection of the Wyville-Thomson Ridge and the continental slope. (a) plot of "typical station" from tabulated data in Ellett and Martin, 1973, p. 599, (b) plot of average temperature (solid curve) and temperature range envelope (between dashed curves) from tabulated data in Ellett, 1978, (c) transect "A" temperature and salinity transects from Hill and Mitchelson-Jacob, 1993.

A recent publication (Holliday, Pollard, Read & Leach, 2000) reports on a further 63 revisits to this section, 38 fully sampled, made by Ellett and his colleagues between 1975 and 1996, and by the Southampton Oceanography Centre between 1996–1998. These firmly establish the climatological average circumstance of a deep DS isopycnal layer at the eastern boundary at this latitude; we do not have the data set and so cannot establish the absence or presence of single sections showing a shallower occurrence of the layer. A section here in 1996 during WOCE (Lynne Talley, personal communication, 1997, data available from the WOCE Hydrographic Office) also shows the DS isopycnal layer remaining deep across the width of Rockall Trough.

Hill and Mitchelson-Jacob (1993) have also considered the northward flow of warm saline water in the Rockall Trough. Fig. 10(c) shows their section near 59°N, about 130km south of the Wyville-Thomson Ridge. It indicates that the 7.5°C isotherm, the nominal top for the DS isopycnal, remained below 1000m throughout. Hill and Mitchelson-Jacob (1993) noted that if density surfaces near $\sigma_1 = 32.00$ are to cross the Wyville-Thomson Ridge, they "must rise very steeply". as that surface lay between 900–1300 m along their section. Warm pool waters above 900 m dominate the section — and on the upper continental slope those waters are warmer and slightly more saline than offshore, a telltale of the "Rockall Slope Current" (reviewed by Huthnance, 1986; also called the "Scottish Continental Slope Current" by Booth & Ellett, 1983).

Moving further north, Tait (1957) described 28 repeats (1927–1952) of a section called "Faroe Bank to Butt of Lewis". This section extended northwest from the continental shelf break, crossing the 1000m isobath near 59.4°N, and crossing the crest of the Ridge near 60.2°N 7.7°W close to what today is recognized as the Overflow Notch in the Wyville-Thomson Ridge crest. In all but two of his section plots, the warm pool in the Trough was thick, filling the full depth of the Trough, which has maximum depth near 1100m along this section. The 8°C isotherm generally lay below 800m along these section plots. In two cases there were very cold temperatures plotted at the bottom of the Trough near 1000m, one spurious (Ellett & Roberts, 1973, p. 826), the other apparently an observation that nearly undiluted Norwegian Sea Deep Water had spilled over the Wyville-Thomson Ridge and descended with little mixing to 1000m (Tait, 1957, his Fig. 25 and discussion pp. 71–72). At that station south of the Ridge (location on Fig. 4(c), the southern of the two filled square symbols), the 7.5°C isotherm was uplifted to about 600m, whereas in the other sections if 7.5°C occurred at all at this location, it was below 1000m. This section showed simultaneously cold water at the Overflow Notch, and a doming upwards of the transition layer between the cold water and the warm pool above the height of the crest, with the 7.5°C isotherm uplifted to ~ 130m depth — compared to the more usual depth ~ 450m depth as shown in Fig. 8(b). This seems to indicate there had been an isolated Overflow event, perhaps eddy-induced as the transition layer that usually occurs near the crest at 600m was very shallow near 300m, quite a different structure to that seen in all the other Tait (1957) sections. A Faroe-Shetland Channel section observed a few days earlier, 250 km to the northeast, showed a similar ridging of the transition layer in mid-Channel that was much more dramatic than the typical ridge (e.g. Fig. 5) indicating some unusual event was taking place along the channel. These 1937 data are the only evidence of an uplift of the top of the DS isopycnal layer near (~25km) the eastern boundary south of the Wyville-Thomson Ridge. From the appearance of the 1937 station it appears to have detected a spillover event involving NSDW occurring rather more to the east than normal (see subsequent discussion in Section 3.4), rather than a single occurrence of northward-rising flow in the DS isopycnal layer.

To summarize, we do find no evidence of the DS isopycnal layer's intersection with the eastern boundary in Rockall Trough rising northwards. Given the layer's depth immediately south of the Wyville-Thomson Ridge's intersection with the eastern boundary, we agree with the conclusion of Hill and Mitchelson-Jacob (1993), that if it is to rise across the Ridge, it indeed "must rise very steeply".

Iorga and Lozier (1999b) presented isopycnal maps from gridded data that we interpret as agreeing with our conclusion that within the Rockall Trough the DS isopycnals remain at depth. Their model circulation

is for a domain south of 60°N, but they state "... however, the climatological pressure fields show a northward shoaling of the isopycnals in the eastern basin". They show (their Fig. 6) pressure for two isopycnal surfaces σ_1 = 31.90 [$\sigma_{0.5}$ = 29.7] and σ_1 = 32.10 [$\sigma_{0.5}$ = 29.5]. The former is actually in the winter convection domain in Rockall Trough, and is thus actually a warm pool isopycnal. The latter surface is the more fully documented in their discussion of inferred circulation, and falls in the DS isopycnal layer as defined here. Their lighter surface rises progressively northward from >800db near 55°N to ~250db at the crest of the Wyville-Thomson Ridge. This is the result of this surface being immediately beneath the depth of winter convection in the south, but being in the seasonal thermocline in the north, which is present near surface in the summer and transitional months, but absent from winter data. On the denser surface, in the DS isopycnal layer, the surface remains near 1200db till 58°N, then in the 1° gridded data is contoured as ~350–600db along the crest of the Wyville-Thomson Ridge. Thus the surface as contoured is deep within the Rockall Trough, shallow north of the Ridge, and within the limits of gridded data, rises northward over 2° latitude. Gridded data cannot be expected to capture the "details" of the surface across the Ridge and show whether the surface is continuous, and if so, where. We next examine the geometry of DS isopycnal surfaces in the neighborhood of the Ridge using individual hydrographic stations and sections, and with current meter measurements describe the regional flow.

3.4. The DS isopycnal layer at the Wyville-Thomson Ridge

In the preceding subsection we demonstrated that the DS isopycnal layer remains deep along the eastern boundary of the Rockall Trough, including immediately south of the intersection of the Wyville-Thomson Ridge and the eastern boundary, e.g. station 23 on Fig. 3. At issue next is to establish whether the DS layer is continuous across part or all of the Ridge, and if so, what flow, if any, occurs across the Ridge in the layer? The section along the Ridge crest (Fig. 8) shows that, indeed, those isopycnals are observed over the western half of the Ridge, within and westward from the Overflow Notch in the Ridge crest near 7.8°W. Because of this east-west contrast, we subdivided our discussion into those two domains. First we address the break in layer continuity across the Ridge near the eastern boundary, and then the nature of the evident continuity of the layer across the Ridge at and west of the Overflow Notch.

3.4.1. The discontinuity of the DS isopycnal layer across the eastern Wyville-Thomson Ridge

We examined 27 available stations to the east of the Overflow Notch in the Wyville-Thomson Ridge near the crest of the Ridge. We select six stations (A1-A6, positions on Fig. 4(c)) to form a non-synoptic eastward extension of the synoptic section shown in Fig. 8. This extends the section to the intersection of the Ridge with the continental slope near 60°N. When stations were not available at the crest, we have utilized data from stations situated a few kilometers south of the crest, accounting for the artificially deeper spots at stations A2 and A4. At the eastern end of the section, station A6 falls just north of the shallower eastern end of the Ridge and is included to show the character of warm waters brought to the Faroe Shetland Current by the poleward flow of warm water along the upper continental slope (e.g. Dooley, Martin & Payne, 1976; Dooley & Meincke, 1981; Gould, Loynes & Backhaus, 1985), which is discussed in a later section. These data indicate that warm pool waters cover the eastern half of the Ridge crest, and that along the eastern boundary the DS isopycnal layer is interrupted by intersection with the eastern part of the Wyville-Thomson Ridge. We have taken this fact into account in the selection of stations for the eastern boundary section of Fig. 3, where station 23 at the Ridge crest is station 75 from the section in Fig. 8, immediately east of the Overflow Notch and about 55 km westward of the 400 m isobath of the continental slope (Fig. 4(c)). This station selection intentionally severs the continuity of the DS isopycnal layer along the eastern boundary section (Fig. 3), to emphasize the discontinuity of the layer at the eastern half of the Wyville-Thomson Ridge. The waters atop Wyville-Thomson Ridge east of the Overflow Notch are wholly warm pool waters present in the same depth range in the northern Rockall Trough, and include

the warmer and slightly more saline waters in the Rockall Slope Current, e.g. Fig. 10(c). We now consider the nature of the DS isopycnal surface's continuity over the western half of the Ridge.

3.4.2. The continuity of the DS isopycnal layer across the western Wyville-Thomson Ridge

In the segment of the Faroese Channels adjacent to the Wyville-Thomson Ridge, the southward descending transition layer grazes the crest of the Ridge, e.g. Fig. 11, and the layer continues a southward descent into the northern Rockall Channel rather than being intersected by topography as it is at the continental slope, e.g. Fig. 5, and at Faroe Bank in the Faroe Bank Channel (see, e.g. Fig. 6 in Johnson & Sanford, 1992). At some places along the Ridge, at some times, the graze of the transition layer leaves a vertical space beneath the warm pool and transition layer, through which NSDW can spill across the Ridge, e.g. station 77 in Fig. 8. This is the spillover described by Ellett and Roberts (1973). When the space is closed to NSDW, the transition layer waters above the NSDW may still be presented to the Ridge crest to be available to spill over, e.g. stations 76, 78, and 79 in Fig. 8. The NSDW spillover may be concentrated at the Overflow Notch in the ridge crest, visible in the section of Fig. 8 and the topography of Fig. 4, because that deepest pathway would generally be the first spot where a rising transition layer would expose NSDW to spillover. In Fig. 8 the deepest part of the water column over and west of the notch in the Ridge crest has about 150m of DS isopycnal layer waters. At the Overflow Notch in the Ridge crest (station 77) are additionally about 150m of waters denser than the DS isopycnal layer, representing the NSDW spillover.

Along the Ridge crest (Fig. 8) the warm pool waters occupy most of the water column, representing a cross-section of a warm pool wedge extending northward from a thick end in the Rockall Trough to a thin end in the middle of the Faroe Bank Channel. Fig. 11(a) (position on Fig. 4(c)) shows that warm pool wedge tapering northward across the Channel: note the compression of the spacing between $\sigma_1 = 31.8$ and 32.0 from 560m south of the Ridge to less than 100m next to Faroe Bank, and that the salinity in the wedge, >35.25, is similar to that observed in the Inflow (Fig. 3(c) and Fig. 5(b)). The DS isopycnal layer coincides with the transition layer between that wedge and the NSDW, and in the Faroese Channels, that cross channel rise represents principally the geostrophic shear between out-flowing NSDW and inflowing warm pool waters.

To extend farther southward into the Rockall Trough than Fig. 11(a), Fig. 12(a) shows a section from the Overflow Notch southwest along a gully on the south flank of the Wyville-Thomson Ridge, replotted from data in the Ellett and Martin (1973) study of the Overflow. The NSDW descends westward along this gully between the Wyville-Thomson and Ymir Ridges, Fig. 4(c), and is encountered as a thin near-bottom layer at stations 189 and 190. The DS isopycnal layer expands in thickness from a thin sheet at station 192 to a less strong gradient layer of 150–300m thickness in the gully (stations 189–191) and finally to a thick layer immediately outside the gully (stations 186 and 188). The NSDW warms and gains salt by entrainment of overlying waters as it descends from spilling over the western half of the Wyville-Thomson Ridge and is delivered to the northern Rockall Trough (Ellett & Roberts, 1973). In the process the plume decreases in density and moves diapycnally into the DS isopycnal layer by becoming lighter than $\sigma_1 = 32.30$.

The continuity of DS isopycnals indicated by Fig. 12 is verified with CTD profiles from a later experiment reported in Saunders and Gould (1988; their stations 80–83), contemporaneous with the Ridge crest section in Fig. 8, crossing the gully near station 189 in Fig. 12. Those data have rather colder NSDW, 2.75°C compared to 4.4°C at station 189, while their station 84 has 1.32°C compared to the nearby 1972 station 190's 4.5°C in Fig. 12. Repeated cross-gully sections observed by Ellett (1991) demonstrated the temporal and spatial inhomogeneity of the near-bottom waters descending westward through the gully, as do the near-bottom temperature maps by Currie, Edwards and Ellett (1974). Common to all these data, however, is an image that the DS isopycnal layer is continuous across the western part of the Wyville-Thomson Ridge, from the layer's occurrence as the transition layer in the Faroese Channels and over the western half of the Ridge through its descent as part of the spillover plume in the gully between the southern flank

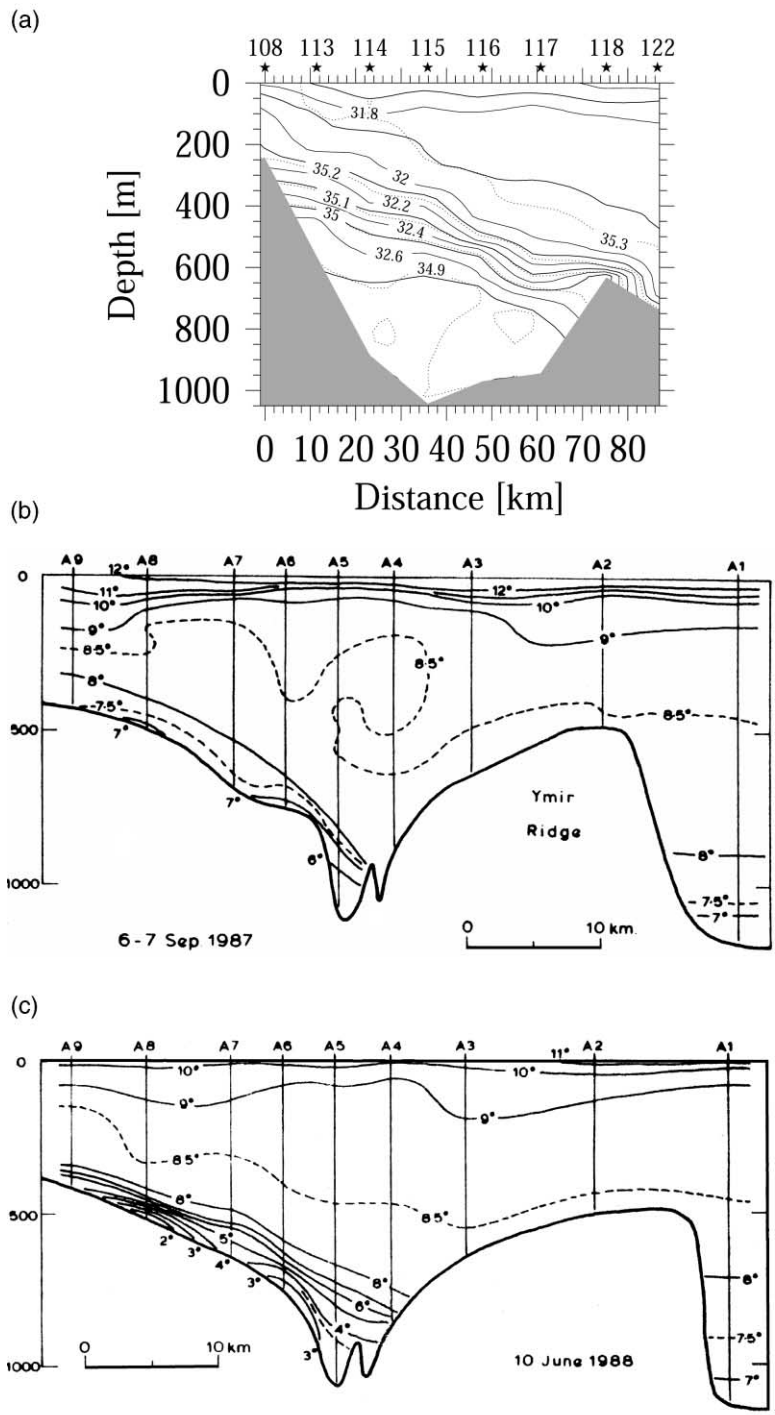

Fig. 11. (a) Distribution of and $_1$ for a section from Faroe Plateau (left) across Wyville-Thomson Ridge (location on Fig. 4c); (b) meridional section across the gully between Wyville-Thomson Ridge and Ymir Ridge, across a mooring north of the axis of the gully (from Ellett, 1991); (c) As Fig. 11b, a repeat occupation of the section (from Ellett, 1991).

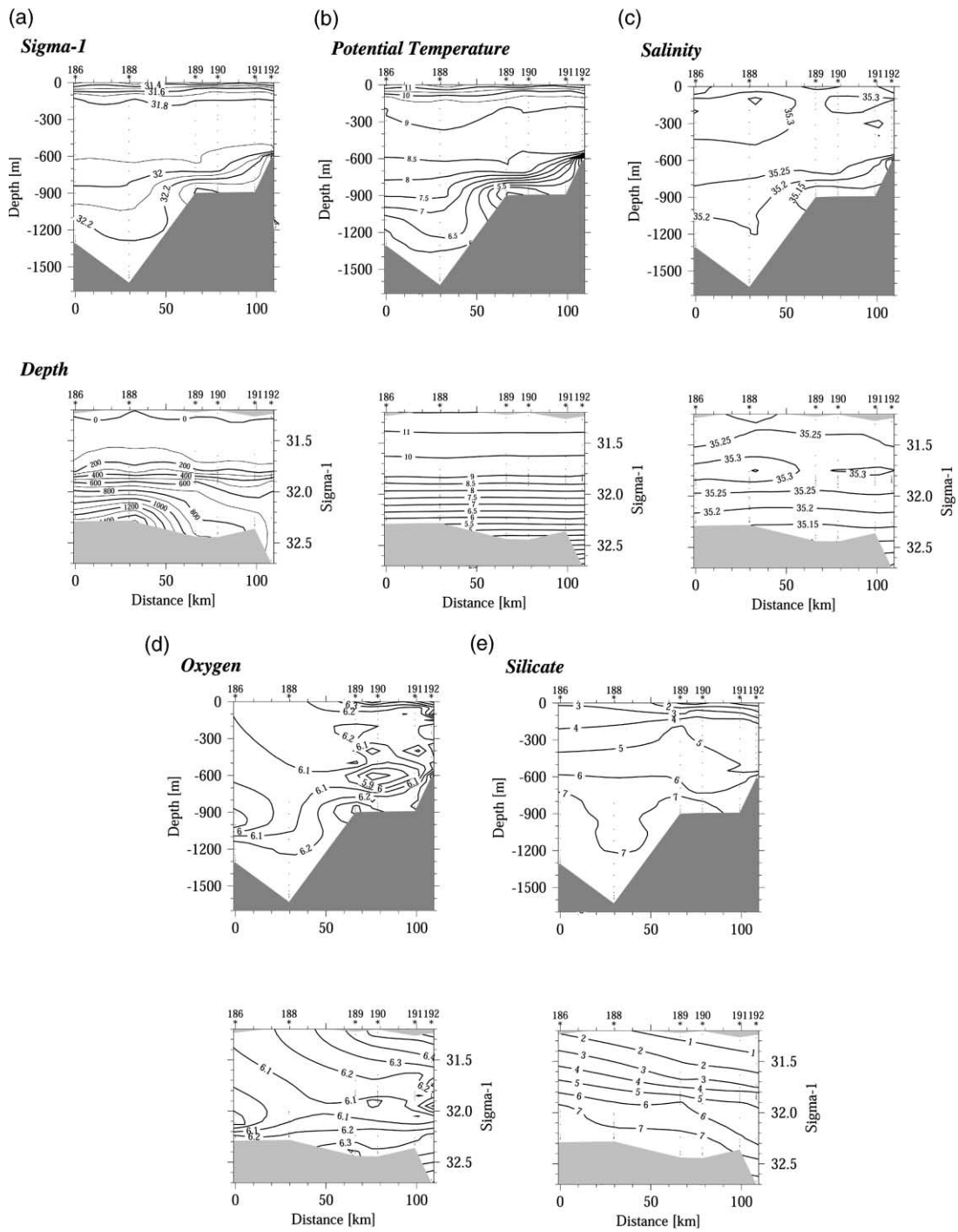

Fig. 12. Property distributions for a 1972 hydrographic section from the spillover notch in the Wyville-Thomson Ridge along the gully between The Wyville-Thomson Ridge and Ymir Ridge. Data from Ellett and Roberts, 1973. (a) depth (m) and potential density parameter referenced to 1000 db reference pressure, (b) potential temperature [°C], (c) salinity, (d) oxygen [ml/l], (e) silicate [μg-at l^{-1}].

of the Wyville-Thomson Ridge and the northern flank of Ymir Ridge, to its presence at depth in the northern Rockall Trough.

Meridional sections across the axis of the gully (Fig. 11((b),(c)), for others see Fig. 2 in Ellett & Edwards, 1978, and Fig. 6 in Ellett, 1991), suggest that the continuity of DS isopycnals is not only confined to the western half of the crest of the Wyville-Thomson Ridge, but may also be confined to the gully. The DS isopycnal layer appears as a relatively thin sheet over the area forming the northern flank of the gully, which is the southern flank of Wyville-Thomson Ridge north of the gully axis (Fig. 11((b),(c)), and has varying amounts of NSDW beneath it, and the wedge shaped warm pool above it. The DS isopycnal layer grounds out on the sea floor near 800–1000m south of the axis of the gully, on the northern flank of the Ymir Ridge. South of the Ymir Ridge the situation looks like that observed south of the eastern half of the Wyville-Thomson Ridge, the DS isopycnal layer is quite deep and intersects the topography without evidence of northward rise.

Putting these pieces together, the DS isopycnal layer's southward continuity from the Faroese Channels begins as a thin layer on the western half of the Wyville-Thomson Ridge, delimited by grounding on the Ridge crest immediately east of the Overflow Notch. A grounding curve descends and turns southwest and then west from that point, intersecting and following the northern flank of the Ymir Ridge. That grounding curve breaks the continuity between the layer within the gully and the DS isopycnal layer waters nearer the eastern boundary south of the eastern Wyville-Thomson Ridge. Northwest of the grounding curve, within the gully, the layer is a thin sheet covering the southern flank of the western Wyville-Thomson Ridge and the southern flank of the Faroe Bank. The slope of the layer carries with it an implied geostrophic shear between the overlying warm pool waters and the layer and the NSDW beneath the layer.

Because the crest of the Ymir Ridge falls in the warm pool, it is only at the deep exits to the gully that the DS isopycnal layer within it connect with the DS isopycnal layer at depths near 1000m in the northwest Rockall Trough. The principle deep exit is south of Faroe Bank, nominally 60.25°N, 9°W and regional hydrographic stations clearly establish continuity through this exit (see, e.g., synoptic survey maps in Currie et al. 1974). In Fig. 4(c) a secondary exit from the gully can be seen from the break in the 700m shading, depending on the details of the geography of the spillover's descent of the gully it is possible that this gap may provide a secondary continuity pathway for the DS isopycnal layer. Data in Currie et al. (1974), Ellett and Edwards (1978), and Ellett (1991), including Fig. 11(b) and (c), indicate that bottom temperatures in this secondary gap are likely to be warmer than 8°C, but the possibility of colder events cannot be ruled out.

We found no explicit example of spillover of NSDW eastward of the Wyville-Thomson Ridge Overflow Notch in available data. The anomalous occurrence of NSDW in the 1937 Tait (1957) section discussed in Section 3.3 could indicate a more extensive spillover. The 1937 station at the Overflow Notch position on Fig. 4(c), 7 km northeast of station 77 in Fig. 8, indicated a greatly uplifted transition layer, 7.5°C and 5°C at 130 m and 310 m, respectively, with about 330 m of colder water beneath. But since that station was at the Overflow Notch (Fig. 4(c)), and no data to the eastward of the notch are available at that time, we are unable to deduce how far the anomalous conditions extended eastwards. The 1937 station showing the anomalous occurrence of NSDW in the eastern Rockall Trough lies southeast of the Ymir Ridge (Fig. 4(c)), and thus could reflect direct spillover of the Wyville-Thomson Ridge at a more easterly site that had descended directly to that station. Alternatively it might reflect such an intense spillover at the Overflow Notch that, rather than being confined to the gully between Ymir and Wyville-Thomson Ridges, the NSDW had spilled over the Ymir Ridge through the secondary gap mentioned in the preceding paragraph to arrive at Tait's 1937 station at a location where NSDW is not normally found.

The topography of the western Wyville-Thomson Ridge, the Overflow Notch, and the double ridge structure with the intervening deepening gully indicates that there is complexity in the geometry of the DS isopycnal layer's continuity. The bottom line is, however, that the combination of Figs. 8 and 11, and 12, and the other data mentioned, establishes the continuity of the DS isopycnal layer across the western

Wyville-Thomson Ridge between the layer's presence below 900m in the northern Rockall Trough and its presence as a shallow transition layer between NSDW and warm pool waters in the Faroese Channels. The restriction of that continuity to the gully between the Wyville-Thomson and Ymir Ridges suggests that its continuity is related to the spillover plume that is banked up against the southern flank of the western Wyville-Thomson Ridge. We next consider the nature of the flow within the DS isopycnal layer over and south of the Wyville-Thomson Ridge.

3.4.3. Steeply rising flow — or steeply descending flow?

Having established that the DS isopycnal layer is continuous across the western half of the Wyville-Thomson Ridge from the layer's shallow regime in the Faroese Channels to its ~1000m depth in the northern Rockall Trough, the next question to address is the nature of the flow in that layer where it makes its descent across the Ridge. The deep source hypothesis requires northwards and upwards flow across the Ridge somewhere in the DS isopycnal, so with the layer being discontinuous over the eastern part of the Ridge, does such ascending flow occur in this western region?

As we began this project we were skeptical about the idea that core layers allied with steeply rising isopycnals indicate rising flow along those isopycnals. What is said in R79 about how the hypothetical upward flow occurs is limited (R79, p. 1214, regarding the rise of the surface in the northern Rockall Trough):

> "The rise, which allows the deeper Atlantic waters to ascend laterally from 1200m to less than 400m and extend through the channel, appears to be the consequence of the vertical geostrophic shear".

While the rise of the DS isopycnals is directly linked to the shear, there is no reason for the rise of the surface necessarily involving ascending flow on the surface. Vertical motion in the ocean is generally gradual, with the crossing angles between the flow streamlines and isobars of a density surface being small, except in the case of dense overflows where more appreciable angles occur. Steep isopycnal slopes are usually interpreted as a reflection of the vertical shear of the horizontal geostrophic flow at right angles to the horizontal density gradient, and not to reflections of strong ageostrophic flow up that gradient. We do not know what physical argument might be made for this steeply rising flow, and none was included in R79. To some degree there is a parallel problem in the more general case of interpreting steeply descending core layers aligned with descending isopycnals, e.g. the northward descents of the Antarctic Circumpolar Current. These, too, are often interpreted as indicative of sinking northward flow, but Reid (1965, p.38) noted that such a signature predominantly represents the geostrophically balanced eastward flow of the Current at right angles to the descending isopycnals. Under the deep source hypothesis the DS isopycnal layer waters to the south of the Wyville-Thomson Ridge are required to climb against gravity from below sill depth, and then to flow across the sill, and in the process deflect the path of a stronger current of lighter water that is flowing towards the sill at depths shallower than the sill.

As it turns out, a variety of current meter measurements were made in this region during the 1980s. Results from a current meter mooring placed in the Overflow Notch in the Ridge crest (H. Dooley, personal communication, 1999) shed light on the variability of the spillover through this notch and the involvement of the DS isopycnal layer. The sill depth of the Overflow Notch is ~ 644m (Ellett & Roberts, 1973), and its width at 600 m is about 7 km. Dooley's mooring was placed very close to the sill (Fig. 4(c)), for about six months beginning mid-November 1982, and instrumented at depths of 102m, 510m, and 633m, in 637m water depth (for reference, station 77 in Fig. 8 was in 630m water depth). The upper instrument failed after three weeks, but full records of currents and temperatures were recorded by the deeper two instruments, and a subsequent resetting of the upper instrument yielded a further 73 days record that we have included in our study. We present these records in two ways. Fig. 13 shows low passed current vectors as time series, panels a, c, and e, and as functions of low-passed temperature, panels b, d, and f, plotted with

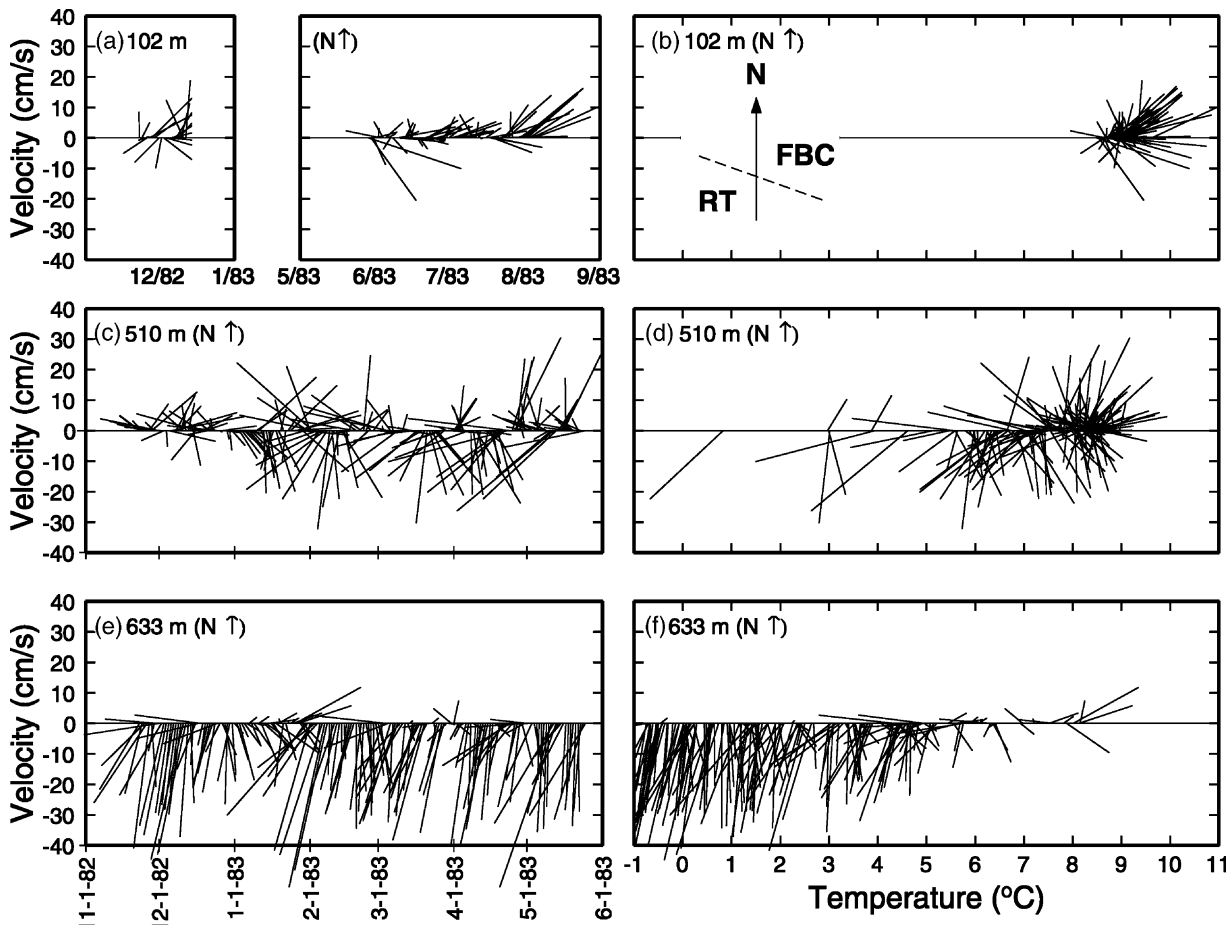

Fig. 13. Current meter data from a mooring in the notch in the crest of the Wyville-Thomson Ridge Crest, mooring 224 (H. Dooley, personal communication, 1999) deployed in 637m water depth, November 23, 1982–May 15, 1983 and instrumented at three levels, 102 m (1), 510 m (2) and 633 m (3). The 102 m instrument record was only 20 days, and is supplemented by a later mooring at the same site with a single instrument at 102 m (4), mooring 231, May 29, 1983–August 5, 1983. Panels a,c,d are daily average current vectors as a time series. Panels b, d, f are daily average current vectors plotted as function of the daily temperature. Position on Fig. 4c.

northward flow up, and with an inserted diagram showing the orientation of the Wyville-Thomson Ridge Crest.

Almost the entire record from the near-bottom instrument (Fig. 13(e)) showed dense spillover, and only a few daily vectors had a slight component northwards. Fig. 13(f) shows the same vectors plotted using the temperature of each vector measurement as the plotting coordinate. At the deepest instrument the dominance of strong southward flow at colder temperatures is obvious. The near-bottom temperatures were quite variable, but dropped to <0°C during only about 12% of the record's duration. Using 5°C or the lower side of the DS isopycnal layer, this record shows that the instrument was measuring dense overspill for most of the time, and only during 17% of the record were water temperatures warm enough to be considered observations of the DS isopycnal layer. The occasional observations of flow with a northward component, involved the strongest three northward flow vectors and were events associated with warm pool waters >8°C, suggestive that there was complete grounding of the transition layer onto the northern

side of the Wyville-Thomson Ridge so that the Overflow Notch filled with warm pool waters from the south. Daily averages with temperatures between 5°C and 7.5°C, nominally the DS isopycnal layer, occurred only on 22 days out of the 184-day record, with those 22 vectors mostly of southward orientation and together averaging a speed 5.1cm/s in a direction of 255°, i.e. in the outflow direction rather then the inflow direction. There is no evidence in the record from this near-bottom instrument that northward flow into the Faroese Channels through the Overflow Notch persisted for a significant time in the DS isopycnal layer or elsewhere. Instead, whenever the DS layer was near the bottom of the Overflow Notch, the flow measured was southward, which corresponded to waters from the transition layer between NSDW and warm pools within the Faroese Channels spilling out through the Overflow Notch into the gully between the Ymir Ridge and the western Wyville-Thomson Ridge.

The time series from the instrument placed 127m above the seafloor of the Overflow Notch at a depth of 510m was above the depth of the crest of most of the Wyville-Thomson Ridge (Fig. 13(c)) shows the daily average vectors were much more erratic in both direction and temperature. They were mostly (146 days out of 184) in the warm pool range >7.5°C (Fig. 13(d)) that was a proxy for the top of the DS isopycnal layer σ_1 = 32.00. Occasionally (7 days out of 182), the temperatures were cold enough to be considered dense spillover (colder than 5°C) indicating, we believe, momentary vertical expansion of the NSDW layer uplifting the transition layer at the Overflow Notch. For 31 days out of 184 days (i.e. 16% of the record) daily temperatures were in the 5° to 7.5°C range of the DS isopycnal layer. Usually whenever the instrument was sampling water typical of the DS isopycnal layer, the flow had a southerly component; during those 31 days the mean speed was 14.3 cm/s at 216°. All but one of the 31 vectors that exhibited a northward flow component also had a strong westward orientation, indicating the flow was not quite parallel to the overall orientation of the Wyville-Thomson Ridge and indicated a slight outflow component even for these vectors. Only one daily vector from this 184-day record was associated with a temperature of 6.7°C, which indicated that there was DS isopycnal layer inflow into the Faroese Channel above the Ridge Overflow Notch. So, as with the near-bottom instrument at this location, the measured DS isopycnal layer velocity indicates a spillover of waters from the transition layer between NSDW and warm pools within the Faroese Channels.

The shallow instrument at the Overflow Notch mooring (Fig. 13 a, b) with its composite record length of 89 days, showed only warm pool temperatures. It indicated a predominance of warm inflow across the inclined Wyville-Thomson Ridge into the Faroese channels, at a mean temperature of 8.94°C, speed 8.4 cm/sec at 68°, i.e. a ridge-crossing angle of about 48°. Some of the vectors had southerly velocity components, but their overall orientation was almost parallel to the Wyville-Thomson Ridge, again at slight inflow angle. About 7 of 89 days exhibited small-amplitude warm outflow.

What of other locations along the Ridge? Two additional moorings (locations on Fig. 4) were placed along the Ridge crest by Dooley (personal communication, 1999), one at each end of the Ridge. One was placed at the western end of the Ridge near its intersection with Faroe Bank for 3.5 months beginning late July 1980. It was instrumented at depths of 37m and 497m in a water depth of 501 m. This mooring was located close to the position of the 1987 station 79 in Fig. 8, where a thin layer of DS isopycnal layer waters was measured near the bottom. The vectors for this mooring's near-bottom instrument (Fig. 14(b)) were predominantly orientated southwards in the spillover direction. While the coldest temperatures at this mooring (Fig. 14(b)) were not as extreme as at the bottom instrument within the Overflow Notch, clearly there were substantial amounts of NSDW spilling over at this location, which was well west of the notch. Temperatures were quite variable, but mostly colder than 5°C (163 days out of total 217 days). Fig. 14(b) shows that nearly all the vectors associated with temperatures colder than 5°C indicated spillover.

For the observations with temperatures associated with the DS isopycnal layer, 5°–7.5°C, the mean speed is 8.6 cm/s at 133°, indicating mean outflow from the Faroese Channels across the Ridge, whose inclination is 115°. The majority of daily average vectors in the DS temperature range had southward flow components, and most of the 15 days with northward components were oriented just north of eastward. The predomi-

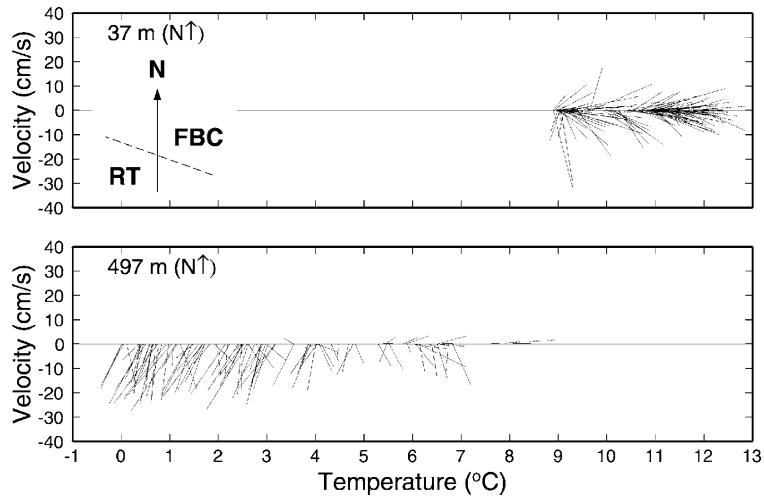

Fig. 14. Current meter data from a mooring at the western end of the Wyville-Thomson Ridge Crest, mooring 198 (H. Dooley, personal communication, 1999) deployed in 501-m water depth, July 30, 1980–November 15, 1980, and instrumented at two levels, 37 m (a) and 497 m (b). Daily average current vectors plotted as function of the daily temperature. Position on Fig. 4c.

nance of the southward-oriented vectors over the eastward oriented vectors accounts for the time average outflow vector for this layer. The eastward-oriented vectors indicate that there was occasional inflow into the Channels in the DS isopycnal layer near the western end of the Wyville-Thomson Ridge, but with trajectories crossing the Ridge from the west, from the area south of Faroe Bank. This is inconsistent with an eastern boundary undercurrent origin for these occasional events, for any remnant of that undercurrent in the Rockall Trough would lie southeastward of this site not westward, and would somehow have to traverse the spillover plume that lies between this mooring and the eastern boundary. Instead, as will be elaborated in a later section, such eastward flows crossing the western part of the Ridge are part of the delivery of Iceland Basin warm pool waters past Faroe Bank to the Faroese channels. In the Iceland Basin, winter convection occurs at the densities of the DS isopycnal layer.

The shallow instrument at the mooring near Faroe Bank (Fig. 14(a)) always sampled warm pool waters. Nearly all the vectors recorded by this upper instrument had an eastward flow component, with a majority of those vectors oriented northwards of 110° and thus indicating warm pool inflow to the Faroese Channels across the inclined Wyville-Thomson Ridge from south of Faroe Bank. Some vectors were turned sufficiently southwards to indicate an outflow of warm waters from the Faroese Channel. Referring to Fig. 4(c) to note this mooring's placement relative to the shoal Faroe Bank, it is likely that these sporadic warm outflows represented waters that had entered the Faroese Channels through the Faroe Bank Channel between Faroe Plateau and Faroe Bank, and then turned southward across the Wyville-Thomson Ridge east of Faroe Bank. Saunders (1990, data in Saunders & Gould, 1989) has reported current-meter measurements showing SE flowing warm pool waters at 300 m on the Faroe Bank side of the Channel northeast of Faroe Bank.

At the eastern end of the Wyville-Thomson Ridge, near its intersection with the continental slope Dooley's third mooring was placed in 501 m water depth on the Rockall Trough side of a notch with sill depth near 450 m (Fig. 4(c), according to the Smith & Sandwell, 1997, 2 nm bathymetry database). This eastern notch separates an isolated shoal on the Ridge crest with depth $<$400 m from the continental slope. This deployment yielded six-month records beginning early June 1983. The upper instrument at 100 m indicated (Fig. 15(a)) warm inflow to the Faroe-Shetland Channel passing through that notch, with no occurrences of water cold enough to be considered DS isopycnal layer water. The lower instrument, which was at 477 m (24m above the sea floor) and probably slightly deeper than the notch sill to its east, recorded

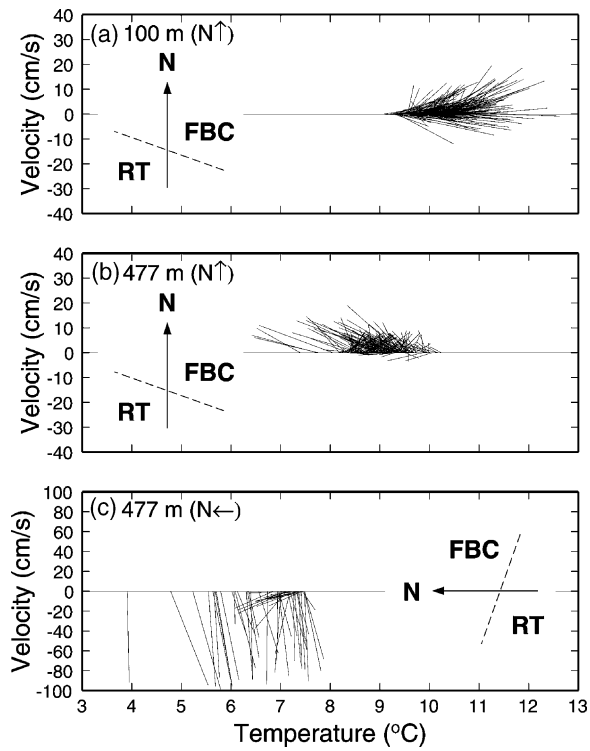

Fig. 15. Current meter data from a mooring at the eastern end of the Wyville-Thomson Ridge Crest, mooring 233 (H. Dooley, personal communication, 1999) deployed in 501m water depth, June 8, 1983–December 8, 1983, and instrumented at two levels, 100 m (a) and 477 m (b) daily average current vectors plotted as function of the daily temperature, (c) unfiltered hourly current vectors plotted as function of the daily temperature, restricted to observations colder than 7.5°C. Position on Fig. 4c. Note 90 degrees of rotation of vector coordinate.

flow (Fig. 15(b)), that was almost always westward, with a small northward component. Its mean vector orientation of 321° suggests a flow following the bathymetric contours of the southern side of the isolated shoal. This could indicate that the Rockall Slope Current flow coming north was being blocked from turning through the eastern notch. Alternatively, it could be indicative of a near-bottom Ekman layer inducing flow to the left of the prevailing flow at shallower levels (the veer between the mean velocity vectors of the two instruments was 117°, while the mean of the low-pass filtered veer between the two instruments was 101°). Both instruments were essentially wholly measuring warm pool waters, whose warmth was suggestive of a dominance of the Rockall Slope Current waters at this site close to the continental slope. This is consistent with the Ridge crest section in Fig. 8, which exhibited temperatures close to 9°C and included station A6 just north of the crest in the southwestern Faroe-Shetland Channel. The warmth of the water at the depth of the upper instrument reflects the summer and fall span of the record.

At this eastern mooring there was only a single occurrence in the low-pass filtered daily average records of temperatures becoming cold enough to be considered as indicating the presence of the DS isopycnal layer (7.4°C), and that vectors measured by the lower instrument were oriented relative to the topography such as to not represent an inflow to the Channel. Examination of the hourly unfiltered data for the lower instrument shows that the higher frequency occurrences of water colder than 7.5°C at the lower instrument were all associated with westward flows, i.e. in 50 hourly data points from a total record of 4524 points. These are plotted in Fig. 15(c): note the rotation of the vector coordinate in this panel relative to the other

two panels. All, but about 10 of these points, indicated flow was nearly westward at relatively high speeds; these are interpreted by Dickson and Kidd (1986) as being indicative of occasional spillover events at this site. Given the temperatures involved, these represent not NSDW spillover but spillover from the transition layer between the warm pool waters and the NSDW. Immediately to the east of the Wyville-Thomson Ridge, the transition layer intersects the continental slope at depths of around 500 m (e.g., Fig. 5), but can be inferred occasionally to be presented to this shallow sill of the passage on the eastern Ridge. The other 10 of these hourly vectors, when temperatures were between 7° and 7.5°C, were oriented NNW, which, given the shape of the 430m and 500m contours around the mooring site (Fig. 4(c)), probably reflected the flow was following isobaths along the southern side of the eastern bump on the Ridge.

Immediately west of the <400 m shoal on the eastern Wyville-Thomson Ridge a fourth mooring (position on Fig. 4(c)) of the same vintage as the above three Dooley moorings, provided records at 50m (102 days) and 447m (64 days) in 450m water depth (data plots not shown; these data were obtained from L. Rickards, BODC). Its upper instrument showed wholly warm inflow, while the near bottom instrument, nearly entirely sampled warm pool waters and showed the same sort of veering that the eastern Dooley mooring exhibited. In its unfiltered half hourly sampled record only four vectors of the 3085 sample record were colder than 7.5°C, and then only slightly cooler at ~7.2°C. The data from both these eastern mooring sites tell a similar story of dominance of warm inflow with only rare occurrences of DS isopycnal layer waters, and without inflow orientation for the associated vectors. They reinforce the results of the preceding sections that along the eastern boundary and eastern half of the Wyville Thomson Ridge the DS isopycnal layer consistently remains deep and seldom if ever rises to shallow enough depths to provide part of the warm Inflow.

Fig. 16 summarizes the above and other current meter measurements, showing the record mean vectors and associated average temperatures. Panel (a) uses near surface instruments, while panel (b) uses near-bottom instruments. Included in these plots are additional moorings from south of the crest of the Wyville-Thomson Ridge, which are discussed in the next subsection, and along the Rockall continental slope at its intersection with the Ridge, revisited in Section 5. The near-surface instruments define inflow of warm pool waters into the Faroese Channels, either after crossing of the Ridge from the west, or by waters flowing northwards from the northern Rockall Trough, which include the flow of the Rockall Slope Current that turns eastward where the Ridge intersects the continental slope. The near-bottom instruments show that inflow across the eastern end of the Ridge is blocked and that the dense spillover across the Ridge occurs farther west. The spillover is, on average, colder than the DS isopycnal layer, and feeds a westward flow that flows along the gully between the Wyville-Thomson and Ymir Ridges (Fig. 4). That westward flow appears to be intense, and while entrainment has resulted in the mean temperatures in the gully becoming warmer then those of the spillover, in the gully it has associated temperatures that are still colder than in the DS isopycnal layer. Fig. 16(c) shows the results of conditionally sampling all the instruments at each mooring for the velocities occurring when the instrument was recording a daily average temperature between 5°C and 7.5°C. At the easternmost site the open-headed vector represents the average of 50 samples of hourly data from the Fig. 15(c), the only hourly observations of water this cold at this mooring. Similarly, the open-headed vector just west of there represents the four samples (half-hourly) out of a 64-day record where the temperature dropped to around 7.2°C, this being a mooring just westward of the bump on the eastern Ridge, but well eastward of the Overflow Notch, Fig. 4(c). This panel thus portrays the flow in the DS isopycnal layer as directly sampled by current meters.

From the distribution of properties along the crest of the Wyville-Thomson Ridge and from the current meter measurements at locations along the crest, we find scant evidence for DS isopycnal layer water ever crossing from the northern Rockall Trough into the Faroese Channels. The velocity measurements indicate that even when the DS isopycnal layer occurs at the crest, the flow in the layer is usually southward out of the Faroese Channels. The only mild exception to this conclusion was the measurement near the western end of the Ridge of occasional flow from the west into the Faroese Channels at DS isopycnal temperatures;

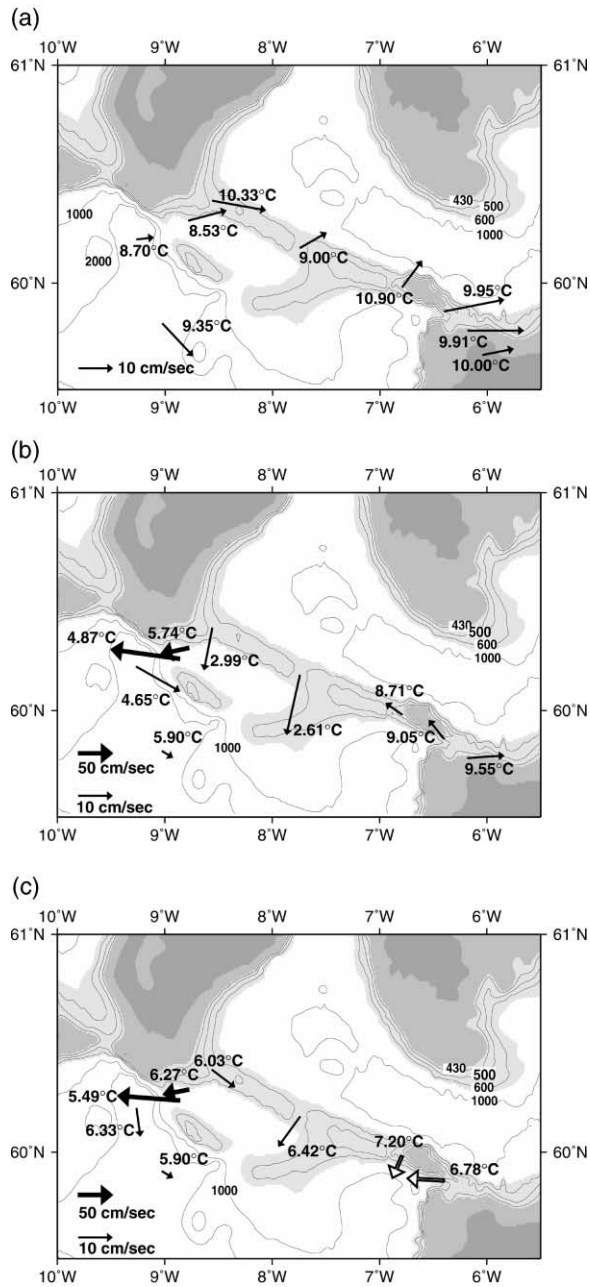

Fig. 16. Record mean current vectors and temperatures at indicated instrument depths in the area of the Wyville-Thomson Ridge. The three moorings from Fig. 13, 14 and 15, and others as indicated in the text. Shade Breaks at 200, 400 and 700 m, white deeper than 700 m. Contours 500, 600 and 1000 m, with 430 m added to show sill in eastern part of the Wyville-Thomson Ridge. (a) near-surface instruments, (b) near-bottom instruments, (c) sampling instruments only when recording daily average temperatures between 5°C and 7.5°C.

but these cannot be attributed to an eastern boundary origin. We next consider the flow conditions on the southern flank of the Wyville-Thomson Ridge.

3.4.4. The spillover plume on the southern flank of the Wyville-Thomson Ridge

The main outflow of NSDW into the subpolar gyre is the westward course of the water through the Faroese Channels. The NSDW flow is confined between the Faroe Plateau on one side, and on the other side by, sequentially, the continental slope off the Shetland Islands, the Wyville-Thomson Ridge, and the Faroe Bank south of the Faroe Islands (Fig. 4(b)). The bulk of the exported NSDW debouches through Faroe Bank Channel into the northern part of the Iceland Basin, to south of the Iceland-Faroe Ridge, from where there are no pathways that connecting back into the Rockall Trough. Saunders (1990) estimated the Faroe Bank Channel outflow to be 1.9 ± 0.4 Sv, based on limited moored current meter data combined with ADCP and hydrographic data and using a temperature of 3°C to define the top of the water mass. His estimate was made at the narrows between Faroe Bank and Faroe Plateau and thus did not include any water spilling over from the Faroese Channels across Wyville-Thomson Ridge to the east of the narrows. More recently long-term moored ADCP measurements by Østerhus, Hansen, Kristiansen and Lundberg (1999) at the same narrows also yielded a 1.9 Sv estimate for the $<$3.0°C water, of which about 1.5 Sv was colder than 0.5°C.

The Wyville-Thomson Ridge Overflow is a smaller amplitude side branch from this main Outflow pathway (Ellett & Roberts, 1973; Ellett & Edwards, 1978; Saunders, 1990; Ellett, 1991), which delivers dense waters from the Faroese Channels to the Rockall Trough. The Wyville-Thomson Ridge Overflow waters as observed in the northern Rockall Trough have been extensively metamorphosed from the NSDW characteristics by considerable entrainment of warmer more saline waters. Saunders (1990) used two shipboard ADCP transects with hydrographic and XBT data to estimate 0.35 Sv (the section in Fig. 8 supplemented with XBT data, see Saunders 1990, Fig. 11) and 0.30 Sv (an XBT section a year later, with the preceding year's T-S relation used to transform temperature section data into geostrophic shear) amplitudes for the Overflow colder than 3.0°C in the neighborhood of the Overflow Notch in the Wyville-Thomson Ridge. This represented roughly a fifth of the amplitude of the remaining part of the Outflow that passes between Faroe Bank and Faroe Plateau. Other estimates of the Wyville-Thomson Ridge Overflow have been made downstream of the point of spillover where substantial warming of the plume has occurred. Comparison is therefore difficult, for a mixing/entrainment model is often used to estimate the fraction of the flow that is "pure" NSDW. Thus Ellett and Edwards (1978) used a hydrographic section and a short-term current meter measurement by J.Crease in 1973 (the highest speed vector in Fig. 16(b)) to estimate a plume transport of 1.2 Sv, of which they estimated 0.33 Sv to be NSDW. Ellett (1991), using a different mooring (see Fig. 4(c) for locations, and the discussion below of the velocity measurements) and hydrographic data (two of his five sections across the mooring site are shown as Fig. 11((b),(c)), estimated the total plume transport to be only 0.3 Sv below 8.0°C, with only 25% of that being NSDW. This estimate is probably a lower bound, as it is based on a width of only 7km near the mooring for converting the velocity it measured to transport, and as Fig. 11((b),(c)) show, the breadth of the blanket of cooler water over the northern part of the gully is at least three times that assigned width.

There are two ways that this spillover could contribute to the flow of DS isopycnal layer water south of Wyville-Thomson Ridge, and both seem to be active. First, there can be direct spillover of the waters in the transition layer that is between the warm pool waters flowing through the Faroese channels to the Nordic Seas, and the NSDW flowing out through the Faroese channels, e.g. Fig. 5. The current meters at the western mooring and Overflow Notch mooring on the crest of the Wyville-Thomson Ridge measured the direct spillover as discussed in the preceding section. In this case, the characteristics of the spillover in the DS isopycnal layer represent the product of the mixing between the NSDW and warm pool waters in the Faroese Channels (e.g. Johnson & Sanford, 1992), or possibly an export of a mixture Arctic Intermediate Water (~ 3°C) from the Norwegian Sea with the warm pool waters (e.g., Dooley & Meincke,

1981). Secondly, the entrainment of warmer waters into the NSDW plume as it descends into the northern Rockall Trough may lead to waters in the entrainment layer moving in the same direction as the Overflow plume. This can be thought of as part of a diapycnal overturning cell where some of the warm water approaching the Ridge is entrained into the descending plume, and at each successive cross section of the plume a reversal of flow direction occurs from northward to southward somewhere in the transition layer. At some point downstream in the gully the plume may warm enough to move diapycnally into the DS isopycnal layer across $\sigma_1 = 32.3$.

The Overflow plume in the gully between the western Wyville-Thomson Ridge and the Ymir Ridge has been examined by several expeditions and experiments. In Fig. 16(b) the near-bottom velocity vectors plotted include two measurements of strong down-gully flow. The stronger is a 24-day record from a mooring in 1140m water depth at the axis of the gully from a short mooring instrumented at 12m and 24m above the bottom (1973 data from J. Crease, personal communication, 1999; data used by Ellett & Edwards, 1978): plotted is the upper instrument average vector speed of 101cm/s. The lower instrument, not plotted, recorded 85 cm/s. Both instruments recorded overall mean temperatures of around 4.5°C, but daily averages ranging between 3.2 and 6.3°C. These measurements indicate the plume was very energetic, with considerable dilution of the NSDW characteristics by entrainment of waters that were both warmer and more saline; occasionally there were even occurrences of water warm enough to be considered DS isopycnal-layer water.

Ellett (1991) reported on a partially successful experiment to get more plume data. In the gully the plume forms a thin sheet along the flank of the Wyville-Thomson Ridge, with the densest waters occurring generally near the gully axis. The transition layer isotherms are usually banked uphill towards Faroe Bank, with occasional pockets of dense water up-slope. Two tall moorings were deployed, one at the axis of the gully in 1115m water depth, the other partly up the Wyville-Thomson Ridge flank in a depth of 710m, which was similar to the sill depth of the Overflow Notch in the Ridge, 60 km up the gully to the east. The deeper mooring was knocked down and failed to release, but when it eventually surfaced on its own, it broke apart before it could be recovered. The shallower mooring functioned, and with a second deployment yielded record lengths of 271 days. These data spanned the period during which the station group transect 75–79 illustrated in Fig. 8 was made along the crest of Wyville-Thomson Ridge, and two of Ellett's five meridional hydrographic sections across the site are shown in Fig. 11((b),(c)). The mean vectors for the full duration of the records from for the mooring's upper and lower instrument results are included on Fig. 16((a),(b)), and well define the overturning cell character of the gully flow regime. Near-bottom at 690m, a mean speed of 42 cm/s down-gully at a temperature of 5.7°C was recorded: the upper instrument at a depth of 270m was in the warm pool and showed a mean up-gully speed of 11.6 cm/sec and a temperature of 8.5°C. In Fig. 17 we show the time series information in the same format as the previously illustrated mooring records, but with the vector coordinate rotated so that the y-axis direction is 258°, i.e. the down-gully direction. The lower instrument record from 20m above the bottom, shows some events of very cold and dense water, and during 64 days out of 273 days total showed temperatures <5°C (Fig. 17(c)). During the majority of its record (190 days out of 273) it was sampling the DS isopycnal layer at ~5°–7.5°C, and the flow direction measured was down-gully, i.e. somewhat south of west.

The middle of the mooring's three instruments, at 540m sampled 150m above the bottom (Fig. 17(b)). It mostly sampled (238 of 273 days total) warm pool waters, with some dominance of up-gully flow over down-gully in that temperature class. Occasionally (26 of 273 days total) its measurements were in the DS isopycnal layer and the colder plume waters were strongly dominated by down-gully flow. The uppermost instrument mostly recorded warm pool temperatures and up-gully flow (Fig. 17(a)).

At this site the occurrences of DS isopycnal temperatures were associated with current measurements showing down-gully flow away from the crest of the Wyville-Thomson Ridge. The water involved seems to be the spillover plume water, containing either NSDW with considerable admixture of warm water through entrainment, or direct spillover of the waters in the Faroese Channels in the DS isopycnal range.

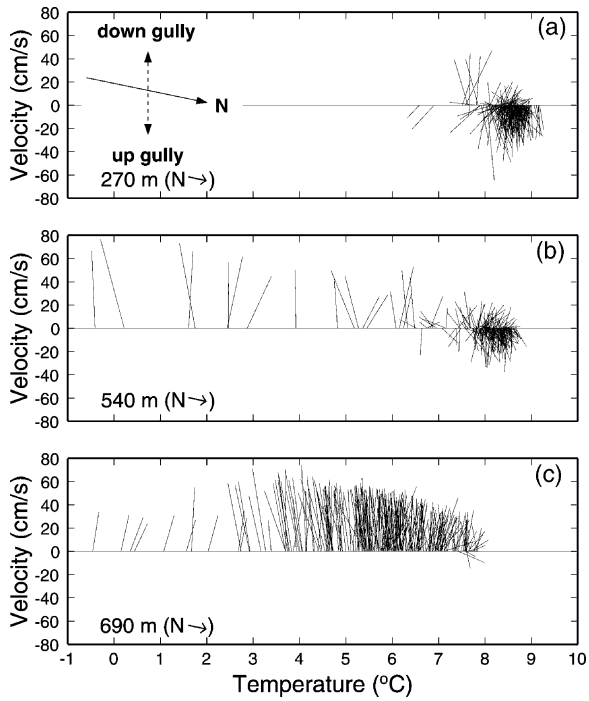

Fig. 17. Current meter data from a mooring (218 two settings) in the gully between Wyville-Thomson Ridge and Ymir Ridge deployed in 710 m water depth, September 8, 1987–February 29, 1988 and March 3, 1988–June 8, 1988, and instrumented at three levels, (a) 270 m, (b) 540 m, and (c) 690 m. Daily average current vectors are plotted as function of the daily temperature. Note the vector coordinate rotation.

On Fig. 16 we have included a vector from a long record (around 900 days between 1978 and 1983, Gould, personal communication, 1999), which is a composite of multiple settings of a mooring to the south of where the plume debouches from the gully, and water depths were between 1370m and 1475m. This mooring was located near station 188 in the along-plume section of Fig. 12, in a local topographic depression outside the gully exit that reaches 1600m and is separated by a 1300m sill to the southeast from the deeper Rockall Trough. The records show (Fig. 16(b)) there was substantial flow of 15.0 cm/s, at the depth of the near-bottom instruments (nominally 1400m) directed southeastward towards into the more open and deeper area of the northern Rockall Trough; the average temperature was 4.65°C, just colder than the DS isopycnal layer. At the mooring's nominal 1000m sampling level wholly DS isopycnal layer temperatures were recorded, averaging 6.6°C, with average current speeds of 10.3 cm/s directed at 202°. At this site, Figs. 12 and 18, station 188, the entrainment process had warmed most of the dense plume into the DS isopycnal layer, and that layer fills the water column below about 750 m. The section shown in Fig. 12, shows the layer had high oxygen and low silicate characteristics derived from the spillover source and the entrained waters. We will return in Section 6.3 to consider the impact of these plume waters on the characteristics of the DS isopycnal layer in the northern Rockall Trough. In Fig. 16(c) we have combined the occurrences of DS isopycnal temperatures at these two sampling levels into a single composite vector to emphasize that the fast westward flow of these waters through the gully exit between Ymir Ridge and Faroe Bank appears to turn south and to decelerate over the local depression outside the gully exit. In the northern Rockall Trough immediately south of the sill of this depression, the last vector on the plot shows weak southeastern flow in this layer.

Over the western part of the southern flank of the Wyville-Thomson Ridge there is ample evidence for

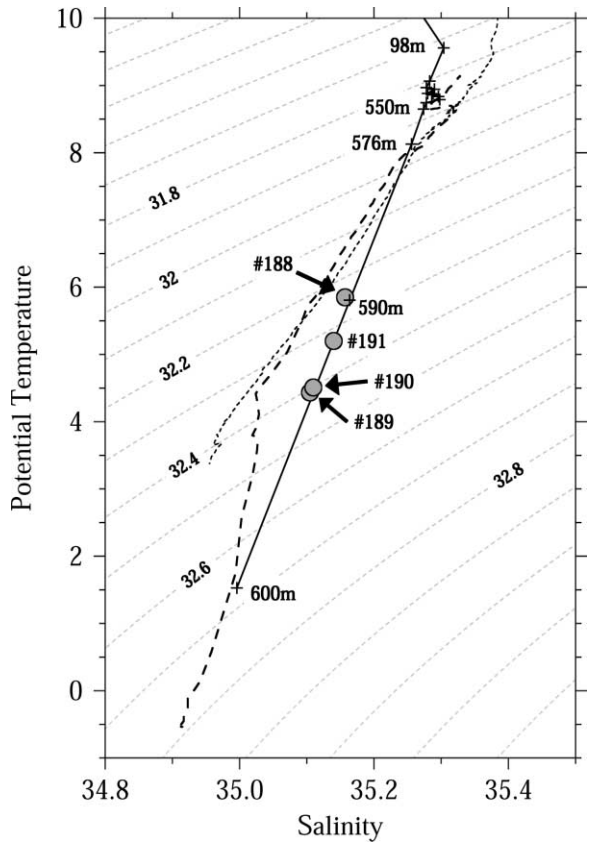

Fig. 18. Temperature-salinity relations for two sets of data from the Wyville-Thomson Ridge Overflow plume in the gully between Wyville-Thomson Ridge and Ymir Ridge. Solid black curve and crosses: Station 192 (Ellett and Roberts, 1973; see also Fig. 13); gray circles: bottom observations from stations 188–191 (Ellett and Roberts, 1973; see also Fig. 13); thick dashed line: station 77 (Saunders & Gould, 1988; see also Fig. 7); thin dashed line: station 86 at 58.4°N, 9.9°W (Saunders & Gould, 1988).

the continuity of the DS isopycnal layer between the Faroese Channels and the northern Rockall Trough. Direct current measurements show that where the layer continuity exists, it is associated with the plume of spillover water descending from the Ridge rather than flow rising towards the Ridge. Our overall conclusion from our examination of data from the Wyville-Thomson Ridge area is that the continuity of the DS isopycnal layer between the Faroese Channels and the northern Rockall Trough reflects the existence of the entraining plume of dense water, descending and flowing westward along the Wyville-Thomson Ridge flank that is confined to the gully between there and Ymir Ridge. That continuity is broken over the eastern flank of the Wyville-Thomson Ridge where the plume is not observed.

Iorga and Lozier (1999b) remarked from a 1998 draft of this paper that we “doubt the possibility of a 500m rise in the isopycnal that carries Mediterranean Water”. That is an incorrect reading in that our doubt focuses on the eastern sector; we have no doubt that there is continuity in this isopycnal surface over the western and central part of the Wyville-Thomson Ridge. However, we do argue that there is no reason to believe that there is any north-to-south-rising flow associated with that continuous surface as required by the deep source hypothesis. Instead, the evidence is that the tilt of the surface over the crest and southern flank of the Ridge, e.g. Fig. 11 is to first-order an indication of the vertical shear between the warm pool waters and the cold overflow waters, with to second-order a descending flow component for the plume.

The absolute velocity of the plume has a cross-isobar component representing this ageostrophic flow, oriented from lower to higher pressure.

3.5. Are there long looping branches from the North Atlantic Current in the eastern subtropical gyre?

The circulation of the North Atlantic Current (NAC) within the deep source hypothesis framework was not substantially described in R79, but as noted in Section 2, the circulation was very explicitly indicated by a set of absolute circulation maps extending from the sea surface through the main thermocline, to the deep and bottom waters. These maps are the primary basis for our cartoon of the circulation within the deep source hypothesis framework in Fig. 1((a),(b)). Here we call into question a key structural element of those absolute circulation maps.

The maps in R94 (its multi-paneled Fig. 8) define a NAC reaching through the main thermocline into the deep water to the depth of the crest of the Mid-Atlantic Ridge, nominally at 3000db. The maps show NAC branches turning to the south near 20°W into the eastern subtropical gyre. Then rather than continuing southward as part of this gyre, some again retroflect west of the Iberian Peninsula, and return northward as an eastern boundary current (and undercurrent) flow to the Rockall Trough. These are indicated as flows at each depth that are so parallel as to vertically integrate to a substantial transport loop (Fig. 9 in R94). The total water column transport shows a subtropical gyre defined as the difference between a gyre center transport stream function minimum of $<$60Sv (but $>$50Sv), and a ridge of maximum transport stream function $>$140Sv (but $<$150Sv) offshore of the eastern boundary, giving a gyre strength of between 80 and 100Sv. Between that ridge $>$140Sv and the eastern boundary where the stream function falls to 132Sv is a northward flow regime of amplitude greater than 8Sv (but $<$18Sv).

We agree with the structure of such looping flow for the upper water column, down to 500–800 m. In this shallow regime is a subtropical recirculation southward, representing the subtropical gyre, that is painted by winter convection influences from higher latitudes subducting southward with the wind-driven anticyclonic gyre flow (McCartney, 1982). Many measurements have documented poleward flow along the upper few hundred meters of the continental slopes of the Bay of Biscay (e.g. Swallow, Gould & Saunders, 1977; Pingree & LeCann 1989, 1990; Dickson & Kidd, 1986); it is this flow that transitions into the Rockall Slope Current (reviewed by Huthnance, 1986; also called the "Scottish Continental Slope Current" by Booth & Ellett, 1983). Above 500m, there is little contrast in water mass characteristics between these upper slope waters and the southward-flowing water offshore, e.g. sections in Fuglister, 1960. In particular, the poleward-flowing waters have present the same sort of convection influences mapped by McCartney and Talley (1982). We return to these upper water considerations in the shallow source hypothesis sections below.

In contrast with the upper 500m, we do not agree with the suggestion that there are such looping flow pathways below nominally 500m. Moving down in the water column beneath the depth of recirculating convection-painted waters, the MOW tongue makes its presence felt. For example, Lozier et al. (1995) mapped properties on the $\sigma_1 = 31.85$ surface near 650db west of Porcupine Bank, which deepens southward to 800db at the eastern boundary of the Bay of Biscay and the Iberian Peninsula, with salinity increasing from ~34.4 off Porcupine Bank to ~34.9 off the southern Iberian Peninsula. Any looping flow through this area has to gain salinity as it moves southwards into the MOW tongue, then loses salinity upon exiting the tongue in the northward flow along the boundary. R94 includes four circulation maps spanning the depth range for the MOW density levels of the deep source hypothesis, 800, 1000, 1500db, and $\sigma_{1.5} = 34.64$ ($\sigma_1 \approx 31.376$). These show southward turning branches from the mid-depth flow of the NAC south of Rockall Plateau, which turn east to converge into the eastern boundary, and flow back to the Rockall Trough as the eastern boundary undercurrent. To illustrate, Fig. 19 shows selected adjusted steric height contours from the R94 800db and 1000db circulation maps, in each case superimposed on R94 salinity fields for density surfaces near those pressure levels. The isobaric circulation maps of R94 do not include

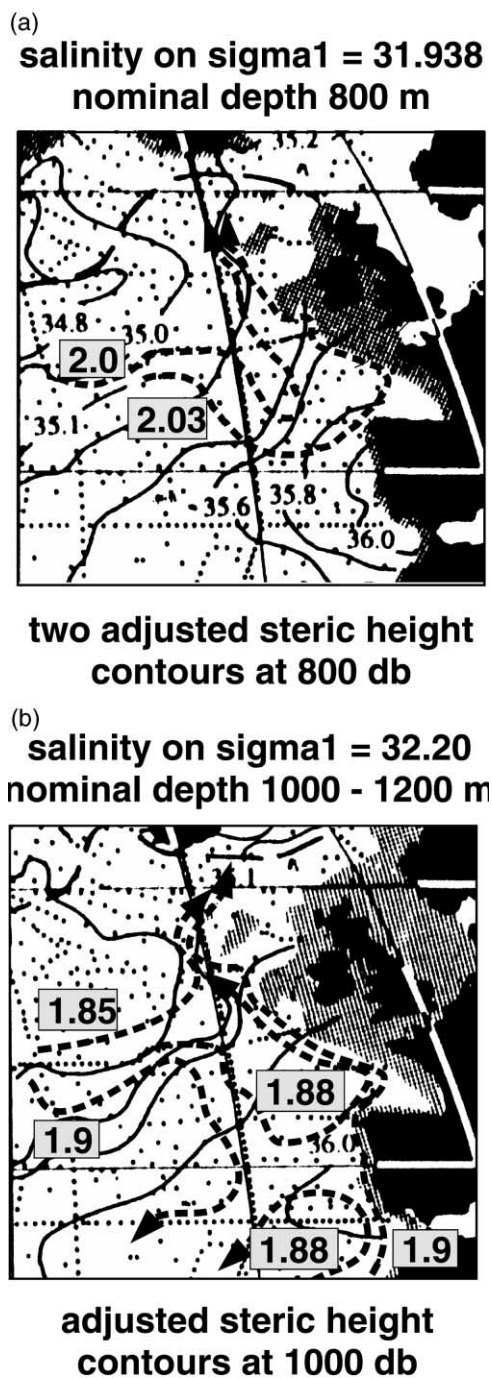

Fig. 19. Salinity and circulation composite maps adapted from Reid (1994) and other sources (a) salinity on 31.938 (solid), circulation on 800 db (dashed), (c) salinity on 32.20 (solid), circulation on 1000 db (dashed).

a representation of the movement of the northward rising DS isopycnal layer waters, so we have cartooned it in Fig. 1((a),(b)), showing the eastern boundary undercurrent rising in northern Rockall Trough to join with upper ocean waters crossing the Wyville-Thomson Ridge.

Along the southward flow segments of these looping pathways the salinity rises to very high values. Practically all of that acquired excess salinity is removed along the northward return flow segments adjacent to the eastern boundary. The waters following these hypothetical looping pathways thus undergo large meridional displacements (3000km path length) and large salinity excursions in order to achieve a small (600km) net northeastward displacement and small net salinity change. In Fig. 20 we further illustrate the implausibility of such pathways by contrasting the small temperature-salinity relationship differences between a typical Rockall Trough station (stars) and two stations (open and filled circles) spanning the width of the NAC flow as it approaches the Rockall Plateau from the southwest, with the large departure from any of these three stations that a station (diamonds) off northwestern Portugal exhibits. Oxygen and silicate characteristics (not shown) similarly show small differences for the direct flow path versus large excursions for the long looping pathways.

The absolute circulation maps of R94 are a combination of the geostrophic shear and a spatially variable barotropic field. The region where the loops are constructed has very little geostrophic shear, indeed at MOW depth can be described as relatively featureless. It is an area where the details of horizontal flow have been elusive, particularly north of the Azores Current and at the depth of the MOW salinity tongue (e.g. Saunders, 1982; Stramma, 1984; Klein & Siedler, 1989). It was the most uncertain aspect of a 1992 North Atlantic synthesis (Fig. 9(c),(d) of Schmitz & McCartney, 1993), and the comprehensive review of the North Atlantic warm water system (Krauss, 1986) indicated little about the northeastern subtropical area north of 36°N. The problem is elucidated best in Saunders (1982) where regional averaged geostrophic shear profiles show a shear reversal in the middle depth of the MOW tongue. Relatively speaking, this means that the pattern and sign of flow at MOW levels are strongly dependent on the applied barotropic field, while the upper ocean (and the deep water) are less dependent — usually amplitude only, not so much pattern or sign. Saunders (1982) chose to apply a wind-driven Sverdrup flow constraint to the full water column flow. For the observed shears, this yielded a three-layer system with an upper ocean (<850m

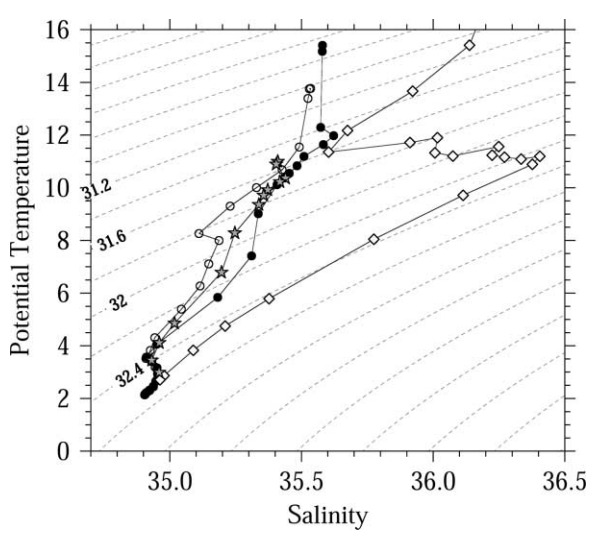

Fig. 20. Property-property plots comparing two NAC stations at 20°W, a Rockall Trough station, and a station from the undercurrent off Portugal. Circles: 47° 59.8′N, 20°_W (black); 50° 04′N, 20°W (white) (July 1988); gray stars: 54°N, 15°W (May 1988); white diamonds: 37.5°N, 10°W (June 1981).

in the calculations) subtropical gyre, including one NAC looping pathway reaching southward to 40–45°N, general southward flow below 1200m, and an intervening MOW layer with little systematic flow. just 0.5Sv flowing from the Mid-Atlantic Ridge towards the Iberian Peninsula near 40°N and turning northward. The fields in R94 require a more substantial barotropic component in this region, leading to stronger upper water looping flow, and penetration of those loops through the MOW rather than only above the MOW.

We reject the long looping pathways of the deep source hypothesis as unnecessarily convoluted, unlikely, and unnecessary for the explanation of the water mass characteristics of the Inflow. This conclusion is primarily dictated by the looping requiring large, but canceling, salinity excursions along the trajectories, and by the lack of shear signatures suggestive of such loops. A direct NAC branching from mid-basin into the Rockall Trough, with small progressive salinity changes adequately explains the water mass found in the eastern subpolar gyre, as will be elaborated on in Sections 4 and 5.

3.6. Summary of evidence against the deep source hypothesis

- Upper ocean silicates in the Norwegian Current are not elevated above values typical of the domain of winter convection. Occasional reports of observed slight elevations appear to be spurious when viewed against the regional data set.
- Within the northern Rockall Trough, isolines of silicate associated with the DS isopycnals do not rise across the Wyville-Thomson Ridge to cause enhanced silicate in the Norwegian Current.
- Within the Rockall Trough where the DS isopycnals are near 1000 m, the very slight enhancement of silicate that is measured can be attributed to a weak Antarctic Intermediate Water influence delivered by the North Atlantic Current.
- Along the eastern boundary of the Rockall Trough, the DS isopycnal layer remains at depth rather than rising to the north. The layer grounds out on the southern flank of the eastern third of the Wyville-Thomson Ridge.
- Over the central and western southern flank and crest of the Wyville-Thomson Ridge and the gully between there and Ymir Ridge, the DS isopycnal layer is continuous with those densities within the Faroese Channels, but direct velocity measurements show the flow within this layer being part of the outflow from the Channels rather than a rising flow moving into the Channels. That outflow is partly direct spillover of the Channels' water in the DS isopycnal classes, and partly warm water entrained into colder spillover waters lightening them into the DS isopycnal layer.
- The rising DS isopycnal over the southern flank of the Wyville-Thomson Ridge reflects principally the geostrophic shear between the upper warm pool and the spillover plume horizontal velocities, with an ageostrophic non-isobaric velocity reflecting the plume descent.
- The hypothetical extended southward branches of the NAC near 1000m, looping back northward along the eastern boundary, require large canceling salinity excursions, with the loops being mainly a construction from additive barotropic velocities. Without those additive components, a direct NAC flow into Rockall Trough with only slight salinity changes results.

4. The shallow source hypothesis

According to the shallow source hypothesis, part of the North Atlantic Current's eastward transport of warm and saline thermocline waters at mid-basin turns northward in the eastern basin to supply the Nordic Seas Inflow. This northward branching is, of course, an old concept in physical oceanography with a substantial literature beginning with Helland-Hansen and Nansen (1909), and Nansen (1912), and including the classic Sverdrup, Johnson and Fleming (1942). In the shallow source hypothesis we recognize the

tendency towards conservation of properties following the dominant geostrophic advection pathways, but we also recognize that water masses of both the directly convected layer and the waters immediately beneath the convection evolve downstream through air-sea exchanges. It is that transformation following the flow along pathways branching northward from the NAC that creates the thick warm pool waters that are delivered to the area south and west of the Wyville-Thomson Ridge and the Faroese Channels.

To develop more firmly the basis for the alternative shallow source hypothesis we show in Fig. 21 a set of upper ocean maps. These maps are based on a huge number of stations (updated from Lozier et al., 1995) compared to the limited data coverage used by the early pioneers reviewed above, and this allows some sharpening of the details of the property and circulation distributions that they first described so remarkably well from very sparse data. We have chosen 400db as a surface for mapping properties because seasonally this is a level that is penetrated by regional convection, so that the maps reflect the properties resulting from that transformation process. Since the crest of the Wyville-Thomson Ridge crest is nominally at 600m, we show a transport map for the upper 600 db to indicate the pathways that may contribute freely to the Inflow by horizontal flow. We have used a deep reference level, 2000 db, reflecting our belief that the entire thermocline shear and the upper deep water shear in the NAC reflect eastward flow across the basin branching to northward flow in the subpolar gyre and southward recirculation in the subtropical gyre. The transport map is only a semi-quantitative guide to the circulation, because of uncertainties of the barotropic flow, and for other reasons elaborated on in Section 4.2. In Fig. 21(a) the contour scaling is such that the numerical contour label is in Sverdrups for a Coriolis parameter value assigned as $10^{-4}s^{-1}$ (latitude ~43°N). Thus the subtropical gyre is indicated as the difference between an eastern boundary contour of 70 and western basin maximum exceeding 95 (at 35°N), with the difference of ~25 being multiplied by the ratio of sin 43° to sin 35° to yield 30Sv. We call your attention to these large-scale features of importance to the shallow source hypothesis:

- The upper ocean baroclinic transport map shows the NAC sweeping eastward from the Newfoundland Basin across mid-basin with a major branch wheeling northward to envelop the eastern boundary, Rockall Trough and Rockall Plateau (we use “to wheel” in this paper in the specific sense of a flow turning about a pivot point while maintaining its lateral structure). The deep referenced net flow in the upper 600m across 50°N is about 22Sv (which would be reduced by southward flow of the Labrador Current inshore of the 2000m isobath at the western boundary not included in this field).
- Isotherms, isohalines, and isopycnals at 400db are roughly parallel to NAC transport pathways, so that, to first order, Rockall Plateau regional temperatures and salinities exhibit a tendency towards conservation following the flow, and the water mass characteristics of the Rockall Trough and Plateau area traced upstream to mid-ocean and the Newfoundland Basin.
- To second order, there are systematic deviations from parallelism of transport and property contours. The deviations are largest along the south and east side of the bundle of NAC transport contours. Oxygen and density values progressively increase following the NAC pathways branching northward into the eastern subpolar gyre, and temperature and salinity values decrease. These cooling, freshening, “densification” and oxygenation trends reflect the progressive action of winter convection following the flow, an evolution called subpolar mode water production.
- The action of convection in homogenizing the upper ocean is visible in the steep decline of potential vorticity along the right side of the NAC, from $<90 \times 10^{-12}$ $m^{-1}s^{-1}$ at mid-basin to $<30 \times 10^{-12}$ $m^{-1}s^{-1}$ northwest of Ireland. It is the vertical homogeneity associated with low potential vorticity that leads to the characterization “warm pool” for the waters south and west of the Wyville-Thomson Ridge, Faroese Channels, and Iceland-Faroe Ridge. These low potential vorticity values contrast with the elevated values along the axis of the Gulf Stream (>130) and its branches southeast of Newfoundland into southward recirculation, and the northward flow initiating the North Atlantic Current, both of which are highlighted by the >100 shading.

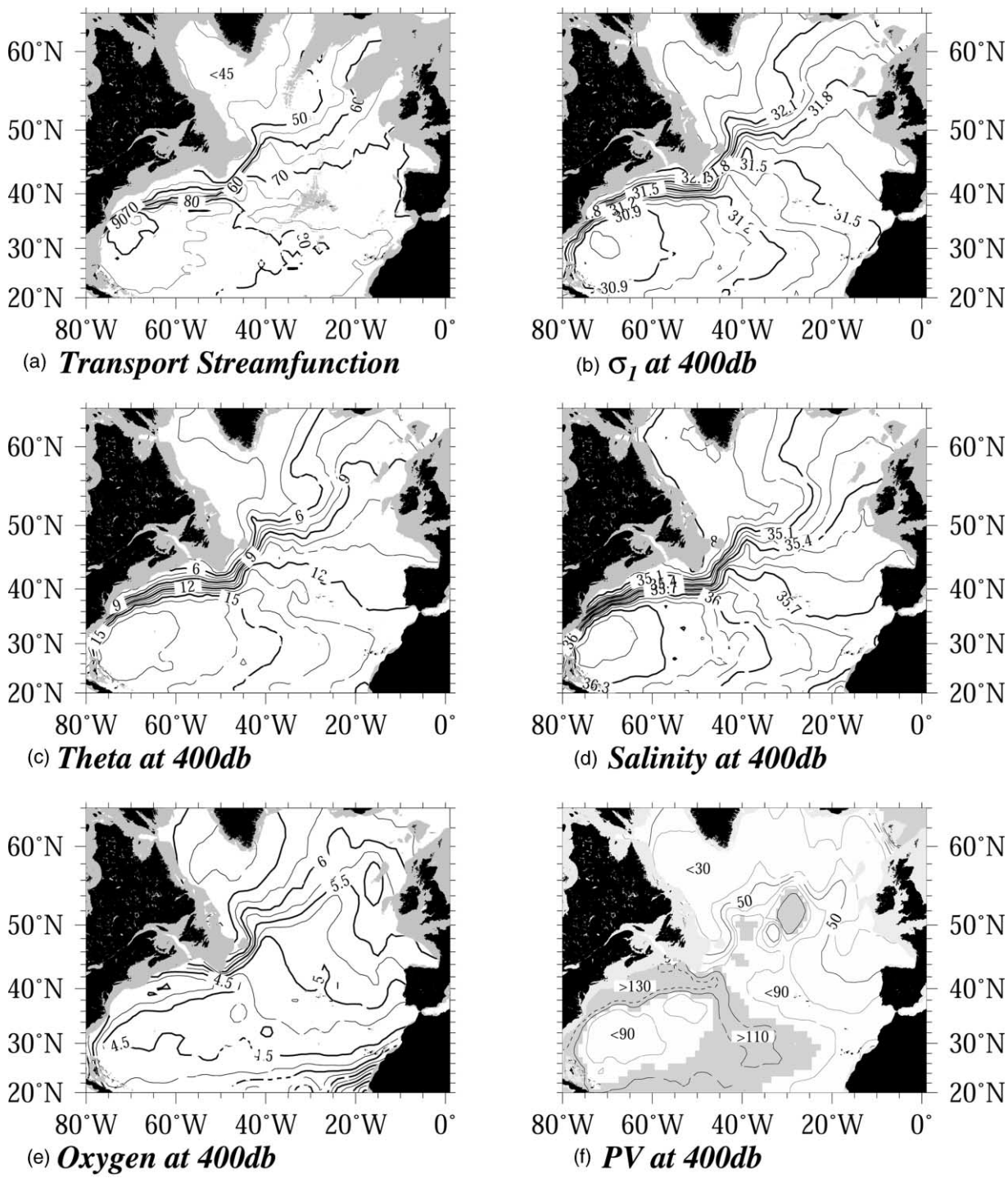

Fig. 21. Upper ocean property distributions (a) transport stream function, 0–600 db relative to 2000 db reference level, (b) 400 db potential density referenced to 1000 db, (c) 400 db potential temperature, (d) 400 db salinity, (e) 400 db oxygen, (f) 400 db potential vorticity [10^{-12} $m^{-1}sec^{-1}$].

- Northward of 56–58°N some upper ocean baroclinic transport contours, e.g. 55, 60, 65 $\times 10^5$ kg s^{-2}, shift from meridional orientation to northeastward, indicative of the flow towards the Wyville-Thomson Ridge, Faroese Channels, and Iceland-Faroe Ridge.
- Near the eastern boundary between 50°N and the Gulf of Cadiz somewhat warmer and more saline waters exist, but in an area of weak baroclinic circulation compared to the NAC. Note the low baroclinic gradient defined by the space between the 75×10^5 kg s^{-2} contour's extension ESE from the Newfoundland Basin past the Azores to the Canary Islands, and the 70×10^5 kg s^{-2} contour extension from the Newfoundland Basis ENE to the Goban Spur and then south past the Bay of Biscay and the coast of the Iberian Peninsula. At 40°N this interval represents about 5Sv southward flow, but spread over a considerable width.

A variety of studies have indicated that the NAC is a deep current system, which is the basis for our use of 2000db as the reference level for the upper water transport map of Fig. 21(a). This choice gives eastward transport of Labrador Sea Water (LSW) within the NAC in mid-basin, as is required by the Talley and McCartney (1982) interpretation of the mean LSW distribution and the Sy, Rhein, Lazier, Koltermann, Meincke, Putzka and Bersch (1997) description of eastward advection of LSW transients. The choice of a deep reference level, at least beneath the LSW, is consistent with the interpretations by Krauss (1986), Sy (1988), Sy, Schauer and Meincke (1992), McCartney (1992), Cunningham and Haine (1995); Pollard, Griffiths, Cunningham, Read, Pérez and Ríoz, 1996 and the synthesis by Käse and Krauss (1996). The wheeling of the NAC flow from eastward to northwards in our climatological average field is not significantly different in pattern or amplitude from that of a regional synoptic survey in 1991 (Pollard et al., 1996, repeated here as Fig. 1(e)). It is also similar to the fields resulting from a recent inversion of an eastern basin set of hydrographic sections (Fig. 1(f)) (Paillet & Mercier, 1997), and a whole ocean inversion by Isayev and Levitus (1995).

The only substantive disagreements between our upper water column transport map (Fig. 21(a)) and R94 adjusted steric height maps at the sea surface, 250db and 500db involve the long southward-looping pathways near the eastern boundary discussed above in Section 3.5. Because our transport field is based on a 2000 db level-of-no-motion, the eastern "edge" of the mapped field is the intersection of 2000db with the European continental slope. The poleward flow of the upper several hundred meters over the upper continental slope is inaccessible to this treatment, and occurs east of the mapped field. In the upper ocean schematic of Fig. 1(c), we have included this poleward flow along the upper continental slope in the Bay of Biscay and the Rockall Trough, a circulation element well documented by direct current meter and surface drifter measurements (e.g. Swallow et al., 1977; Booth & Ellett, 1983; Dickson & Kidd, 1986; Huthnance, 1986; Booth & Meldrum, 1987; Huthnance & Gould, 1989; Pingree & LeCann 1989, 1990). At mid-basin, our use of a deep reference is in agreement with R94 maps showing NAC flow extending as deep as 2500 db. Our transport function is inadequate for representing the western boundary current in the subpolar gyre, because so much of that occurs inshore of the 2000m isobath. Thus in the west, the R94 maps give a more complete picture. The transport map (Fig. 21(a)) has an Azores Current defined by the 75 and 80 $\times 10^5$ kg s^{-2} contours, representing about 6Sv. A relative plateau found between there and the main NAC flow north of 42°N is a common feature in regional circulation studies. A clear signature of southward subducting subpolar mode water is seen in that area (McCartney, 1982), limited in southward extent by the Azores Current (Robbins, Price, Owens & Jenkins, 2000).

The main action on the transport map is the northward wheel of most of the NAC contours. The changes in water mass characteristics along such wheeling pathways are very small compared to the long looping pathways in the R94 schematics. In Fig. 20 we deliberately selected two stations spanning these wheeling NAC pathways at 20°W to emphasize the comparatively small water mass changes that occur along the direct baroclinic pathways from there (southwest of Rockall Plateau) to the Rockall Trough. That is a stark

contrast to the large property changes en route required along the pathways of the deep source hypothesis, which depart on long excursions away from and back to the baroclinic stream function contours.

We have chosen to illustrate flow with a mass transport function for the upper layer rather than a velocity stream function for one or more surfaces. While there is considerable vertical shear of the geostrophic flow of the NAC across the upper 2000m, there is very little veering with depth. Maps of dynamic height on 0, 200, 500, 800, 1000 and 1500db, all relative to 2000db, show parallelism of the NAC isopleths to first order, e.g. Fig. 22. Thus, while our map shows the baroclinic transport of the upper 600db, relative to 2000db, the patterns of baroclinic flow at levels within the upper 600db and for the rest of the main thermocline essentially parallel this upper transport field. The small veering that does exist will be subsequently discussed in an appropriate context in Section 4.3.

The maps and other evidence lead to our version of the shallow source hypothesis: The Nordic Seas Inflow is supplied from the warm pool of waters enveloping the Rockall Trough and Plateau, including the upper continental slope of the Trough. This thick warm pool in turn is supplied by a northward turning branch of the NAC joining the Rockall Slope Current, with upper waters progressively cooled, freshened, oxygenated, and made denser by the action of air-sea exchanges following the flow. This is schematically illustrated in Fig. 1(c) as a direct flow of NAC waters towards the Rockall Plateau area, which splits into northward flows through the Rockall Trough, including the Rockall Slope Current, through the Hatton-Rockall Basin, and along the western flank of the Rockall Plateau (Hatton Bank), and thence to the area immediately south of the Iceland-Faroe-Scotland Ridge. There they can provide the warm Inflow to the Nordic Seas, both north of the Faroe Islands and through the Faroe-Shetland Channel. This represents a NAC that completes its divergence into northward and southward flows at the eastern boundary rather than offshore of that boundary as required in the deep source hypothesis (Fig. 1(a)). Under the latter hypothesis a “space” is required where the upwelling eastern boundary undercurrent pushes the NAC branches out of the way in order to make its way northward and upward to the Wyville-Thomson Ridge crest. We now explore some aspects of the flow and transformation processes producing the warm pool waters.

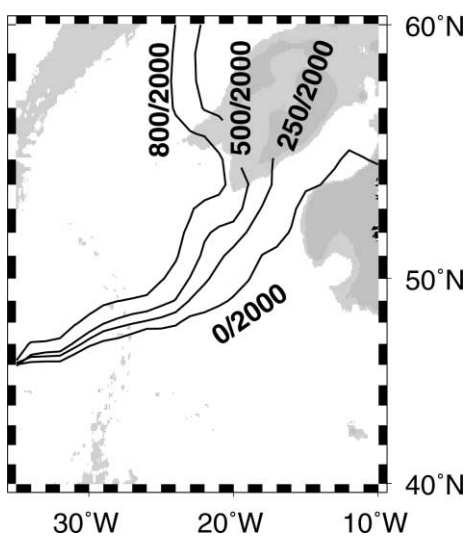

Fig. 22. Dynamic height contours in the northeastern North Atlantic for several pressure levels, all referenced to 2000 db, and selected so as to pass through a common geographic point south of Rockall Plateau.

4.1. The role of transformation in upper ocean circulation and setting water mass characteristics

We have constructed a composite vertical section (Fig. 23) roughly following the NAC pathway from the Newfoundland Basin eastwards across the Mid-Atlantic Ridge, and the northward NAC branch pathways in the eastern subpolar gyre through the Rockall Trough into the Norwegian Current (see Fig. 4(a),(b) for positions). The stations have been selected as lying on the subtropical side of the eastward flow regime of the NAC, as evidenced by the lower main thermocline (e.g. ~4°–7°C) remaining at depths near 1km or deeper all along the section. This layer outcrops on the northern side of the NAC in the central subpolar gyre, and the layer slope is a signature of the geostrophic shear of the NAC. In the northeastern area, we selected stations near the easternmost of the three pathways for NAC water flow branching northward in Fig. 1(c), as the Rockall Trough pathway is most relevant to the contrast of the two hypotheses for Inflow origin. The section is not a composite of random stations scattered in time, rather it is comprised of segments from four synoptic sections appended to each other. For this and other reasons discussed below the section is not strictly aligned with a streamline of the broad warm water flow path. Within the synoptic segments of the composite section, there are visible (Fig. 23(a)) lower thermocline undulations of order 100–200m, compared to the order 500m rise across the NAC; these are indications that the NAC wanders laterally across the linear segments of the section by a fraction of the NAC width.

In Fig. 23, the NAC enters from the left, including transport in all the density classes $\sigma_1 \leq 32.4$, and considerable water in the lighter classes $\sigma_1 \leq 31.7$, collectively with average temperature of roughly 12°C and salinity of about 35.5. Much of that lighter transport has disappeared by the mouth of the Rockall Trough at 54°N, partly through circulation to the south in the eastern limb of the subtropical gyre (discussed in Section 4.2), and partly by the transformation into denser water. This along-path transformation of water is the so-called “subpolar mode water” (SPMW, McCartney & Talley, 1982). A defining characteristic of SPMW is its weak vertical temperature and other property gradients resulting in a visually “thick” layer. These weak gradients reflect persistence of the vertical homogeneity imparted by winter convection. The most appropriate indicator of SPMW is its relative low potential vorticity (hereafter PV) (Fig. 23(f)). We have added shading to indicate the low PV waters on the other property sections of Fig. 23, and have similarly treated many other section figures in this paper, including the eastern boundary section in Fig. 3. At 54°N, ~ 2000km along the section ordinate, the PV minimum core is near $\sigma_1 = 31.7$, and aside from a seasonal thermocline atop the water column, we infer that convection has consumed all the lighter waters upstream along the section producing the thick layer of weak vertical stratification. Moving northward along the section to the station at the Wyville-Thomson Ridge crest, station 58 near 3150km, the continuing transformation has chewed downwards into the thermocline to $\sigma_1 = 31.9$ yielding the warm pool waters of the northern Rockall Trough and the Banks and Basins of the Rockall Plateau complex.

It should be noted that there is some interannual variability of winter convection density and depth that results in small variability of the regional SPMW characteristics. Generally speaking these are on the order of a few tenths of a degree temperature for the local PV minimum. Ellett and Martin (1973) remarked that in their repeat section near 56°N “beneath 150m depth a band of low variability extended across the section, being least in the vicinity of the Irish continental slope”. Their illustration (their Fig. 6(a)) of standard deviation shows the layer is characterized by temperature standard deviations of <0.2°C, centered near 500m. This relatively small variability reflects the well-known climatic stability of mode waters (e.g. Warren, 1972; McCartney & Talley, 1982). In Ellett and Martin (1973), their Figure 7 showed similar low

Fig. 23. Property distributions along a section following the eastward NAC pathway across the basin and northward through Rockall Trough (see Fig. 4a for location), as function of depth, upper panels, and of density, lower panels. Low PV is shaded. The section is comprised of four synoptic sections: *Gauss* 1993, *Oceanus* 1988, *Knorr* 1996 and Bord Est 1988, with additional historical data at the northern end. (a) depth and sigma^{-1}, (b) potential temperature, (c) salinity, (d) oxygen, (e) silicate, (f) potential vorticity [10^{-12} m^{-1}sec^{-1}].

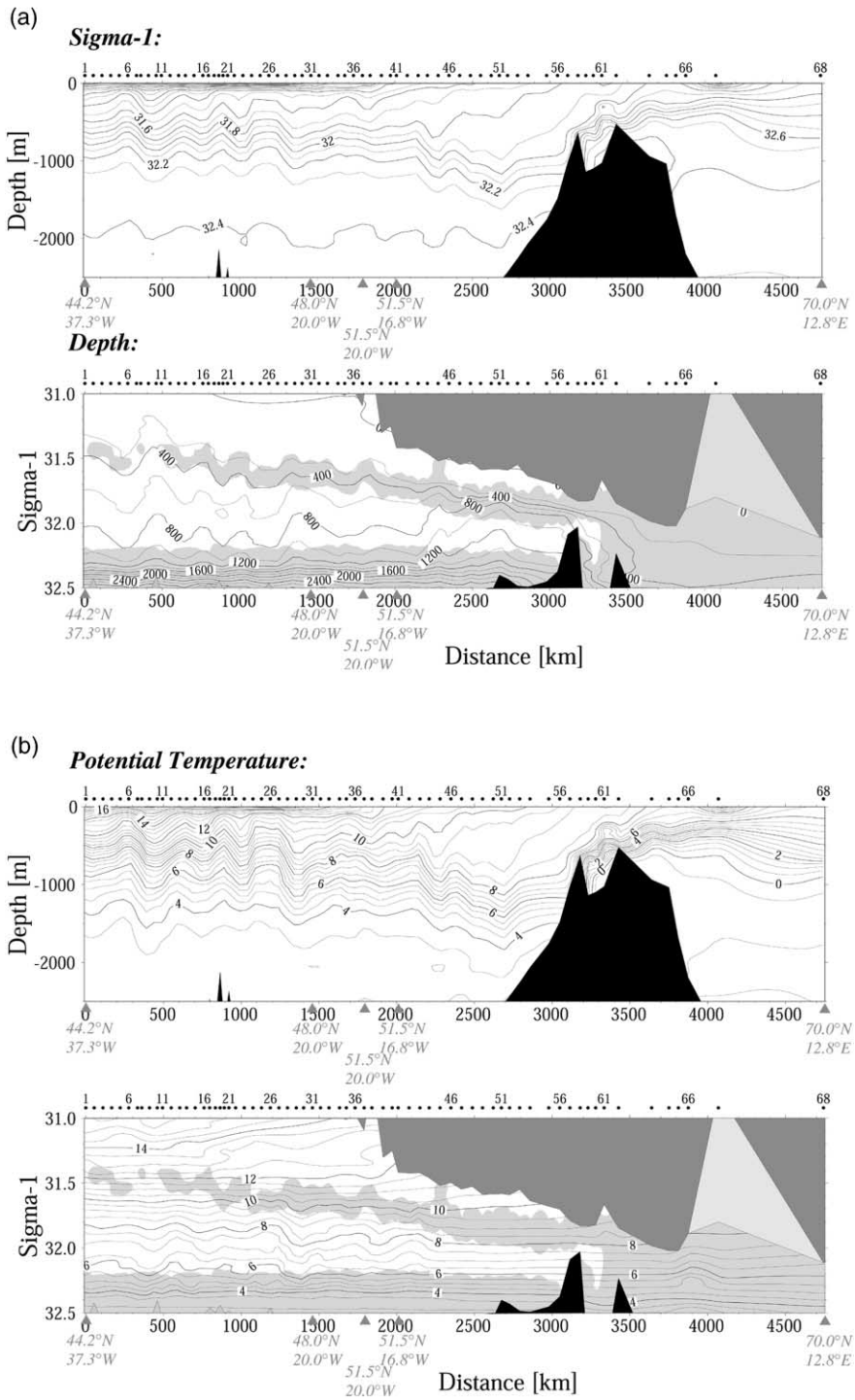
(a)
Sigma-1:
Depth [m]
Depth:
Sigma-1
Distance [km]
(b)
Potential Temperature:
Depth [m]
Sigma-1
Distance [km]

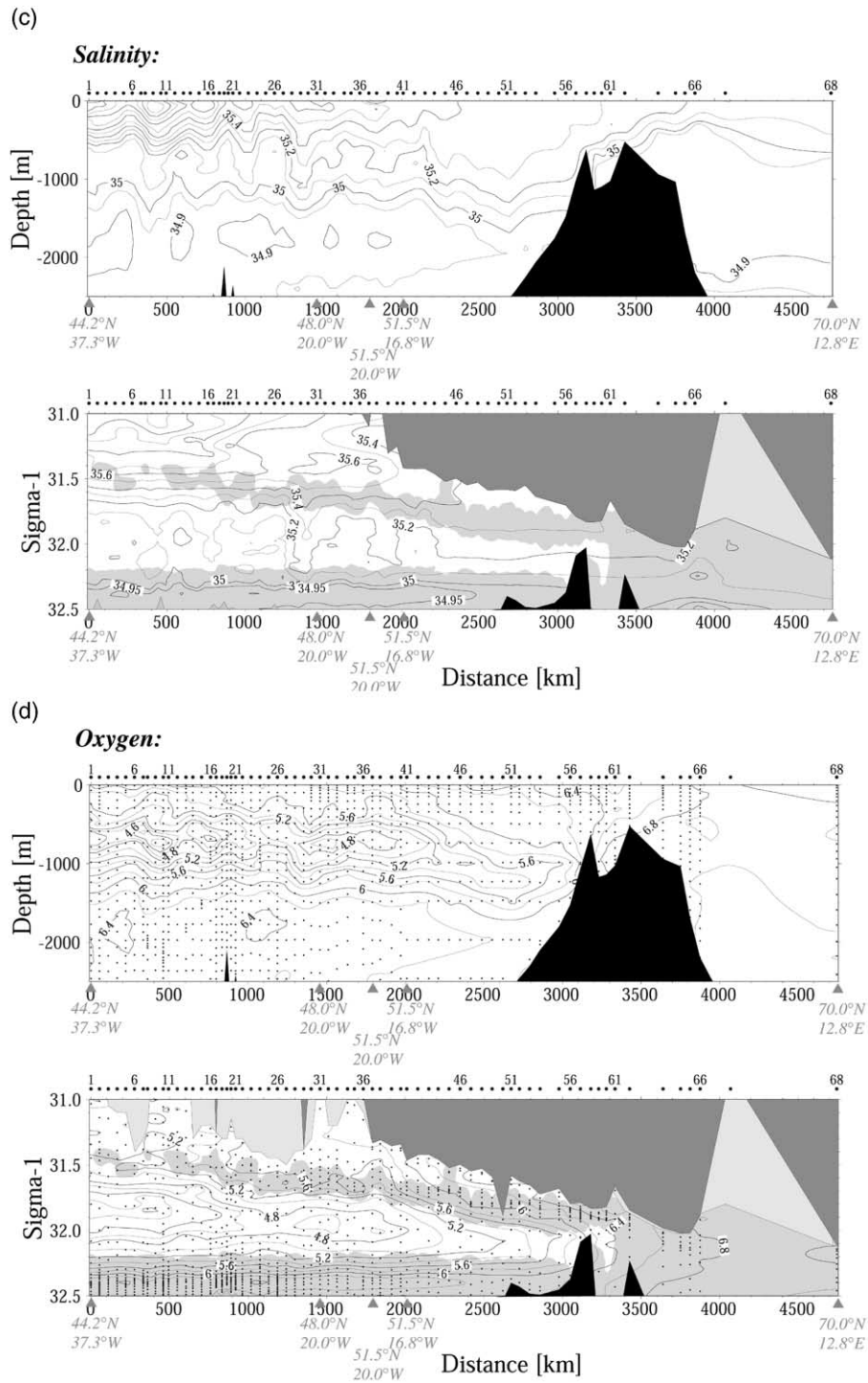

Fig. 23. (*continued*)

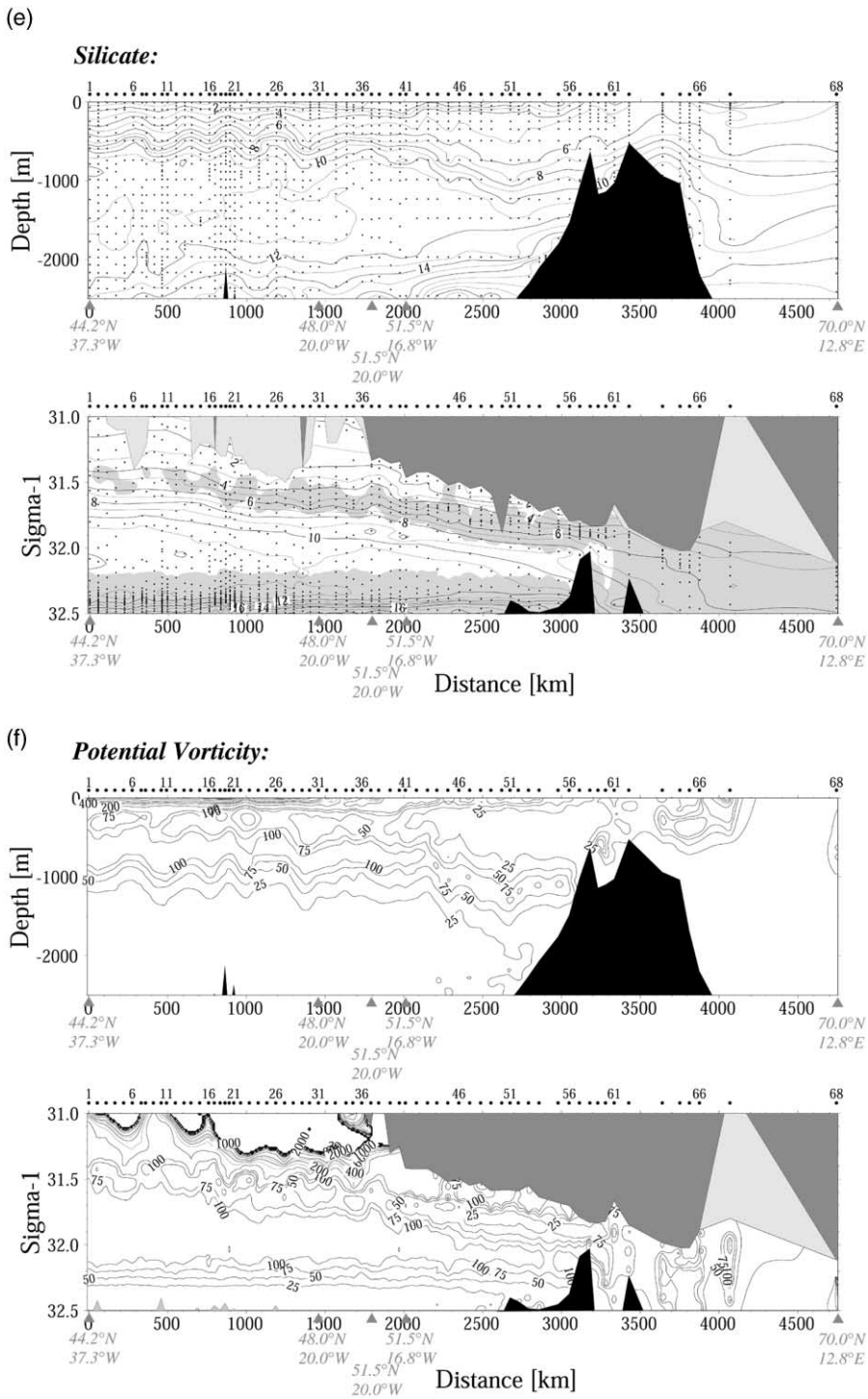

Fig. 23. (*continued*)

amplitude temperature variability at station "FBL" near the eastern boundary immediately south of the Wyville-Thomson Ridge (59.5°N, 7.1°W). Pollard, Read and Leach (2000, and personal communication, 2000) report similar stability; between 1975 and 2000 the average temperature of the upper 800m between Rockall Bank and the continental slope near 57°N when adjusted for the seasonal cycle exhibited a standard deviation of only 0.19°C about the mean value of 9.15°C, with much of that variability being a warming trend for 1996–2000. These temporal variations are small viewed against the scale of the progressive evolution of SPMW following the flow, e.g., the isotherm distribution of Fig. 23(c).

The along-section cooling of the SPMW reflects a stage of the overall warm-to-cold water transformation of the northern North Atlantic. The total high-latitude transformation nominally north of 50°N, was estimated to be about 15Sv by McCartney and Talley (1984) (apportioned roughly equally between the subpolar gyre and Nordic Seas transformations) and at 13Sv in the North Atlantic in a synthesis by Schmitz and McCartney (1993). In whole ocean inversions presented as zonal averaged meridional sections, such warm to cold water transformations show up as the upper limb of the meridional overturning circulation, with net northward flow in light density classes progressively "descending" into denser classes at higher latitudes. Two differently initialized inversions of the IGY (1957) "48°N" section by Roemmich (1980) were rather indeterminate as to the amplitude of the overturning, yielding estimates of 22.1Sv and 8.9Sv; but after constraining these by independently estimated heat flux divergences between 48°N and other locations these results changed to 24.4 and 25.5Sv. Two full North Atlantic inversions described by Wunsch and Grant (1982) gave 13.7Sv and 13.2Sv for the net northward flow of the overturning circulation at 50°N. Wunsch (1984) estimated 16.9Sv at the IGY "48°N" section, when a constraint of maximizing heat transport at 24°N was applied, and between 10Sv and 15Sv when that flux was minimized. In Macdonald (1998), (Figure 2) in an inversion of a global data set indicated 27Sv warmer than 3.5°C flowing northward across a second realization of the 48°N section 1982, an estimate higher than these others for unknown reasons. A more recent global inversion by Ganachaud (1999), using the 1993 occupation of the 48°N section, indicated an overturning intensity of 19Sv. Koltermann, Sokov, Tereschenkov, Dobroliubov, Lorbacher and Sy (1999) estimated 9.2Sv, 18.9Sv, and 14.7Sv for, respectively, the first, second and third realizations of the 48°N section, with a focus on the decadal changes of overturning intensity.

We review here some terminology involved with the physics of water mass formation and transformation, see Woods (1985), Cushman-Roisin (1987), Speer and Tziperman (1992), Marshall, Nurser and Williams (1993) and Qiu and Huang (1995) for more complete treatments. The mixed layer instantaneously entrains mass from or detrains mass to the pycnocline depending on the sign of the sum of the instantaneous rate of change of mixed layer depth, the vertical velocity across the base of the mixed layer and the horizontal flow "across" the mixed layer base, if the base is sloping. The latter term is called the lateral induction term, the dot product of the horizontal velocity vector and the horizontal gradient of mixed layer depth. Annual average exchange is calculated from the time average of that sum, either an Eulerian calculation at a point or an integration along a Lagrangian trajectory for a year, yielding a net annual subduction rate (see Qiu and Huang for discussion of differences of definitions of annual subduction). A positive subduction rate represents a net delivery of mixed layer waters to the pycnocline (net detrainment), a process dominant in the interior of the subtropical gyre. Negative subduction rate reflects net entrainment into the mixed layer, and that has been called "obduction" by Qiu and Huang (1995). The entrainment process is dominant along the Gulf Stream and NAC and within the subpolar gyre. Marshall et al. (1993) and Qiu and Huang (1995), working with climatological mixed layer data and deep referenced geostrophic circulation of the mixed layer, demonstrated that the lateral induction term dominates the vertical velocity term within the mixed layer response to the surface fluxes in the entrainment domain. They estimated, using somewhat differing formulae, rates reaching 250–350 m/y along the Gulf Stream and NAC. Marshall et al. (1993) additionally used climatological sea surface data to demonstrate the dominance of heat flux over evaporation minus precipitation and Ekman transport contributions to the surface buoyancy forcing of mixed layer density. The relevance of these concepts and estimates to the present work is that the fields they present

show that the NAC pathway, including the northward branching into the subpolar domain, dominates the entrainment domain, implicating the obduction process as that setting the SPMW transformation following the flow. That transformation is a buoyancy-driven entrainment reflected in the downstream deepening of winter convection, the densification of the mixed layer, and dominated by the horizontal flow across sloping isopycnals. Note that the mixed layer entrainment can involve both lighter and heavier waters; the former is transformed into the layer in the lateral induction term involving the cooling downstream of the lighter waters, the latter moving vertically "upwards" from the denser waters into the mixed layer that deepens and increases in density, down-stream.

A regional study by Paillet and Mercier (1997) focused on circulation and transformation in a domain restricted to the east of 35°W and south of 54°N. It improved on the above transformation studies because it involved a full water column calculation with a dynamically constrained reference level in an oceanic data inversion. Fig. 1f shows the total transport in the upper 800m from their calculation. A transport of 36Sv above 800m enters the northern domain from the west, and an additional 9Sv enters via the Azores Current in the southern domain. Of that 36Sv, 10Sv represents cold fresh subpolar gyre waters recirculating across the NW corner of the domain, and the other 26Sv represents warmer subtropical waters, which divides into a northward wheeling branch of 15Sv destined to envelop the Rockall Plateau and Trough, a residue of 2Sv that diverges into the >800db layer, and a southwards recirculation of 9Sv that joins with the Azores Current in a curious fashion (see Jia, 2000 and Özgökmen, Chassignet & Rooth, 2001, for an exploration of that interaction — the Azores Current's structure may be partly defined by the entrainment of warm waters into the MOW plume in the Gulf of Cadiz). The northward wheeling NAC segment geographically corresponds to the first 45 stations of our NAC pathway section (Fig. 23).

An estimate of 11.9Sv of buoyancy driven entrainment within the domain resulted from the Paillet and Mercier (1997) dynamically-constrained inverse calculation of hydrographic data, which is the domain's net entrainment into the winter mixed layer that is dominated by the lateral induction process and is also their estimate of SPMW formation within their domain. Largest obduction rates, >400 m/y occur in a patch in the northern part of their domain, with peak value of >600 m/y occurring near 52°N, 20°W corresponding to the area where winter mixed layer depth increases steeply to the northeast, combining with the horizontal flow field to give a large lateral induction into the mixed layer. About 2.5Sv of this SPMW formation subducts southward (Section 4.2), supplying the low PV tongue observed in the eastern subtropical gyre (McCartney, 1982). The remaining 9.4 Sv they indicate as divided (in unspecified proportions) between one component that passes northward into the Rockall Plateau area, and another that recirculates southward and restratifies into lighter layers through the action of air-sea fluxes farther south. We infer from their figures that the northward pathway is the dominant pathway for the rest of the obducted water, given their estimated transport pathways and strengths, Fig. 1f. Recirculating subducted SPMW representing 4Sv of the estimated 10Sv of subtropical gyre recirculation across 40°N, and other figures in their study suggest the other 6Sv of southward gyre flow is not from the obduction regime in the north but rather represents a southward turning of part of the 26Sv entering the domain from the west, a trajectory that may be essentially adiabatic flow beneath the subducting water, rather than restratification of waters above the subducted layer. Therefore, taking 9.4Sv as an upper bound on the SPMW transformation following the northward wheeling NAC branch, we infer that up to 63% of their estimated total delivery of 15Sv of warm subtropical waters to the eastern subpolar gyre in the upper 800m represents warmer waters transformed to SPMW in the northeastern subtropical gyre domain south of 54°N. Stated another way, 37% or more of the 15Sv of northward branching NAC water passes through the domain essentially adiabatically, whereas 63% (or less) is transformed from lighter density classes to heavier within the domain dominated by the lateral induction process of horizontal flow across sloped isopycnals. In our own transport map (Fig. 21(a)) the northward flow across 54°N in the upper 600m east of 25°W is about 12Sv, a somewhat smaller value than that estimated by Paillet and Mercier, reflecting our restriction to the upper 600db. There is a good mutual agreement between the Paillet and Mercier (1997) transformation estimate, which

infers the required buoyancy forcing from the oceanographic data, and the estimates of the required ocean transformation that results from applying estimated buoyancy forcing in the same domain (Marshall et al., 1993; Qiu & Hang, 1995), keeping in mind the formulation differences for the various annual average entrainment estimations (Paillet & Mercier, 1997, use the formulation of Marshall et al., 1993, not that of Qiu & Huang, 1995).

The 9.4Sv can be viewed both as the first stage of the total high-latitude transformation and as a "preconditioning" of the subtropical gyre waters being delivered to the eastern subpolar gyre. Additional transformation occurs in the subpolar gyre and Nordic Seas as that 9.4Sv continues its buoyancy driven increase in density, and growth in transport as a result of continued entrainment (dominated by lateral induction). That is inferred because the 9.4 Sv of transformed subtropical waters delivered to the subpolar gyre does not return southward as warm light waters but rather as the cold dense waters of the lower limb of the overturning circulation. Continued convection will chew downwards through denser levels north of the Paillet and Mercier domain along pathways around the Nordic Seas to the dense overflows and around the subpolar gyre to the Labrador Sea convection area. In Fig. 21(c), the 400db temperature, a good indicator of the local winter convection temperature of the SPMW, is about 10°C at 54°N. The part of the northward flow across 54°N that forms the Inflow still has about 2°C of cooling to undergo before crossing the Iceland-Scotland Ridge. The part that turns westward in the subpolar gyre undergoes about 6°C additional cooling on its way to the Labrador Sea. Using the estimates of overturning cell strength above, total high-latitude transformation of 13–19Sv, then northward of 54°N an additional transformation of 4–8Sv is expected to be added to the 9.4 Sv estimate. For example, in their solution, part of the 15Sv delivered to the eastern subpolar gyre, 15–9.4 (or less) Sv = 5.6 Sv (or more), is denser than the waters that undergo obduction within their domain. Continued buoyancy forcing causes a continuing increase in density of the winter mixed layer, and lateral induction of that transport. The Macdonald (1998) estimate of 27Sv of total high latitude overturning strength near 50°N is problematic, since it requires the addition of about 18 Sv of higher latitude transformation. Qiu and Huang (1995) included as a byproduct of their calculations an estimate of 23.3Sv total North Atlantic obduction, with 13.3Sv of that corresponding to the SPMW transformation of the subpolar regime and the rest being subtropical mode water transformation.

4.2. Subduction: limited southward recirculation of transformed NAC waters

In the Paillet and Mercier (1997) diagnosis of the eastern basin circulation and transformation (Fig. 1(e)), an estimated 2.5Sv of the warm subtropical waters transformed to SPMW subducts southward with the subtropical gyre interior circulation. This represents about 30% of the illustrated subtropical gyre recirculation across 54°N above 800m. Earlier work has inferred this circulation from the low-PV character of the subducted waters (McDowell, Rhines & Keffer, 1982; McCartney, 1982; McCartney & Talley, 1982; Pollard & Pu, 1985; and Pollard et al., 1996). In the eastern boundary section (Fig. 3), the impact of this southward flow of SPMW is visible as the fairly isopycnal low-PV layer near σ_1 = 31.5–31.7 extending southward from station 13 near the southern tip of Porcupine Bank, weakening southward but still detectable off the Gulf of Cadiz. This density range corresponds to winter convection immediately west of Porcupine Bank and Goban Spur. Paillet and Arhan (1996) estimated that a winter deep mixed layer beginning a southward journey near 45°N, at expected gyre velocity, might be exposed to convection again the following winter near 43–44°N, but thereafter would be remain permanently submerged. A meridional section near 20°W by Tsuchiya et al. (1992) showed the associated PV minimum layer was detectable to 27°N, and a section at 36°N discussed by McCartney (1982) showed the layer extending westward to about 25°W. Robbins et al. (2000) suggested that the Azores current may delimit the SPMW influence in the southwest; a finding similar to McCartney's (1982) discussion of limited subtropical recirculation of mode waters in the northeast North Atlantic. This SPMW contribution to the overall subtropical recirculation takes place in the area of weak baroclinic flow on the transport map of Fig. 21, between the 70×10^5 kg s^{-2} contour

west of the Iberian Peninsula and the 75×10^5 kg s^{-2} west of the Azores; the difference representing about a flow of 5.3Sv in the upper 600 m. The recirculating SPMW appears as a low-stratification layer above the MOW, and because the warmer subtropical waters above are more saline than the SPMW, as is the MOW below, the recirculating SPMW is often to be seen as a salinity minimum. Neither the PV nor the salinity of the SPMW is conserved as it flows southward.

It appears from the climatological database that the SPMW is not only an extensive pool in the subtropical interior off the Bay of Biscay, and northward to off Porcupine Bank, but it also blankets the upper continental slope (the Armorican and Celtic shelf/slope sectors of the Bay of Biscay). Winter convection on the slope may exceed 500m where the bottom is deeper than that, or reach the bottom at inshore locations. In summer a seasonal thermocline builds, sequestering the SPMW as a subsurface PV minimum over the upper slope. Many measurements have documented the poleward flow of these waters and it is this upper slope flow system that enables there to be loops defined in the upper 800m of our circulation schematic, where southward-flowing SPMW in the interior is partly opposed by return northward of SPMW along the upper continental slope. The transition from the poleward flow along the upper slope to southward flow in the interior may be quite close to the eastern boundary, and we have contoured it that way in Fig. 1(c). Our climatological stream function (Fig. 21(a)) shows no structure at the contouring interval — but note that the reference level used here restricts the field to water depths greater than 2000db. Pollard et al., 1996) (Fig. 1(d)) reported on a synoptic survey and identified an anticyclonic gyre just west of the Bay of Biscay in the upper 2000 db transport field. This echoes very early fields by Helland-Hansen and Nansen (1926), and is suggestive of the NAC branching west of Goban Spur into northward and southward turning paths, the latter providing a flow counter to the upper slope current on the Celtic Slope. In Pingree (1993), Figure 4 illustrated the circulation in this region, based on trajectories of surface drifters drogued at 50–550m and supplemented by data from moored current meters on the upper slope (see also Pingree & LeCann 1989, 1990). They found an anticyclonic flow in the Bay of Biscay that reversed to a poleward flow that was restricted to the upper continental slope. It has been postulated that this northward flow on the upper continental slope has been caused by a poleward along-slope pressure gradient, which in turn is tied to large-scale meridional variation of upper ocean density (see, e.g., Huthnance, 1986). There may, therefore, be a link between the buoyancy forcing of SPMW winter convection, and the upper slope poleward current at the eastern edge of the convection regime.

4.3. Dynamics and circulation in the transforming flow along the NAC: implications of non-conservation of density

The existence of air-sea buoyancy fluxes and the resulting increase of density following the flow imply that flow pathways will cross from lower to higher density in Fig. 21(b). The trace of the axis of the tongue of increasingly lower potential vorticity along the right side of the NAC projects northward into the Rockall Trough in Fig. 21f, crossing density contours. This is a manifestation of the accumulated effects of buoyancy loss on the upper water column yielding increasing vertical homogeneity of the upper water column in the process of increasing density through convection, which is the underlying process of the upper limb of the meridional overturning circulation. Cooling dominates in the downstream “densification” of the SPMW. The regional excess of precipitation over evaporation is a surface fresh water flux that acts in opposition to the cooling flux with regards to this density forcing, but is generally considerably smaller in magnitude, according to the estimates made by Schmitt, Bogden and Dorman (1989).

One major difficulty in being quantitative about transport amplitudes and pathways is that in the eastern subpolar gyre winter convection penetrates many hundreds of meters, and the net annual average buoyancy loss of the region means that the layer we are interested in is not an adiabatic flow regime. This density increase compounds the difficulties of circulation inference beyond the usual sorts of problems associated with reference level velocities. Here are some of the complicating aspects.

Since baroclinic velocity and transport functions (dynamic height and potential energy anomalies) are vertical integrals of specific volume anomalies, the density changes following the flow will be reflected in these functions (Dynamic height and potential energy are pressure integrals of and p, respectively, where is the specific volume anomaly, which decreases for the buoyancy driven densification following the flow. The transport function in Fig. 21 is the sum of a potential energy term for the upper 600db and a dynamic height term for the shear between the reference level 2000bd and the base of the layer at 600db). The changes will be progressive and systematic downstream in the entrainment regime where air-sea exchanges convectively drive upper ocean densification. Flow streamlines will cross from higher baroclinic stream function to lower in Fig. 21(a) as the average density of the upper ocean increases along the flow, resulting in decreasing dynamic height and potential energy anomaly along the flow. The upper 600m flow trajectories will thus wheel somewhat more sharply northward than the contours of constant baroclinic transport stream function in Fig. 21(a), even if the usage of a 2000db level of no motion were a perfect choice. Tracing such actual flow trajectories upstream from the Rockall Plateau area would give water origins rather further south within the NAC and subtropical gyre than given by the baroclinic contours of Fig. 21(a). Given the large uncertainties of the heat and fresh water contributions to annual average surface buoyancy forcing, and the additional complexity of the related process of the veering with depth of horizontal velocity induced with buoyancy forcing discussed below, we have not attempted to go beyond the knowledge of the sign of this effect to an estimate of the amplitude of the change of transport stream function along the flow. In a numerical simulation of the "cooling spiral" process by Spall (1992), the effect can be seen by comparing the trajectory of a subpolar particle (his Fig. 3(a), parcel "A" once it leaves the Gulf Stream recirculation) to the transport stream function (his Fig. 1(a)).

As noted in the preceding section we discussed the downstream evolution of the SPMW as a buoyancy driven entrainment process, indicated in some model calculations as a negative-signed subduction (Marshall et al., 1993; Paillet & Mercier, 1997) termed "obduction" by some (Qiu & Huang, 1995), which is the opposite of the detrainment process of subduction. Most of this entrainment is "lateral induction", defined as the horizontal flow across sloping isopycnals, rather than vertical flow across the mixed layer base. Thus horizontal velocity vectors do not lie on isopycnal surfaces but cross the isopycnals from light to heavy. This is the central process for the water mass transformation at mid- and high-latitudes. The entrainment into the mixed layer involves both the denser waters immediately beneath the mixed layer being "consumed" by the deepening mixed layer, and the lighter waters from upstream, driven across the mixed layer isopycnal by buoyancy forcing. Upper ocean density advection is to first order balanced by the buoyancy forcing because of the dominance of the induction term in transformation, so the non-parallelism of isopycnals and flow trajectories is an essential dynamical consideration of upper ocean circulation.

The buoyancy forcing has additional dynamical implications. We noted earlier that there is no large veering of the horizontal velocity with depth in the upper ocean of the eastern North Atlantic. The sense of rotation and the amplitude of the veering with depth that are observed (up to ~30°, Stommel, 1979) within the NAC south of the Rockall Plateau area are consistent with the idea of a cooling spiral induced by the annual net buoyancy loss of the upper ocean caused by air-sea fluxes (see also Schott & Stommel, 1978; Spall, 1992). For a given buoyancy forcing, the veering scales with the inverse square of the horizontal speed, and thus becomes larger in areas where the transport stream function contours diverge near the eastern boundary than along the faster-moving NAC at mid-basin. Stommel's veering estimate was made at a point 52.5°N, 20ºW where, on Fig. 21(a), the contours appear rather far apart and therefore the speeds are relatively slow; thus his result of 30° veer can be considered to be on the high side of the likely regional range. In Spall's (1992) OGCM simulation of cooling spirals, the veering is typically $<20°$ along his model NAC and northward branching, but rises to $>40°$ close to the eastern boundary, where speeds are slow; this is diagnosed by Spall as convection driven spiraling. A more recent study of convection near a boundary (Spall & Pickart, 2001) indicates a spiral in such a regime with a flow component towards the boundary's continental slope at shallow levels, enhances sinking along that slope, and generates a flow

component away from the boundary in the lower part of the convective layer. This folding over may have relevance to the Rockall Slope Current and other slope currents that occur along the eastern and northern boundaries of the SPMW domain.

Stommel's (1979) velocity hodograph illustrated the spiral of the geostrophic flow relative to 850db south of Rockall Bank veering to be only about 30° and mostly in the upper 200m, with the near surface geostrophic flow to the right of the thermocline flow. This veering means that in following a depth averaged thermocline flow path of the NAC (e.g. the synoptic survey transport field in Fig. 1(e)) the near surface waters move from left to right relative to waters deeper in the thermocline, which move right to left relative to the depth-averaged flow. These crossing angles are not large, but they are systematic and so can accumulate significant lateral displacements of the apparent trajectories at different depths. Fig. 22 illustrates this with a set of dynamic height contours for several pressure surfaces, calculated from the same data set used for Fig. 21(a), with the contours chosen so as to pass through a common geographic point southwest of Rockall Trough.

Thus there are two distinct effects of density of the upper ocean increasing that confound attempts to deduce flow in the layer penetrated by winter convection. There is the systematic increase of layer baroclinic transport stream function following the flow, so that the layer transport isolines veer systematically left of the stream function contours. Relative to this layer average transport pathway, within the layer flow streamlines rotate with depth, so that the surface flow of the layer is systematically to the right of the deeper flow in the layer.

Luyten et al. (1985) considered the vorticity balance implications of the lateral induction for this area. They found that the lateral induction term dominates over Ekman suction in defining the regional flow, which additionally "feels" the bottom and is a departure from simple flat-bottom Sverdrup dynamics (see also Wunsch & Roemmich, 1985). Paillet and Mercier (1997), Figures 9 and 10, have emphasized the contrast between their estimated total transport pattern and intensity and the Sverdrup transport estimated from the same wind field they used in their dynamically constrained inversion. The quantitative studies of the regional buoyancy forcing by Marshall et al. (1993) and Qiu and Huang (1995), have confirmed this inference of induction being dominant over Ekman suction.

4.4. Pathways of warm water approaching the Nordic Seas

In Fig. 1(c) we have illustrated the northward wheeling NAC dividing into three branches; one traverses the Rockall Plateau complex, the second joins the Rockall Slope Current, and the third delivers warm water to the area south and west of the Faroese channels. Conditions along these three pathways are somewhat different, as the path-integrated transformations along each yield somewhat different variants of SPMW. Generally speaking, along a latitude north of 50°N, the coldest freshest modes are found along the Hatton Bank pathway, whereas the warmest and most saline occur along the Rockall Slope Current pathway. As a backdrop for the warm pathways discussions in this and the next subsection, Fig. 24 shows a view of this region combining the 400db temperature distributions of Fig. 20(c) with velocity vectors from moored current meter measurements in the warm pool waters.

As mentioned earlier, for our primary NAC pathway section (Fig. 23) we have elected to use the easternmost of the NAC pathways through the Rockall Plateau complex, as that is the pathway along which conditions are in most direct conflict with the deep source hypothesis of rising MOW flow along the eastern boundary of Rockall Trough. That section approaches and crosses the Wyville-Thomson Ridge at the Overflow Notch (Fig. 8) where the mooring data shown in Fig. 13 were collected in 1982–1983. At the Ridge-crest station 58, the PV minimum is at a density 31.91, associated with salinity of ~35.30 and temperature ~8.6°C. These values were recorded in early May 1988 (Arhan, Colin de Verdiere & Memery, 1994) 12 months after the sections in Figs. 5 and 8; the latter's stations 75–79 show essentially identical warm pool characteristics along the central and western Wyville-Thomson Ridge. Furthermore, the Ellett

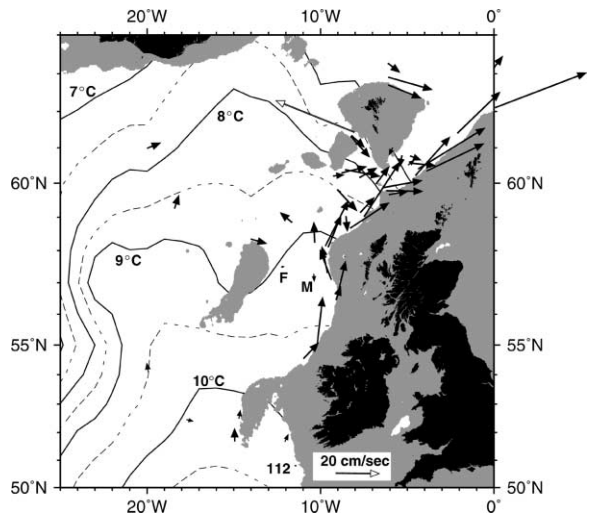

Fig. 24. Temperature distribution at 400 db, and 400 m bathymetry, with mean velocity vectors from a variety of current meter mooring measurements of upper ocean flow.

(1991) current meter data from 1987–1988 in Fig. 15 from the gully between Ymir and Wyville-Thomson Ridges overlap in time with these same hydrographic stations and sections, and the temperatures recorded at the mooring's upper pair of instruments, 270m and 540m show water temperatures were the same as those in the flow along the gully towards the Wyville-Thomson Ridge crest, and above the sill depth of the crest of the ridge. Recalling our discussion of the Paillet and Mercier (1997) results in Section 4.1, at 54°N their 15Sv of flow in the upper 800m was interpreted as delivering to the eastern subpolar gyre about two thirds transformed warmer waters and one third waters as yet not contacted directly by winter convection delivered from adiabatic flow through their study domain. From Fig. 23(a), at station 45 near 54°N the density at 800m was 31.9; the low PV indicative of winter convection center is near a density of 31.7–31.8. It seems then that the adiabatic component (i.e. about one third of their estimate) falls within the density range of 31.8–31.9, which is the density range of the warm pool at the Wyville-Thomson Ridge. We therefore infer that the on-going transformation northward through the Rockall Trough, continues to transform the lighter two-thirds into that denser class, and combines it with the previously adiabatic one third, which is also driven by buoyancy forcing into the winter mixed layer, and so produces SPMW near density 31.9, the warm pool density at the Wyville-Thomson Ridge. Not all the 15Sv flow above 800m is destined for Nordic Seas inflow, as some is utilized for continued transformation within the subpolar gyre that leads to Labrador Sea Water production.

While this emphasizes the warm pool south of the Wyville-Thomson Ridge in the northern Rockall Trough as the immediate source of waters flowing across the Ridge to the Faroese Channels, the other two NAC branches on Fig. 1(c) could also be involved in delivering warm pool waters to the area south of the Ridge, with the Rockall Slope Current delivering slightly warmer water across the eastern end of the Ridge.

A section along 20°W collected about three months later (July, 1988 not shown, see Tsuchiya et al., 1992) provided nearly synoptic data from the Hatton Bank branch of the NAC along the western flank of the Rockall Plateau complex. This section documented the PV minimum along 20°W over the northern Hatton Bank and the Iceland Basin south of 60°N at a somewhat lighter density of about 31.83, fresher salinity ~35.20, and about the same temperature 8.6°C. The Hatton Bank pathway waters are generally slightly fresher at a given density than the Rockall Trough pathway waters. The westernmost NAC branch

in turn may branch into pathways passing both to the south and to the north of the Faroe Islands. SPMW flowing eastward to the south of Faroe Bank to enter the Faroese Channels over the western Wyville-Thomson Ridge is typically 8.5°C, while that entering the Channels via the Faroe Bank Channel between Faroe Bank and Faroe Plateau is cooler, typically at or slightly cooler than 8°C. SPMW passing eastward to the north of Faroe Plateau is near 7.5°C (van Aken & Becker, 1996; Hansen & Østerhus, 2000). Within this band of eastward flow north and south of Faroe Plateau the SPMW density changes from $\sigma_1 \leq 32.0$ to $\sigma_1 \geq 32.0$, so that direct inflow of SPMW occurs in the DS isopycnal layer. For example, in the 1987 data that Saunders (1990, in Saunders & Gould, 1988) collected between Faroe Bank and Faroe Plateau, the SAMW forming the warm pool inflow to Faroe Bank Channel was $\sigma_1 \approx 31.96$–31.99, while along 7°W northward of Faroe Plateau the density of the PV minimum was $\sigma_1 \approx 32.01$–32.06. While the latter are DS isopycnal layer densities, they do not represent a flow of modified MOW, instead they represent the density that the warmer waters have reached for this area through convective transformation. For more detail about the Faroe Plateau regional circumstances, extensive information is given in van Aken and Becker (1996) and Hansen and Østerhus (2000). The sense of the arrangement of temperature, salinity, and density of these inflows from the west can be gathered from the contours in this area in the maps of Fig. 21(b), e.g. the $\sigma_1 = 31.8$, 31.9, and 32.0 contours of Fig. 21(b).

The third principal northward path for NAC flow is between the Hatton Bank and the Rockall Trough pathways. Atop the Rockall Plateau between Hatton Bank and Rockall Bank is the Hatton-Rockall Basin, which is wide open to the south at thermocline depths, but in the north the George Bligh Bank forms a significant barrier. This Basin is filled to near 1000m by SPMW warmer than 8°C (Tsuchiya et al., 1992; van Aken & Becker, 1996), and it is likely that there is a net northward flow through this Basin, passing to either side of George Bligh Bank, and thereby entering the northern Rockall Trough. Van Aken (personal communication 1998, other aspects of the data set described in van Aken & de Boer, 1995 and van Aken & Becker, 1996) indicated that a synoptic section in 1991 from Hatton Bank eastward across George Bligh Bank and thence northeast to Lousy Bank was blanketed in mode water near 8.5°C with salinities near 35.25.

4.5. Direct measurements of warm water flow towards the Norwegian Sea

The moored current meter results described in sections 3.3.3 and 3.3.4, summarized in Fig. 16, are the most direct evidence for the flow of warm pool waters across the Wyville-Thomson Ridge. They, and the other data in Section 3.3, demonstrate that only warm pool waters flow into the Faroese Channels, from the south and west. Waters denser than the warm pool either have their entry to the Channels blocked (by the eastern half of the Ridge), or they flow out of the Faroese Channels into the Rockall Trough (over the western half of the Ridge). A tightly constrained estimate of the flow of warm pool waters across the Ridge is precluded by sampling issues: i) the three moorings along the Ridge crest may not resolve the horizontal and vertical structure of the flow; ii) there is considerable mesoscale variability and iii) there are indications of seasonality of flow as discussed by Dickson, Gould, Griffiths, Medler and Gmitrowicz (1986). In spite of these shortcomings, what level of warm water transport do the moored measurements suggest?

Fig. 16(a) shows six vectors along the Ridge crest and on the continental slope. In the latter region the moorings have additional warm water measurements below the surface instruments (some are on Fig. 16(b)). The continental slope region can be approximated as a triangular cross-section of 400 m and 30 km sides, and the various instruments from those three mooring suggest an average inflow speed through that triangle of between 10 and 15 cm/s, or a contribution of 1.2–1.8 Sv, a range consistent with Rockall Slope Current estimates to the south (Huthnance, 1986; Huthnance & Gould, 1989). We model the flow across the Wyville-Thomson Ridge crest westward of this continental slope triangle as a warm pool layer with an average thickness of 400 m and a width of 150 km, spanning the crest from the Faroe Bank to

the continental slope. Each 1 cm/s of average flow normal to the Ridge crest through this cross-section corresponds to 0.6 Sv. The average for the four vectors recorded at the Ridge crest in Fig. 16(a) have components normal to the Ridge crest axis of 1.6, 7.4, 9.5 and 17.9 cm/s from west to east. An additional factor is that these near surface speeds may decline significantly with depth, particularly on the western ridge where there is a reversal to a cold outflow below 400m, e.g. Figs. 8, 13, 14 and 16 b, c. We use estimates of 4–8 cm/s for the warm inflow across the Ridge offshore of the continental slope, which yield a transport estimate of 3.2 to 4.8 Sv. Combining the transports for the two domains yields a total estimated warm inflow across the Wyville-Thomson Ridge and Continental slope of 4.4–6.6 Sv. These are substantial transports, of the same order as the expected import of warm water to the Nordic Seas.

A year-long moored array deployed in 1983–1984 across the continental slope in the Faroe-Shetland Channel at 61°N yielded an estimated transport of 7.65 ± 2.58 Sv (Gould et al., 1985): 2.17 Sv of the variability is attributable to a seasonal cycle that peaks in winter. Huthnance and Gould (1989), (see also Huthnance, 1986) noted that a variety of measurements at the continental slope of Rockall Trough south of the Wyville-Thomson Ridge indicated a northward flow of warm water along the upper slope, i.e. the "Rockall Slope Current", that is not nearly that large. The Rockall Slope Current flow is strongest and most organized in the upper 500 m, and is estimated at 1.2–2.2 Sv (measurements reviewed by Huthnance, 1986). In Fig. 10(c), the isolated core of somewhat higher salinity marks this upper ocean flow, and, according to Hill and Mitchelson-Jacob (1993), it originates from the upper waters farther south in the Rockall Trough and not from deep MOW. The Rockall Slope Current delivers the warmest and most saline warm pool waters to the Inflow. Huthnance and Gould (1989) noted the requirement for substantial additional flow from the west of warm water into the Faroese Channels to explain the increase from the ~1–2 Sv Rockall Slope Current to the ~7 Sv flow measured in the eastern Faroe-Shetland Channel, and pointed to flow across the Wyville-Thomson Ridge as the explanation of the much larger Faroe-Shetland Channel transport. The results of the six moorings we have summarized here clearly support their inference of a large component of inflow in addition to the Rockall Slope Current.

Some of the additional flow originates from the warm pool waters within the northern Rockall Trough offshore of the Rockall Slope Current. Booth and Meldrum (1987); (see Booth & Meldrum, 1984, for additional details) described seven drogued surface drifters that in 1983 and 1984 were deployed in the middle of Rockall Trough at two sites (57.5°N, 11.7°W and 59.5°N, 9.0°W) south of the Wyville-Thomson Ridge. Six of these drifters crossed the eastern half of the Ridge and followed the continental slope through the Faroe-Shetland Channel (average speed of 33 cm/s there); the seventh immediately lost its drogue. After passing the longitude of the Shetland Islands, four continued well up the coast of Norway to 66°–69°N in the Norwegian Current, while the other two, whose trajectories in the Faroe-Shetland Channel were closest to the continental shelf, diverted south into the Norwegian Trench west of southwestern Norway.

The perceived requirement for substantial confluence of waters from the west to boost the Inflow has not changed over the years since it was inferred by Gould et al. (1985). There has been a focus during the past few years on contributions of warm Inflow across the Iceland-Faroe Ridge, passing north of the Faroe Islands, and by-passing the Faroese Channels, e.g. van Aken (1988), Krauss (1995), and van Aken and Becker (1996). Preliminary results of recent Nordic WOCE measurements using moored ADCP instruments suggest there is a smaller warm inflow of 5 Sv along the Faroe-Shetland Channel continental slope (Turrell, Hansen, Østerjus, Hughes, Ewart & Hamilton, 1999; Hansen, Larsen, Østerhus, Turrell & Jónsson, 1999; Hansen & Østerhus, 2000). They also indicated that this 5 Sv had actually been supplemented by a retroflection of 1.3 Sv of southward-flowing warm water on the Faroe Plateau side of the Channel, so the net inflow through the Channel was only 3.7 Sv. They reported on simultaneous measurements north of the Faroe Islands showing 3.3 Sv eastward flow of warm water that they attributed to flow across the Iceland-Faroe Ridge; it was the 1.3 Sv of this flow that in their schematic turns southward and retroflects in the Faroe-Shetland Channel. In this interpretation, the Norwegian Current gains less of its transport from the flow across the Wyville-Thomson Ridge than in the Gould et al. (1985) result, but this is compensated

by the flow passing north of the Faroe Islands to give a similar total delivery to the Norwegian Current of ~7 Sv.

However, there is an alternative interpretation of the relative contributions of the two pathways to the their inferred 3.3/3.7 Sv split. We believe that the idea that the southward flow on the Faroe Plateau side of the Faroe-Shetland Channel retroflects to join the inflow along the Shetland continental slope originated with Dooley and Meincke (1981), but this is just one of two possible interpretations of the reversed geostrophic shear distribution of "domed" cross-Channel sections like Fig. 5. Saunders (1990) reported on results from three moorings with warm water measurements near 300m at the Faroe Bank Channel. The two of the instruments (362 and 307 day duration records) on the Faroe Bank side of the Channel showed warm water from the Iceland Basin flowing into the Faroese Channels, see Fig. 24, whereas the third mooring, on the Faroe Plateau side of the Channel, indicated there was strong (39 cm/s) outflow at average temperature of 6.9°C, for the 75 hours of measurement, a suggestive but not definitive observation. His repeats of ADCP referenced hydrographic sections similarly showed the cross-Channel flow reversal, as did a fourth section farther west where the Channel enters the Iceland Basin. It is possible, therefore, that rather than retroflecting at Faroe-Shetland Channel, the warm water from north of Iceland that branches southward into the Channel follows the Faroe Plateau side of the Faroese Channels all the way to the Iceland Basin. In this alternative hypothesis, without the retroflection, the measurement of 5 Sv of inflow along the continental slope remains undiminished and represents a net delivery across the Wyville-Thomson Ridge of 5 Sv of warm water from the northern Rockall Trough domain. The 3.3 Sv of warm water flowing eastward to the north of Faroes is diminished by the 1.3 Sv that turns south through the Faroe-Shetland Channel, traverses the Faroese Channels, and is delivered back to the Iceland Basin sector of the subpolar gyre, thus yielding a net delivery via the northern inflow pathway of 2 Sv. The two pathways split 2:5 in this scenario.

A geostrophic estimate of the split between the pathways passing north and south of the Faroe Islands is given by Krauss (1995) who used drogued surface drifters to adjust geostrophic shear estimates. He used surface drifter data to show that the shallow flow over the Iceland-Faroe Ridge southern flank is eastward, as first described by Helland-Hansen and Nansen (1909), not westward as illustrated subsequently by some later authors. Krauss estimated that this eastward flow is a source for 7.6 Sv of Nordic Seas warm inflow, of which 4.6 Sv passes to the north of the Faroe Islands and 3.0 Sv traverses the Faroese Channels, entering the Norwegian Sea through the Faroe-Shetland Channel. The subsequent trajectories of some of the drifters outline these alternate pathways. Three drifters deployed at 62°N south of Iceland ultimately crossed the Iceland-Faroe Ridge and after passing eastward close to the northern flank of the Faroe Plateau turned northeast to enter the Norwegian Sea; one after first undertaking a southward excursion and retroflection in the Faroe-Shetland Channel. A fourth drifter from this deployment arrived in the Norwegian Current by traversing the Faroese Channels from west to east.

van Aken and Becker (1996) (see also Otto & van Aken, 1996) described the routes of four drogued surface drifters deployed west of Hatton Bank in a small region near 57°–58°N; all four ended up in the Norwegian Sea northeast of the Faroe Islands. One, launched in March 1993, traveled eastward to the south of Hatton Bank, and passed between George Bligh and Rockall Banks. It then turned northward until near Lousy Bank before turning eastwards to the south of Bill Bailey's and Faroe Banks, and crossing the Wyville-Thomson Ridge near the site of Dooley's westernmost current-meter mooring observed thirteen years earlier. The drifter traversed the Ridge at an average speed of around 14 cm/s, which was similar to the mean velocity recorded earlier at Dooley's mooring (Fig. 16(a)). A second drifter, deployed in April 1991 passed eastward to the north of Hatton Plateau, and of George Bligh, Lousy, and Bill Bailey's Banks, but then dipped south of Faroe Bank to enter the Faroese Channels by crossing the Wyville-Thomson Ridge southeast of the Faroe Bank, again near the site of Dooley's westernmost current-meter mooring. This drifter stalled at the northern end of the Faroe-Shetland Channel, becoming temporarily trapped there in a cyclonic eddy before escaping into the Norwegian Sea. A third drifter, launched in January 1991,

became stuck for 46 days in anti-cyclonic loops over Faroe Bank, and upon escaping followed the western flank of Faroe Plateau and passed over the Iceland-Faroe Ridge just northwest of the Faroe Islands, and then traveled eastward into the Norwegian Sea north of the Faroe Islands. A fourth drifter, deployed in March 1993, avoided the Faroese Channels completely and arrived at the Iceland-Faroe Ridge well west of the Faroe Islands. It then followed the southern flank of that Ridge towards the Islands and crossing the Iceland-Faroe Ridge just west of the Islands, traveled into the Norwegian Sea to the north of the Faroe Islands.

Booth and Meldrum (1987) also described the tracks of three drogued surface drifters deployed at the southern entrance to the Rockall Trough, to the south of the Rockall Bank. These drifters initially circled together around an anticyclonic eddy, but subsequently diverged. One, which was shallow-drogued (16m), went eastward across Porcupine Bank and onto the continental shelf. A second, more deeply drogued (66 m), also headed east but then followed the Rockall Slope Current northward to about 56°N before moving onto the shelf. The third, drogued at 166 m, headed west, circled the western side of the Rockall Plateau and ending up west of the Faroe Islands with the last stages of its trajectory in the Iceland Basin being similar to some of the Krauss's (1995) and Otto and van Aken's (1996) drifters discussed above.

All the drifters discussed were deployed at sites where warm pool waters fill the upper water column, according to the hydrographic section plots in Krauss (1995) and van Aken and Becker (1996). The float trajectories, therefore, imply a delivery of those warm waters to the Norwegian Sea. Moored current meter records on the western slope of Hatton Bank and the central Iceland Basin (van Aken, 1995) and on the northern flank of Rockall Bank (Dooley & Henderson, 1980) indicate eastward flow of these warm pool waters towards the Faroese Channel. Moored measurements support the continued flow of these warm pool waters eastward across the Wyville-Thomson Ridge (Fig. 16) and to the north of the Faroe Islands (Hansen et al., 1999). Estimated transports are adequate for these flows and pathways to be the totality of the source for the warm Inflow.

To link the warm pool visually with the direct measurements of flow, Fig. 24 combines the field of 400m temperature with the current meter velocity measurements previously discussed (Section 3) in the Wyville-Thomson Ridge area, together with several additional sites in the Iceland Basin, Rockall Bank, the Faroe Bank Channel, the Porcupine Bank, and the Rockall continental slope. These mooring records were collected at various levels between 10s of meters and a few hundred meters, so we have restricted the plot to vectors clearly sampling the warm pool, and have included no mooring data from the continental shelf. Many of the records are from the upper continental slope, and so while they document the existence of the Rockall Slope Current well, they may over-emphasize that feature relative to the under-sampled offshore flows; the latter, while being arguably slower, are of larger lateral scale than the Rockall Slope Current, which is confined to the upper continental slope.

4.6. The transformed water masses within and beneath the warm pool

There are two notable effects of the transformation on the warm pool waters. The first is a net cooling and freshening of the upper water column's water mass through the action of the buoyancy forcing. The second is that the resulting transformed water mass is, somewhat paradoxically, warmer and more saline at a given density than at the same density upstream of transformation.

4.6.1. The downstream cooling and freshening of winter mixed layer waters

The starting point of the R79 development of the deep source hypothesis was to seek a source for the "high" salinity (>35.2) of the Inflow. In actuality, the starting point could have been the reverse, to explain why the salinity of the Inflow is that low given that the entire thermocline of the subtropical waters delivered to area south of the Rockall Plateau is more saline. The preconditioning by the convective transformation achieves most of the explanation, delivering to the Rockall Plateau area the deep warm pool waters.

The observed upper ocean transformation following the NAC involves a cooling and freshening of the downstream-deepening winter mixed layer (McCartney & Talley, 1982). How does this cooling and freshening come about? At the surface along the course of the NAC the sea-air heat flux cools the ocean, while the excess of precipitation over evaporation freshens the convecting layer. As mentioned earlier, in terms of contributions to the buoyancy flux, the cooling dominates over the freshening (Schmitt et al., 1989) to yield the annual average buoyancy loss that drives the convection, and results in densification. As noted in Section 4.1, Marshall et al. (1993) also estimated the source term corresponding to Ekman layer transport, whose contribution competes in amplitude with the evaporation minus precipitation contribution, but also is dominated by the heat flux contribution to buoyancy forcing.

While the combination of these fluxes is the air-sea buoyancy flux causing convective instability, and dominates the large lateral induction term in the entrainment, the flux balance of the deepening mixed layer, which determines its evolving temperature and salinity, also includes a significant entrainment flux at its base as a result of the vertical velocity at the base of the mixed layer. For the SPMW transformation that part of the entrainment process provides additional cooling and freshening of the mixed layer, since the waters below the convective mixed layer are cooler and fresher than the convecting layer.

There are additional contributions to a mixed layer evolution budget. The excess of precipitation over evaporation alone appears to be inadequate to explain the net freshening along the NAC pathway. Ekman layer advection yields a left to right flow across the geostrophic flow of the NAC that is up-gradient for both surface temperature and salinity distributions, and thus is an additional source of cooling and freshening influences to be mixed downwards by winter convection (Marshall et al., 1993). An additional contribution to the heat and salinity budgets comes from the veering with depth of the horizontal flow in the observed regional geostrophic spiral, which acts to slide colder and fresher upper layer waters from left to right across the NAC relative to deep levels (Fig. 22 and discussion in Section 4.3). The latter effect is interesting, for the surface buoyancy flux which reaches to depth through convection simultaneously is the homogenizing agent that creates the PV minimum as well as the forcing for the veering (cooling spiral) of the horizontal flow. The veering of the flow causes, as mentioned above, transport of relatively fresher waters across the NAC which, in turn, through the annual cycle of convection, is mixed into the evolving SPMW. Our point here is that the various fluxes which combine to give net densification following the upper ocean flow yield net cooling and net freshening of the deepening mixed layer.

The winter convection that causes the densification of the SPMW also determines the other characteristics of the Nordic Seas Inflow. Convection causes near saturation in oxygen concentrations, and the oxygen saturation value increases with declining temperature. Thus in Fig. 21(e) the upper water column oxygen progressively rises along the flow path suggested by Fig. 21(a), and a strong rise of the oxygen of the low PV layer is also evident in the NAC pathway section view (Fig. 23(d)). Convecting waters are also nearly stripped of silicate (and other nutrients) resulting in the low silicate values all along the NAC pathway for the low PV layer in section view (Fig. 23(e)). As discussed in Sections 3.1 and 3.2, the modern silicate data utilized here show no increases in silicate values in either the Norwegian Current or the warm pool enveloping the Rockall Plateau and Trough, thus no source of additional silicate is required. In Fig. 21(f), the PV progressively decreases as the transformation systematically reduces the average stratification of the upper water column along the various NAC pathways, and in Fig. 23(f), the deepening and densification of the convection is evident in the PV distribution.

4.6.2. Downstream salinification of density surfaces

In Fig. 23((a)–(c)) the overall downstream evolution of the upper water column is a densification, cooling and freshening for the waters both within and above the low PV SPMW layer. Somewhat paradoxically, as a function of density the situation is the reverse. There is an increase in salinities along the isopycnals following the flow, with the SPMW of a given density actually being more saline and warmer than the properties on that same density surface upstream of its winter outcrop. On Fig. 23(c) this salinification is

apparent through the downstream declination of the isohalines relative to the isopycnals. For example, at $\sigma_1 = 31.8$, salinity is about 35.1 in the NAC at mid-basin, whereas in the Rockall Trough, around station 51, it is about 35.35, while the compensating isopycnal temperature has risen by more than 1°C. One could mistake this as an indication of a MOW influence, since it results in a map of salinity on an isopycnal showing salinity increasing along an NAC pathway towards the Nordic Seas. The shading of the low PV layer on the salinity section (Fig. 23(c)) clarifies the situation. Most of the salinity change occurs between stations 38 and 45, the segment of the section where the low PV layer first intersects this isopycnal. The other water mass properties are similarly affected; the isopycnal temperature increases from ~9°C to >9.5°C (Fig. 23(b)), its oxygen increases from <5.0 to >5.4 ml/l (Fig. 23(d)), while the isopycnal silicate declines from >8μmol l^{-1} to <7μmol l^{-1} (Fig. 23(e)). The intersection of the low PV layer with this isopycnal indicates that not only does the isopycnal outcrop seasonally in this segment of the section but also the salinification and other water mass modifications are associated with the production of SPMW.

The association of the along-NAC points where isopycnal salinification occurs and where SPMW convection reaches that surface has a simple explanation. Suppose one begins with a water column from the southern Newfoundland Basin, say from a branch of the Gulf Stream supplying North Atlantic Central Water into the NAC. North Atlantic Central Water itself exhibits a positive temperature-salinity correlation, and thus the depth-averaged salinity of the water above a given density surface is higher than that at that density surface. Deepening convective cooling driven only by sensible heat exchange at the sea-surface would preserve that average salinity. In such a hypothetical pure cooling scenario, once the progressive convection has reached a given density surface within the North Atlantic Central Water, that surface will have become more saline than the North Atlantic Central Water at that density (see the vertical transformation arrow on Fig. 25(a)), as discussed by Pollard and Pu (1985). In the real ocean, evaporative cooling exists and dominates over sensible cooling, and that implies an impact on salinity. Adding the effect of evaporation, the real cooling process would increase the average salinity of the convecting layer, and would rotate the transformation vector on the T-S plane so as to point towards higher salinity (Fig. 25(a)). Thus, without consideration of other fresh water forcing of the system, the transformation of the mixed layer would be a cooling and salinification when viewed on isopycnals. Without something to oppose these tendencies, the salinification on density surfaces that occurs when the convection reaches that density would be much greater than observed. The tendencies opposing salinification are the regional excess of precipitation over evaporation, the ageostrophic Ekman layer flow of eastern basin fresh subpolar waters across and converging with the geostrophic NAC, the veering with depth of the horizontal flow in the regional geostrophic spiral, and entrainment from below of colder fresher waters into the deepening mixed layers.

The net result of all these effects is that the water mass in the thermocline is more saline than North Atlantic Central Water, explicitly defined as Eastern North Atlantic Water (ENAW) by Harvey (1982), a terminology now in common use. We use these two water mass relations as the backdrop to the schematic of the salinification effect on isopycnals (Fig. 25(a)), with Harvey's ENAW curve extended to temperatures warmer than his own 12°C cutoff in a manner described in Mauritzen et al. (2001). While attributing its general origins to winter surface conditions, Harvey also ascribed its elevated salinity to a MOW component in the winter-convected layer. The studies of McCartney and Talley (1982), Pollard and Pu (1985), Pollard et al. (1996), as well as our own discussion herein, all suggest that the subpolar mode water winter convection generates slightly elevated salinity in the ENAW compared to North Atlantic Central Water. Mauritzen et al. (2001) have implicated diapycnal mixing from the MOW tongue upward into the overlying thermocline waters within the Gulf of Cadiz as an additional mechanism contributing to the east-west variability in the North Atlantic Central Water temperature/salinity relation. One might indeed say that the surprise about isopycnal salinification is not that eastern basin thermocline waters are observed to be more saline than North Atlantic Central Water, but rather that the degree to which the salinity is elevated is not larger than observed!

This completes our development of the shallow source hypothesis for the origin of the warm inflow to

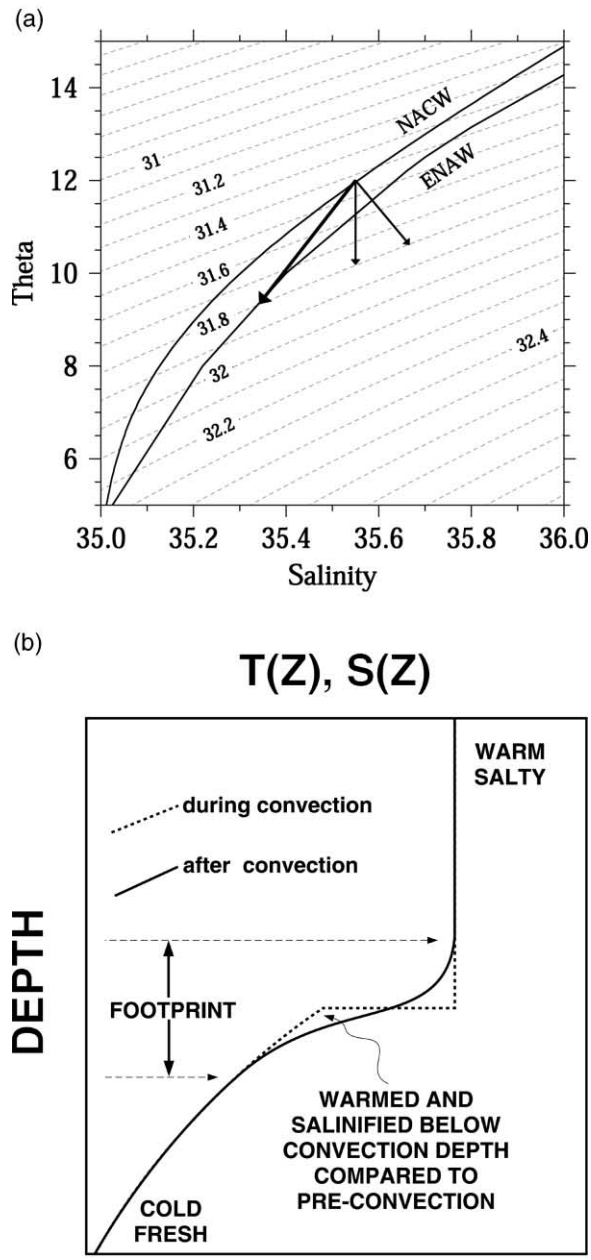

Fig. 25. (a) pure cooling driven salinification of a density surface, also the effect of adding evaporation, and the actual vector, (b) schematic *T(z) S(z)* with steps, with footprint rounded shoulder

the Nordic Seas. For complete closure on issues of the contrast between the shallow source and deep source hypotheses, we lastly discuss the fate of the eastern boundary undercurrent and the origins of the water mass characteristics in the DS isopycnal layer in the Rockall Trough and Plateau region.

5. The DS isopycnal layer in and south of Rockall Trough: the fate of the eastern boundary undercurrent

In the preceding sections the conflicts between the shallow and deep source hypotheses were discussed with a focus on the characteristics of the Inflow and whether they result either from horizontal advection of transforming upper ocean waters delivered to the Rockall Plateau and Trough areas by the northward branch of the NAC or from deep water delivered by the eastern boundary undercurrent to Rockall Trough upwelling and crossing the Wyville-Thomson Ridge. Our conclusion in favor of the shallow source hypothesis leads to the natural question of what happens to the water of eastern boundary undercurrent if it does not rise up over the Wyville-Thomson Ridge?

The initial thought might be that the undercurrent moves past Porcupine Bank and either through or round the Rockall Trough, but without upwelling so that it leaves the Trough still at depth. There are two such pathways available. It could circle the Trough and exit passing westward to the south of the Rockall Plateau into the Iceland Basin. Alternatively, there are passages north of the Plateau silled at about 1100 m (see the dashed contour on Fig. 4(b)) between the various Banks between Rockall Plateau and Faroe Bank. With the σ_1 = 32.0 density surface generally between 800m and 1000m in the northern Rockall Trough (excluding the spillover plume regime in the gully between the Ymir and Wyville-Thomson Ridges), pathways from the Trough north of the Rockall Plateau into the Iceland Basin are also possible. While both of these suggestions for the continuation of the deep flows has the appeal of providing a simple answer to the question of the fate of the undercurrent, there is little evidence for either in the Rockall Trough data.

5.1. Conditions in the DS isopycnal layer in the southern Rockall Trough

What are the conditions with which a regional circulation scheme for the Rockall Trough needs to be consistent at the depth of the DS isopycnal layer? The cross-section of Rockall Trough just north of Porcupine Bank shown in Fig. 7, is 700 km south of the Wyville-Thomson Ridge, and crosses the Rockall Trough somewhat north of Porcupine Bank. While this is a late fall section, displaced in time by perhaps 10 months from the preceding winter's convection, the low PV layer is interannually persistent and dominates the section's upper water column to 800 m and σ_1 = 31.9. Immediately under that warm pool the maximum stratification (the highest PV) is centered on σ_1 = 32.1. The salinity cross-section (Fig. 7(b)) shows a complete absence of the salinity maximum that is the prominent marker of the MOW in the eastern boundary undercurrent south of the Bank. Particular care was taken along this section crossing the eastern boundary to maintain close station spacing and small bottom triangles at the eastern boundary. So we are confident that the sampling did not miss a narrow remnant of the undercurrent. The section's salinity range across the DS isopycnal layer is shown to have been 35.0–35.23, distinctly lower than in the eastern boundary undercurrent southward of Porcupine Bank, e.g. 35.2–35.55 at stations 11 and 12 off Goban Spur in Fig. 3(b). In the North Atlantic as a whole, these salinities of 35.0–35.23 are distinctly lower than those typically associated with a strong MOW influence. Consider, for example, the salinity of ~ 35.23 on the cross-section's σ_1 = 32.0 surface. Tsuchiya's (1989) chart of salinity on this surface shows the eastern boundary salinity rises southwards to $>$36.2 at the core of the MOW salinity tongue along the Iberian Peninsula, but that the 35.2 contour sweeps far west in the subtropical domain, crossing the Mid-Atlantic Ridge to define the western "nose" of the MOW tongue near 55°N that reaches the western boundary with salinity a little greater than 35.1.

Looking at the Trough's oxygen cross-section (Fig. 7(d)) the presence of an oxygen minimum layer indicates subtropical influence. Overall, that minimum layer exhibits an eastern boundary intensification, which could be taken as indicative of a cyclonic recirculation in the Trough at this level. However, that possibility is clouded by a single station on the Rockall Bank side of the Trough, which actually, has the

strongest minimum. Since evidence for this minimum was present in data derived from both the bottle data and the CTD oxygen sensor data, it is viewed as a real feature. Additionally that station falls in the middle of a narrow band of intensified northward shear over the slope of Rockall Bank, suggestive of a northward flow regime as reported by Ellett and Martin (1973). But the general overall intensity of the oxygen minimum layer (<5.2 ml/l) and its most extreme value (4.95 ml/l) is not nearly as low as that observed in the undercurrent south of Porcupine Bank, e.g. <4.5 ml/l at stations 11 and 12 off Goban Spur in Fig. 3(d). Thus while being suggestive of a subtropical influences, such an oxygen minimum does not particularly evoke MOW.

5.2. Conditions in the DS isopycnal layer in the NE Atlantic immediately south of Rockall Trough

5.2.1. Climatological distributions

Fig. 26 shows the distribution in the northeastern North Atlantic of salinity on three DS isopycnals, σ_1 = 32.0, 32.1, and 32.2, the pressure on one viz. σ_1 = 32.0, and the dynamic height distribution at 900 db relative to 2000 db. Being constructed from a climatology, with smoothing and uneven time/space sampling, the maps can be presumed not to represent the field well at the eastern boundary, if there are strong gradients there. We will address that concern subsequently through examination of three high-resolution synoptic sections around Porcupine Bank expressly collected to alleviate such concerns. Maximum salinity observed on these three synoptic sections are annotated on these maps to give indications of the action of smoothing on the contoured field. We begin by characterizing the DS salinity field based on the three salinity maps to establish the interior fields. The Rockall Plateau and Trough are enveloped by DS isopycnal layer waters with salinity ~35.1–35.3, and these isohalines trace southward past Porcupine Bank and thence swing southwestward into the interior of the subtropical gyre. The higher salinities are northeast-southwest-oriented contours that terminate at the eastern boundary southward of 50°N and Porcupine Bank.

The sweep of the DS isopycnal layer salinity contours is essentially the same as the sweep of the pressure contours of the surfaces, e.g. the σ_1 = 32.0 surface (Fig. 26(b)). For comparison, R94 included salinity and pressure contours for σ_1 = 32.2 and 31.938, and the R79 DS isopycnal maps ($\sigma_1 \approx 32.24$) have been repeated here as Fig. 2. The sweep of the DS isopycnal layer salinity contours is also essentially the same as that of the 2000 db referenced upper 600 db transport field (Fig. 21(a)). The orientations of pressure contours define pressure gradients that are indicative of the directions of vertical shear of the horizontal velocity, and, as discussed earlier, those orientations do not change much from the sea surface down through the DS isopycnal layer in the NAC regime, e.g., Fig. 22. Basically, the entire upper 1500 db of the water column is to first order an equivalent barotropic field, with considerable baroclinic shear of the horizontal flow, but small veering of it. In Fig. 26(e) we show the field of dynamic height at 900 db relative to 2000 db, reinforcing the image of near-parallelism of isobars and isohalines with deep-referenced flow contours for the level of the DS isopycnal layer.

As we did with the upper water column, we take the alignment of isobars, isohalines, and baroclinic stream function isolines in the lower thermocline (DS isopycnal layer) as an indication of a dominance of advection in determining the pattern of salinity, with the NAC being a deep reaching current. So a first order interpretation of the maps is that they indicate that DS isopycnal layer waters enveloping the Rockall Plateau and Trough sweep in from the southwest as the lower thermocline flow of the NAC, and that the salinities found to either side of the Plateau are those carried there from mid-basin. To second order there will be fluxes that disrupt the parallelism of flow and isohalines and need to be considered. Comparing the salinity and pressure contours for σ_1 = 32.0, the salinity contours cross isobars from right to left as the contours swing past Porcupine Bank from the southwest, indicative of salinification along the isobars. The pressure contours are only indicative of the vertical shear of the horizontal flow, but the dynamic height contours in Fig. 26(e) compared to the isohalines on Fig. 26(a) reveal salinification on the 48 through 56 dyn.cm contours as they sweep into the subpolar domain, with the 58 and 60 dyn.cm contours switching

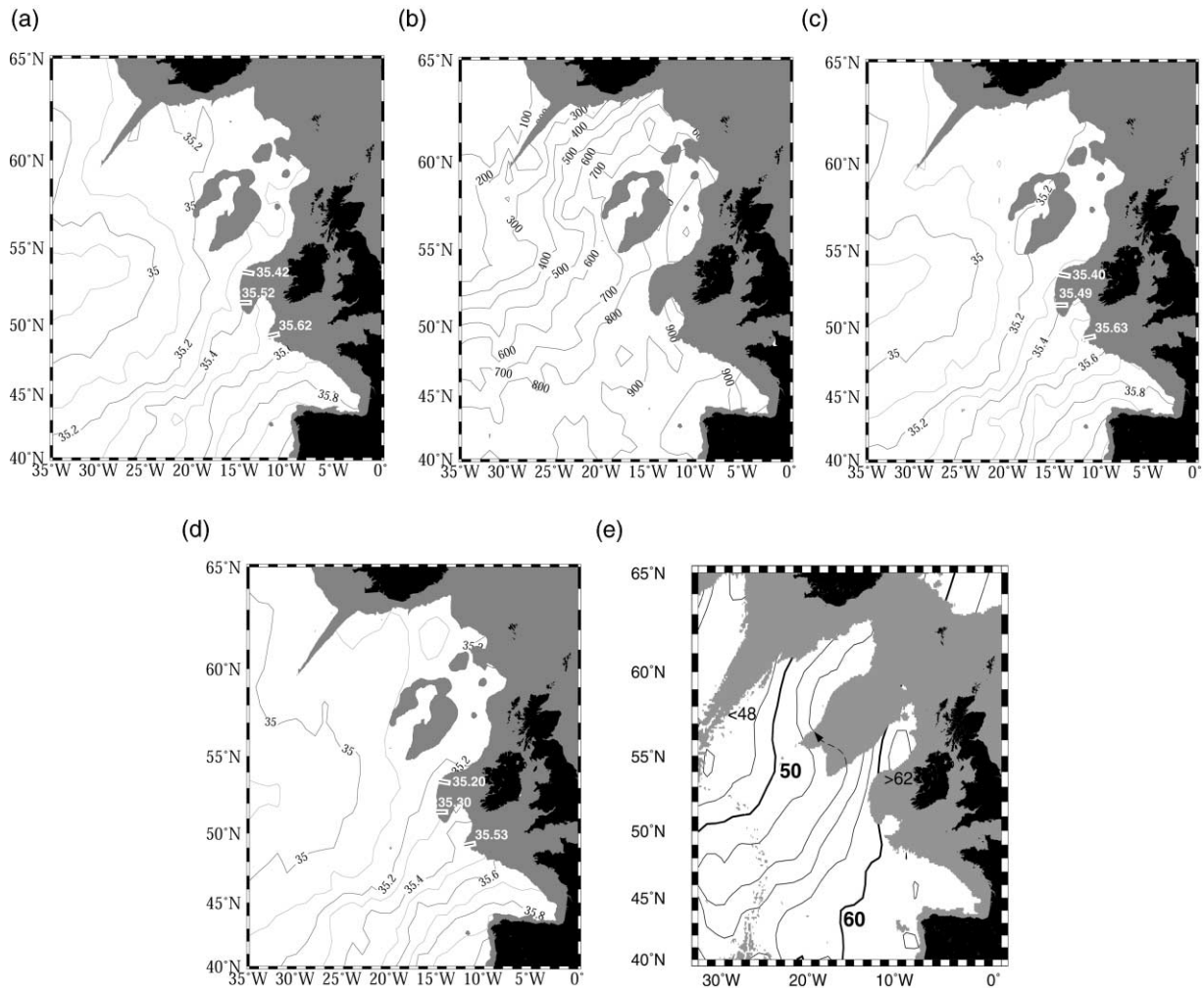

Fig. 26. Salinity on three DS isopycnal layer density surfaces: σ_1 = 32.0 (a); σ_1 = 32.1 (c); σ_1 = 32.2 (d), and pressure at σ_1 = 32.0 (b), all the above with shading indicating depths less than 1000 m; and dynamic height on 900 db relative to a level of no motion at 2000 db, with shading indicating depths shallower than 2000 m, (e).

to mild freshening. The latter signal is perhaps an artifact of the resolution issue at the edge of the fields, as these baroclinic flow contours pass close to Porcupine Bank. There the annotated synoptic section salinity observations show higher salinity values than the climatological field and that could negate the mild freshening signal in the climatology. These considerations lead us to a conjecture that the lack of absolute flow and/or trajectory measurements may preclude "proof".

Conjecture one: The waters approaching Rockall Trough from the south within the DS isopycnal layer represent a northward-wheeling branch from the lower thermocline flow of the NAC, wheeling northward from mid-basin to flow northward adjacent to Porcupine Bank.

5.2.2. Synoptic sections across the eastern boundary at Porcupine Bank and Goban Spur

As part of 1996–1997 U.S. WOCE project on the transformation of warm waters within the eastern subpolar gyre, two short sections were made across the eastern boundary at the northwest and southwest

flanks of the Porcupine Bank, and a third at the flank of the Goban Spur south of the Bank (locations on Fig. 4(b)). These sections were made immediately subsequent to the Rockall Trough cross-section illustrated in Fig. 7. Together these four boundary crossings were made within a 12-day period in 1996. Single stations from each of these "spokes" are part of the Fig. 3 composite section, enabling the continuity of the eastern boundary section past the critical Porcupine Bank sector of the boundary. Fig. 27 shows some properties along the southern three spokes, in density-distance coordinates. These should be contrasted to the Rockall cross-section of Fig. 7 collected northeast of the Bank. A particular effort was made during these crossings to maintain a close station spacing so as to resolve the structure of the dilute MOW along the eastern boundary south of Rockall Trough. These have enabled us to scrutinize at small lateral scales the pattern of dilute MOW at the eastern boundary south of Rockall Trough. To expose the fields further, Fig. 28 shows density and salinity for the four sections in depth-distance coordinates, and compares them to a section along 20°W across the NAC.

The Rockall Trough cross-section of Fig. 7 has DS isopycnals in the depth range 800–1400 m, which are relatively flat and featureless across the Trough, Fig. 28(a). They show no particular organized pattern indicative of a current shear where they reach the eastern boundary. In contrast, the DS isopycnals descend more than 300 m towards Porcupine Bank over about a 300 km distance along the two sections across its northwest and southwest flanks, Fig. 28(b,c). This eastward descent is the geostrophic shear that supports the northward flow of warm waters to the Rockall Plateau and Trough according to the shallow source hypothesis, if referenced to a deeper reference level. For a reference level beneath the DS isopycnal layer, that layer also will have northward flow. Where these descending DS isopycnals intersect the Porcupine Bank, they are approximately at the same depth as in the cross section of the Rockall Trough, Fig. 28(a), while at the offshore end of these two spokes the same isopycnals are more than 300 m shallower than anywhere along the Trough cross-section. Thus, in addition to these two Porcupine Bank spokes defining a large isopycnal descent towards the Bank and deep-referenced northward flow adjacent to the Bank, they also define an isopycnal descent into the Trough from its mouth, also over a distance of about 300 km.

This area of relatively shallow DS isopycnals, just a couple of hundred kilometers west of Porcupine Bank and south of Rockall Bank, is also in the regional historical data-base, albeit smeared by the gridding. It is the cause of the compression of the spacing of the 54, 56, 58 dyn.cm contours at the Trough mouth shown in Fig. 26(e), and their termination at the 2000 m contour of Rockall Bank. The synoptic sections (including the 20°W section) suggest that the mid-depth NAC flow approaches Porcupine Bank from the southwest, turns northward to flow in a narrow band to the west of the Bank, and then turns northwestward to cross the mouth of the Trough and flow onwards along the southern flank of the Rockall Plateau to the Iceland Basin west of the Plateau. In the 20°W meridional section shown in Fig. 28(e), the northward descent of isopycnals begins at station 26, in 2800 m water depth, and extends northward, interrupted by a single eddy, across the southern Rockall Plateau to the crest of Hatton Bank at a depth of ~1000m at station 17 near 57°N. Most of this delivery of warm pool and DS isopycnal layer transport to the Hatton Bank pathway is not accessible to the 2000 db referenced geostrophic transport calculation of Fig. 26(e), but would emerge from a bottom referenced calculation. Dickson and Kidd (1986) reported the results from a mooring deployed in 1982–1983 at 54.1°N, 19.9°W; its 11-month average vector in the warm pool is included on Fig. 24, and its nearly due northward orientation defines the Hatton Bank pathway well. Its other instrument, at 1300 m was sampling water near the dense side of the DS isopycnal layer, beneath most of the shear of the hydrographic section. It yielded a 7-month average speed of 5.7 cm/s oriented about NNW, which supports the inference of the participation of the DS isopycnal layer in the westward flow over the southern Rockall Plateau to the Iceland Basin.

Does the undercurrent turn offshore at Porcupine Bank and follow this pathway, rather than entering Rockall Trough? Notwithstanding the deep source hypothesis, this is the pathway indicated by the long looping pathways in the R94 circulation maps at 800m and 1000m, and repeated here in Fig. 19. It is, however, not a likely undercurrent pathway because this region does not show MOW characteristics any

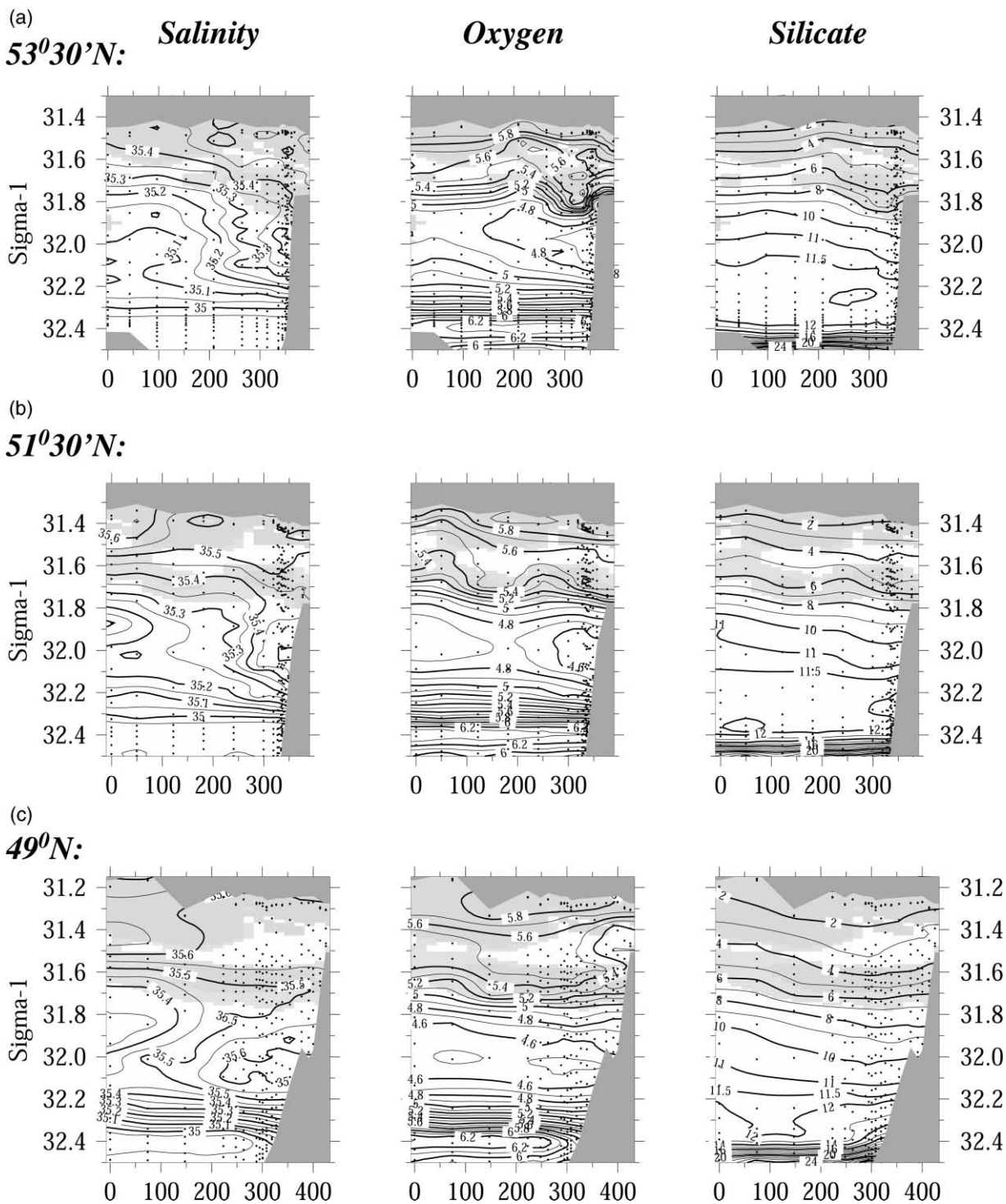

Fig. 27. Salinity, oxygen and silicate for sections at the eastern boundary. Low PV is shaded. (a) northwestern flank Porcupine Bank (b) southwestern flank Porcupine Bank (c) western flank Goban Spur

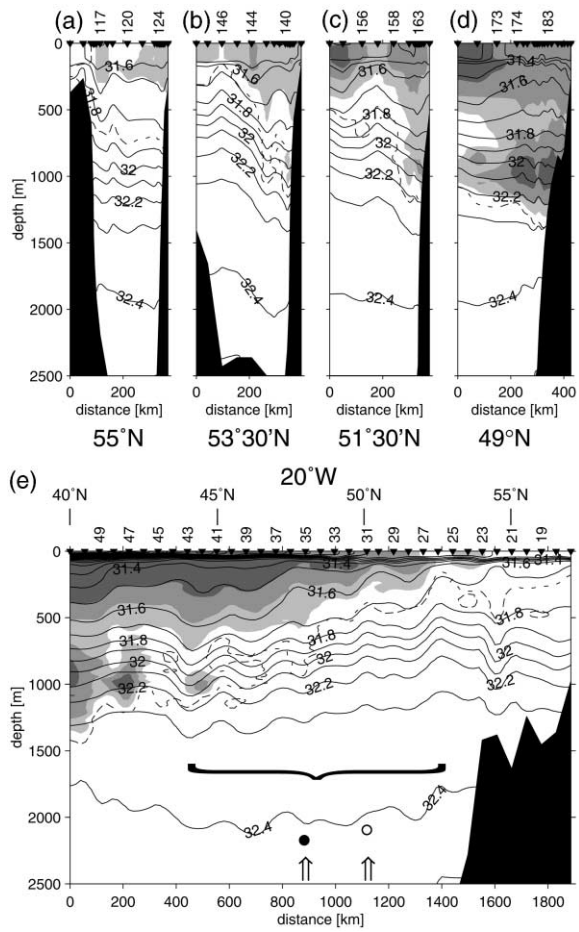

Fig. 28. Isopycnals for sections in the northeastern North Atlantic, with dashed contours showing the 35.3 isohaline and increasing shading indicating the salinity ranges 35.4–35.5, 35.5–35.6, and >35.6. (a) Rockall Trough cross-section near 55°N. (b) Northwest Porcupine Bank spoke near 53.5°N. (c) Southwest Porcupine Bank spoke near 51.5°N. (d) Goban Spur spoke near 49°N. (e) Meridional section at 20°W. Curly bracket indicates band of eastward shear of North Atlantic Current. Arrows and black and white circles indicate the two NAC stations used in Fig. 20.

more than the Rockall Trough cross-section does. Compare Figs 28(a) and (e) and note the absence of waters as saline as 35.3 within the DS isopycnal layer. In Fig. 23, the northward isopycnal descent for stations 41–52 defines the northwestward flow regime across the mouth of the Trough, from Porcupine Bank to the regime described above in the 20°W section segment across the southern Rockall Plateau. Here, as farther northwards in the Trough and westward at 20°W, the DS isopycnal layer waters do not resemble the undercurrent south of Porcupine Bank, having no particular salinity elevation.

On the two Porcupine Bank spokes (Fig. 27 top and middle rows), the most saline deep DS isopycnal layer waters occur at the continental slope where the isopycnals are deepest. The density-coordinate salinity section for the northwest spoke (Fig. 27, top row), shows a transition in the DS isopycnal layers from the fresh SAIW, <35.1 in the west to dilute MOW in the east. The least diluted MOW in this section has a maximum salinity >35.4 and a minimum oxygen content <4.7 ml/l, at a density $\sigma_1 = 32.0$, which is about 0.2 more saline than the deep Rockall waters at this same density, and lower in oxygen by 0.5 ml/l (Fig. 7). On the southwest spoke (Fig. 27, middle row), a similar transition from SAIW to dilute MOW is

observed; here the maximum salinity is >35.5 and the minimum oxygen is <4.6 ml/l. Comparison with the climatological maps (Fig. 26) suggests that with the resolution afforded by these synoptic sections, the area west of Porcupine Bank shows a compressed transition from SAIW to dilute MOW in the same band over which the isopycnal descent towards the Bank occurs. The 35.5 contour terminates on the eastern boundary in between the two Porcupine Bank spokes, while the 35.4 contour terminates on the northern flank of the Bank. Within less than 200 km of the Bank the fresh SAIW becomes dominant. Thus these two spokes define a band of northward flow past the Bank with a "tube" of dilute MOW on its eastern side, and this tube extends neither into the Trough nor northwest past Rockall Plateau.

5.3. The fate of the eastern boundary undercurrent

5.3.1. Alternative interpretations of the northward fading of the undercurrent

The eastern boundary section in Fig. 3 documents the eastern boundary undercurrent extending northward with diminishing MOW. As noted in Section 5.2, the distinctive MOW character along the eastern boundary off the Iberian Peninsula has weakened at the Porcupine Bank, and is absent from the Rockall Trough and from over the southern Rockall Plateau. It appears then that there is no recognizable penetration of the undercurrent waters into the subpolar domain northward of Porcupine Bank. There are three alternatives for the fate of the eastern boundary undercurrent.

Firstly the undercurrent does enter the Rockall Trough, but is consumed by the deepening convection within the Trough, in effect it is mixed into the warm pool and homogenized by the convection. Two aspects of the observations argue against this possibility. Along the eastern boundary section (Fig. 3), the low PV layer can be taken as indicative of the local winter convection northward of about stations 11 and 12, whereas to the south of there, it reflects the southward recirculation of SPMW (see Section 4.2). But the density of the low-PV layer fails to penetrate the DS isopycnal layer at all along the eastern boundary. Within the Trough the low-PV layer density approaches the DS isopycnal layer, but that is well north of where the eastern boundary undercurrent salinity anomaly has already disappeared. Whatever causes the northward decay and termination of the salinity maximum along the eastern boundary, it has essentially completed that process south of Rockall Trough. Fig. 3(b) shows the last stage of salinity decay taking place between Goban Spur (stations 11–12) and the northern Porcupine Bank (stations 13–17), with Figs. 27 and 28 detailing the final fading of the anomaly in synoptic sections. Consumption by convection would be expected to have a seasonality that is strongest in winter, when the convection is active and enhances diapycnal mixing immediately below it, and weakest in late fall when convection has barely started to remove the seasonal restratification. But the sections in Figs. 7 and 27, and 28 are from close to Porcupine Bank in late fall at a time and location that would maximize the likely strength of MOW signal, and yet there is no expression of the undercurrent at all at this site.

The second alternative is that the undercurrent reaches the Trough as a mass transport, but on the way to the Trough it has lost its salinity and other property anomalies through lateral mixing with the waters of the NAC in the DS isopycnal layer. On Fig. 26 low salinity (and, not shown, high oxygen and low silicate) SAIW flows eastward across the North Atlantic within the northern half of the NAC. Moving southwards across the southern half of the NAC, the water mass progressively metamorphoses through "neutral" ENAW and to dilute MOW. In this second alternative, the transports of DS isopycnal waters by the NAC and by the eastern boundary undercurrent compete for space as the NAC approaches the eastern boundary. Both deliver mass transport past Porcupine Bank to the Trough, but as they pass by Porcupine Bank, they are pressed together against the Bank and the last signature characteristics of the undercurrent are washed out by lateral mixing. That seems to match the character of the distributions along the spoke sections in Figs. 27 and 28.

But is it the undercurrent that is delivering the most saline waters in those spokes? If it does, then data demand considerable dilution to occur over the last 300 km of path from Goban Spur to the southern

Porcupine Bank. The bottom row of Fig. 27 shows the spoke that extends offshore from the Goban Spur. This shows a much broader area and less dilute MOW indicative of the eastern boundary undercurrent in the Bay of Biscay. The isopycnal depth distribution along this spoke, Fig. 28(d), shows the DS isopycnal layer intersecting the continental slope at about the same depth as the other sections, but in contrast to the Porcupine Bank pair of sections, there is very little depth variation in the layer offshore along the Goban Spur section, and thus little geostrophic shear to use to build a circulation scheme. The DS isopycnal layer waters in the two Porcupine Bank spokes are much more dilute with regard to their MOW characteristics, and in fact have characteristics similar to those in the DS isopycnal layer within the NAC to the southwest of the Bank, as suggested by the fields in Fig. 26. Thus rather than the second alternative, the data make the third alternative plausible; that is that the undercurrent does not reach the northwestern continental slope of the Porcupine Bank, and instead it is the weak positive salinity anomalies of the right-hand part of the NAC that delivers the slightly more saline waters of the DS isopycnal layer to that location.

Thus the third alternative is that the undercurrent never reaches the Rockall Trough, but instead the mass transport of the undercurrent is expelled from the eastern boundary region into the interior of the subtropical gyre, and dwindles to zero south of Porcupine Bank. In this scenario, it is the flow of the NAC in the DS isopycnal layer that "wins the battle" with the eastern boundary undercurrent for space at Porcupine Bank, so that it is the NAC that delivers DS isopycnal waters to the Rockall Trough area — waters that include SAIW, "neutral" ENAW and dilute MOW all of which are present in the approaching NAC. The disappearance of the dilute MOW to the north then reflects a continuation of the cross NAC mixing process, perhaps enhanced by the compressed gradients immediately west of Porcupine Bank across the wheeling NAC branch, and the elimination of the saline end-member for that mixing northwards of 52°N. A section normal to the boundary at Porcupine Bank would still progress from negative salinity anomaly offshore, through "neutral" ENAW near the boundary to dilute MOW at the boundary, as in the second alternative, with subsequent mixing eliminating the last traces of MOW. There is no particular way to differentiate these two alternatives from just the water masses and the geostrophic shear. The difference is in the pathway along which the dilute MOW is delivered to Porcupine Bank. The report on an inverse model of the eastern North Atlantic by Paillet and Mercier (1997), discussed above in Section 4, primarily deals with flow and transformation above 800m. But it does present 1° gridded velocity vector plots for 50, 500, 1000, 2500 and 3500 m. The 1000 m field intersects the DS isopycnal layer and indicates NAC flow towards the eastern boundary turning northward along the boundary at the Goban Spur, with no organized flow in the Bay of Biscay, much as they cartooned for the upper 800 m (Fig. 1(f)).

5.3.2. The fading of the eastern boundary undercurrent through expulsion of its mass transport

The presence of the tube of dilute MOW off Porcupine Bank and its presence in a region of sloping isopycnals suggesting northward flow, combine with the absence of a significant northward extension of dilute MOW within that tube to argue for lateral mixing with the SAIW as being required to alter the characteristics to those observed at the mouth of Rockall Trough and in the northwestward flow across the mouth. But the tube itself can be explained as originating in the flow of weak MOW within the NAC, e.g., the sweep of the dynamic height contours in Fig. 26(e), rather than a northward continuation of the eastern Boundary undercurrent, particularly since the SAIW part of that NAC flow is found within 200 km of the Bank. Our interpretation of these sections leads us to a conjecture complimentary to our first conjecture:

Conjecture two: The eastern boundary undercurrent fades northward both in its MOW anomaly and in its mass transport, not only through mixing with the subtropical gyre waters, as has long been recognized, but also through expulsion of its transport into the southwestward flow of the subtropical gyre, a flow whose direction lies parallel to the isohalines of the north side of the basin scale MOW tongue. The undercurrent does not pass Porcupine Bank to enter Rockall Trough, having depleted its mass transport between Goban Spur and Porcupine Bank.

Under the third alternative, the decline in the salinity of the eastern boundary undercurrent that occurs steadily northward from the Gulf of Cadiz in Fig. 3 reflects not only a mixing of the salinity anomaly away into the interior, but an expulsion of the undercurrent's northward mass transport, until it becomes zero between the Goban Spur and Porcupine Bank. On Fig. 26 the northeast-southwest orientation of isohalines to the west of the Iberian Peninsula and the Bay of Biscay would then reflect the trajectories of the expelled waters moving southwest in the subtropical circulation, again the idea of first order parallelism of flow and isohalines, but one that requires a shift from the deep reference level of the NAC regime to a shallower reference level farther south at subtropical latitudes. This reference level transition actually is a familiar idea: The NAC is most often represented as a deep referenced circulation element, while the subtropical gyre to the south is often represented as in intermediate reference level system. The core difficulty is that to the west of the Bay of Biscay and the Iberian Peninsula, and north of the track of the Azores Current, there is little shear across the DS isopycnal layer to help guide the selection of the reference level. To aid the reader in visualizing the results of this progressive expulsion of the undercurrent, Fig. 29 compares three meridionally-oriented salinity sections. The salinity contours define the westward projection of the classic MOW tongue away from the eastern boundary, with fading maximum salinities and a sweeping southwestward of the isohalines of the northern side of the tongue. The conventional interpretation often is oversimplified as a subtropical gyre circulation with a diffusive source of salinity at the eastern edge of the domain. Our interpretation replaces that diffusive salinity source with a progressive expulsion

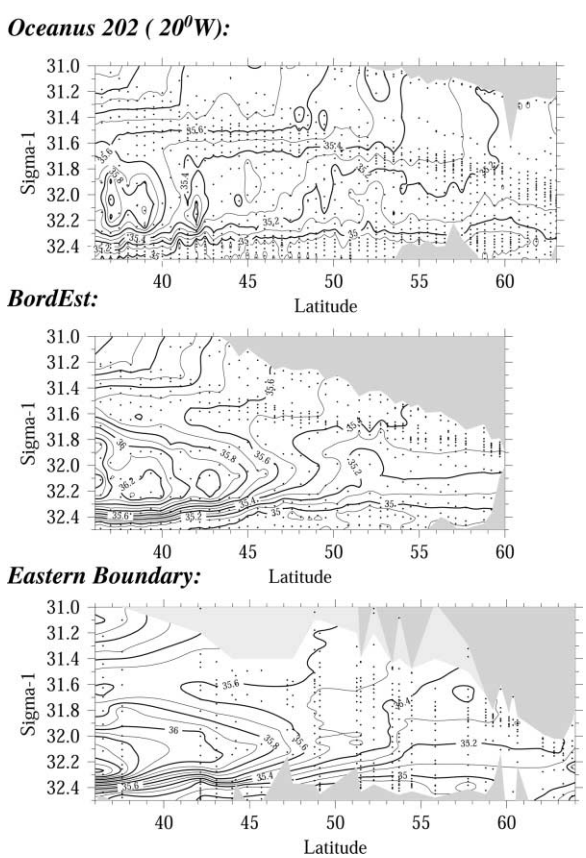

Fig. 29. Salinity distributions along quasi meridional sections top: 20°W (See Tsuchiya et al., 1987). middle: "Bord Est" (See Arhan et al., 1994) bottom: eastern boundary (same data as Fig. 3)

of eastern boundary fluid into that gyre, so that on the northern side of the MOW tongue, there are southwest trending flows quasi-parallel to the isohalines but with small crossing angles from more saline to fresher water, and with streamlines originating from the eastern boundary along the Iberian Peninsula, the Bay of Biscay and with the last expulsion occurring between Goban Spur and Porcupine Bank (Fig. 1(d)). RAFOS floats were deployed for A. Bower and P. Richardson across each of the high-resolution eastern boundary crossings of Figs. 27 and 7 on a density surface intersecting the MOW, specifically to address the issue of the EBUC fate. Bower et al. (2000) give a preliminary assessment of the set of trajectories from the two thirds of the floats that had their subsurface drifts at that time, and a flow synthesis schematic (their Fig. 3b) supports our second conjecture.

We interpret the data as indicating not only a dilution of the salinity of the MOW but a diminution in undercurrent transport: as it flows northwards the undercurrent expels its mass transport and MOW into the interior circulation of the subtropical gyre (Fig. 1(d)). In Fig. 29 we compare the salinity distribution along the eastern boundary (from Fig. 3(b)) with that along the Bord Est section at lower latitudes. The latter section lies well offshore of the undercurrent but shows that strong MOW influence is nonetheless found well north of the latitude of the Gulf of Cadiz, to the west of both the Iberian Peninsula and the Bay of Biscay. Such expulsion of MOW from the undercurrent is included as far north as 42°N (R78) or 35°–45°N (R94). We believe that this expulsion of MOW from the undercurrent continues as it transits the Bay of Biscay so that by the time it reaches the Porcupine bank it is completely drained. This continuation of expulsion to Porcupine Bank is consistent with the shape of the MOW tongue in Fig. 2(b), with the decline in MOW core strength along the undercurrent, and with the expelled MOW being the source waters for the northern side of the MOW tongue. However, this interpretation is at odds with the R94 mapping of circulation and properties, e.g. Fig. 19, where this region is indicated as one of confluence into the eastern boundary currents, shown through the diagramming of long looping trajectories that turn towards the eastern boundary and return northward. Our eastern boundary undercurrent is neither divergent nor convergent. The fate of the transport in the eastern boundary undercurrent is to supply high salinity to the subtropical gyre all along its pathway from the Gulf of Cadiz through the Bay of Biscay to its ultimate demise at the Porcupine Bank. In Fig. 26(e), this interpretation means that somewhere in the southeastern part of the contoured domain, away from the higher gradients of the deep NAC, some choice of reference level is required other than the 2000db we have used. The flow we describe would then be a flow away from the Bay of Biscay, roughly following the isohalines of the northern side of the westward extending MOW Tongue into the lower thermocline of the subtropical gyre.

If the undercurrent were to be considered the direct source for the dilute MOW in the two spokes at Porcupine Bank, it would result in another circulation geometry problem. The NAC does deliver SAIW quite close to Porcupine Bank. If the more saline water observed at the Bank is the extension of the eastern boundary undercurrent, then where does the NAC's northeastward flow of ENAW and dilute MOW in the DS isopycnal layer go? If it does not turn northward past Porcupine Bank then it has to diverge relative to the flow of the rest of the NAC at shallower levels, turning southward offshore of the undercurrent, to provide "space" for the undercurrent to continue northward through the gap (Fig. 1(b)). This seems to us an unnecessarily contorted circulation. Our conclusion is that it is the northward wheeling deep NAC flow that provides the saline waters immediately west of Porcupine Bank. This replaces the divergent shallow and deep pathways of the deep source hypothesis with more or less parallel pathways of NAC flow, as contoured in the shallow source hypothesis circulation schematics (Fig. 1(c) and (d)).

5.4. Discussion of the Iorga and Lozier (1999) diagnostic model for the undercurrent

Iorga and Lozier (1999a,b) have made an extensive study of the climatological fields and circulation to address the nature of the circulation of MOW in the eastern North Atlantic. The end product of their analysis has an eastern boundary undercurrent that extends with undiminished mass transport all the way

from the Strait of Gibraltar to the northern edge of their study domain at 60°N. Since that domain boundary is immediately south of the Wyville-Thomson Ridge, and since they find large northward flow there on $\sigma_1 = 32.1$, we categorically reject their solution because it is in direct conflict with actual flow measurements at the Ridge as discussed here in Section 3.4. How did they arrive at their interpretation? We discuss here the several steps they took to get from starting fields of relative dynamic height to their final solution that they felt represented the absolute circulation. We have some issues to raise about those steps. But it turns out that as the penultimate step in the evolution of the solution, they actually made an ad hoc selection of what to do with the undercurrent around Porcupine Bank, choosing to take it northward into Rockall Trough rather than to expel the undercurrent's transport into the interior southwards of there. Until that choice was made, their evolving solution alternative still retained both possibilities. Thus their solution has a step of subjective interpretation, and since the flow measurements at Wyville-Thomson Ridge are in conflict with their interpretation and the solution that it yields, we are confident in rejecting their solution. Nonetheless we will progress through the steps of their analysis and point out some other issues.

The alternatives of eastern boundary undercurrent versus deep NAC flow as the immediate source for northward flow in the DS isopycnal layer off Porcupine Bank are visible in the intermediate solutions of the Iorga and Lozier (1999b) diagnostic model study of the climatological average fields in the northeastern Atlantic south of 60°N. They start with alternative deep and shallow referenced (their Fig. 1) stream functions for the geostrophic flow on $\sigma_1 = 32.1$ with the two alternative reference surfaces lying 300–400 db above and 1000–1200 db below the $\sigma_1 = 32.1$ surface. They also did a parallel calculation on a shallower surface 31.9 but only the final results for that surface are illustrated in the paper, but it is a less relevant surface as it lies within the SPMW in the central and northern Rockall Trough. Their Intermediate Solution I applied mass conservation to these fields and a "no-flux" condition at the parts of the domain edge where the surface grounds on topography. We have doubts about implementation of this no-flux condition in a climatological field where the edge is poorly resolved in the various synoptic station sets, since this leads to gridding difficulties, and then requires smoothing near the edge of the data domain. Essentially you have to make up data at the domain edge, with only sporadic data control from high resolution sections, which themselves have their content smeared by the gridding. Additionally, a deep referenced stream function field terminates by definition at the intersection of that deeper reference surface with topography, offshore of the edge of the density surface, so that the edge of the domain cannot be required to be a streamline even if there are no resolution issues from the gridding. Dynamic height contours "running into the bottom" are a familiar problem in mapping geostrophic circulation.

The starting two stream function fields (their Fig. 1) demonstrate the resolution problems, most notably a multiple contour "half" bull's-eye at the tip of the Goban Spur; a spot that is critical in our own interpretation of a fading undercurrent, for it is only southwards of there that substantial MOW salinity anomalies are seen in the synoptic or climatological data. More generally, those two fields show haphazard intersections of streamlines with the boundary, dominated by two regions, the Goban Spur bull's-eye, and the disappearance of streamlines that emerge from the Gulf of Cadiz into the coast of Portugal.

The Intermediate Solution I fields for $\sigma_1 = 32.1$ (their Fig. 3) resulting from the adjustments still have the oppositely directed NAC flows that result from the shallow and deep referencing, but, unaccountably, also still have streamlines intersecting the eastern boundary in spite of the stated application of a no-flux condition at the boundary. At this stage of their final solution construction an eastern boundary undercurrent only appears to the south of the Gulf of Cadiz, in the Canary Current domain, where it appears on both maps, as a sharpening and organization of uneven structures in the unadjusted fields.

The shallow-referenced field additionally shows broad northward flow between the southern Iberian Peninsula and the Azores, with some eastward concentration suggestive of the undercurrent. However, one by one those contours hit the eastern boundary of the northern Peninsula and the Bay of Biscay until by the time the Goban Spur is reached all have disappeared and the bull's-eye appears in the unadjusted fields. These contours re-emerge from the boundary between Goban Spur and the Porcupine Bank, turning west-

ward then southwestward as part of the general southwestward flow of the deep NAC that results from the shallow reference level. For the adjusted shallow-referenced field, the Goban Spur bull's-eye is a dividing point between a southern region of flow towards the eastern boundary to the south of a line from the Spur to the Azores, and flow away from the eastern boundary to the north of that line, which is dominated by the reversed deep NAC flow that results from the shallow reference level.

In the deep-referenced field, the mid-basin waters northward of the Azores flow northeastward, and mostly turn northwards with a bifurcation point for the smaller southward flow into the Bay of Biscay being the bull's-eye at the Goban Spur. There is no eastern boundary undercurrent northward of the Gulf of Cadiz in this deep referenced field, and the only significant feature is the Goban Spur bull's-eye.

Their Intermediate Solution II re-computes the shallow and deep referenced fields of Solution I with the addition of a specified velocity (stream function difference) across the mouth of the Strait of Gibraltar. That step also raises for us implementation issues for a smoothed gridded data field, because the MOW plume in the northern Gulf of Cadiz, the central circulation element transforming the raw MOW at the Strait of Gibraltar into an undercurrent off the southwestern Iberian Peninsula, is particularly vulnerable to poor representation in gridded data. In their first paper (Iorga and Lozier, 1999a), the problem is apparent: within the Gulf of Cadiz the pressure of that surface is represented in the gridded data as a set isobars crossing the Gulf meridionally, defining a Gulf-wide pressure ramp from $<$500db west of the Strait to ~1000db south of Portugal. This clearly represents the ageostrophic downstream descent of the Outflow plume isopycnals rather than the cross-plume descent of isopycnals of the plume's geostrophic flow. The applied stream function difference on this surface represents a 14 cm/s velocity across the pair of grid points representing the Strait. While that is a reasonable recasting of the dense export transport into an average speed at the width of the Strait in the grid, it is not obvious how to use that upstream plume condition to derive the downstream distribution of stream function on the plume in its evolved state in the Gulf of Cadiz. According to Baringer and Price (1997), in the process of descending from 300 m at the mouth of the Strait to about 700 m at 7°W in the eastern Gulf, the plume nearly doubles in transport through entrainment. The entrainment lightens the plume, but its core still is characterized by salinity $>$36.4 and temperatures $>$12.5°C. Iorga and Lozier (1999b) state their boundary condition to be a stream function jump across the Strait, and with no normal flow applied as a boundary condition north and south of it, their solutions would seem to constrain it in a peculiar way. If you draw a semicircular arc through the ocean interior, with the two ends of the arc intersecting the eastern boundary north and south of the Gulf of Cadiz, then aside from the impact of variable Coriolis parameter in the calculation of flow from stream function, the horizontal flow across that arc has to equal the amount imposed at the Strait. Perhaps their application of mass balance in the interior enables divergence from the layer into the waters above and/or below, but it could be anticipated that most of the vertical exchange occurs in the plume within the Gulf of Cadiz, and along the undercurrent along the Iberian Peninsula's western flank.

It is the application of the jump condition on the eastern boundary stream function that creates an eastern boundary undercurrent where one did not exist in the unadjusted fields. The two Intermediate Solution II fields (their Fig. 4) both show a pronounced eastern boundary undercurrent created northward of the Gulf of Cadiz by the altered eastern boundary condition. The applied stream function jump at the Strait, about 0.67 m^2s^{-1} becomes a jump at the eastern boundary edge of the domain corresponding to more than three mapped contours at their interval of 0.2 m^2s^{-1}! The shallow-referenced field (their Fig. 3(a)) had part of the required jump in the data west of the Iberian Peninsula, and therefore is only augmented by this new flow. The deep-referenced field did not have any expression of an undercurrent northward from 37°N, so its appearance at this stage (their Fig. 4(b)) is wholly a construct of this specification of a differing stream function at the eastern boundary, and is not a feature of the observations. In both Intermediate Solution II fields this step adds a continuous eastern boundary current in the Bay of Biscay and past Goban Spur where none is present in the original reference fields.

Putting aside our concerns about how the fields were developed, the contrast between the deep- and

shallow-referenced fields of Intermediate solution II reveals a dilemma similar to that we have addressed in Section 5.3 for the region west of Porcupine Bank. The shallow-referenced field has its eastern boundary undercurrent turn west and then southwest off Porcupine Bank, so that it becomes a reversed deep NAC flow. There are some embedded structures, but overall the southwest trending flow fills the domain northwards of a line connecting the southern Porcupine Bank and the eastern-most Azores. On the deep-referenced field the bundle of stream function contours at the edge of the surface in the Bay of Biscay and Goban Spur remains a narrow bundle against the Porcupine Bank, turning up the Rockall Trough and leaving the domain at its northern boundary of 60°N. That bundle displaces the deep flow of the NAC approaching from the south and southwest. On this field all the NAC waters entering from the west turn northwards, joined by most of the Azores Current waters from this depth branching northwards, and the undercurrent.

It is at this point that an ad hoc choice is made. They merge these two fields into a Final Solution (their Fig. 5(c)) as a weighted sum of these two fields, stating (p. 26013) that their goal was "using the shallow level of no (slow) motion in the area of the salty Mediterranean waters and the deep level of no motion in the areas away from these salty waters, such as the northeastern portion of the domain where the relatively fresh waters of the North Atlantic Current reside". They go on to say that this was implemented by using the normalized salinity distribution on the isopycnal to set the weight. The result of this last of a series of steps has the contours that most clearly reflect almost all the deep NAC passing west of Rockall Plateau, while the eastern boundary undercurrent passes undiminished in amplitude, although steadily crossing isohalines, from the Gulf of Cadiz all the way along the eastern boundary past Porcupine Bank, through Rockall Trough, and leaving the Trough across the northern domain at 60°N. The flow represents 45% of the northward flow on the surface between Porcupine Bank and 20°W, and all of that boundary flow arrives there by passing through the point next to Goban Spur where the original fields had the data bull's-eye. Almost all of that northward flow eastward of 20°W turns into Rockall Trough and by their discussion they indicate an expectation that it rises over the Wyville-Thomson Ridge northward of their solution domain.

We have considerable doubts about many of the steps leading to this final solution, particularly the ad hoc determination of the weights and the "control" of the bull's-eye grid point near Goban Spur. But ultimately our rejection of their solution is on a simple basis: however they got there, their Final Solution has major northward flow on the $\sigma_1 = 32.1$ surface immediately south of Wyville-Thomson Ridge, a flow that would have to rise over that Ridge. No such flow exists in nature. While perhaps the problem resides in the selection of weights, we think there is something more peculiar going on with their methodology. It is the step to Intermediate Solution II that created the eastern boundary undercurrent in most of the domain, and that Solution's deep-referenced field is the one where the undercurrent penetrates through the Trough, adding to the deep NAC flow into the Trough that the deep-referenced field of Intermediate Solution I exhibited. The existence of the bull's-eye extreme stream function value in their climatological data set at a grid point next to Goban Spur has local control over how streamlines between the Bay of Biscay and the Porcupine Bank develop through their succession of steps, and could easily preclude recognizing an expulsion of undercurrent mass transport along the Bay of Biscay through Goban Spur sector of the eastern boundary, and additionally by distorting the interior stream function could mask the possibility for a SW flow of such waters away from the boundary for some choice of weighting.

5.5. Salinity beneath the warm pool in Rockall Trough and south of Rockall Plateau

For closure of issues related to the shallow source and deep source hypotheses, we finally discuss the water mass observed beneath the warm pool within and to the south of Rockall Trough and over the southern flank of Rockall Plateau. Our analysis of the water mass observations there combines with the inferences of the NAC origins of northward flow past Porcupine Bank and the measurement of spillover of the Wyville-Thomson Ridge to lead us to a third conjecture:

Conjecture three: The characteristics of the DS isopycnal layer in and south of Rockall Trough are a modification of the waters wheeling through that area from the NAC flow past Porcupine Bank. Small increases in salinity and more substantial oxygenation and depletion of silicate following the advective pathways result from diapycnal fluxes from the convected warm pool waters immediately above the DS isopycnal layer, and by interaction with the southward flow of Wyville-Thomson Overflow Water through the Trough; both processes impacting the dilute MOW delivered past Porcupine Bank by the deep NAC.

To develop the basis for this conjecture, we first briefly review the idea that deep water in Rockall Trough involves an MOW component. We examine two potential contributors to the setting of salinity in the Trough, diapycnal fluxes across the base of the warm pool deep convection, and the Wyville-Thomson Ridge spillover into the DS isopycnal layer in the northern Trough

According to Nansen (1913) the first deduction that MOW influences the deeper thermocline waters of the Rockall Trough was by Nielsen (1907). It is now commonplace to attribute the elevated salinity in the Trough to MOW, often using the name "Gulf of Gibraltar Water". Hill and Mitchelson-Jacob (1993) interpreted their observations as indicating a weak MOW influence near 1200 m as far north as 59°N (Fig. 10(c)), with similar amplitude to influences described by Nansen (1913) using data he collected in the Trough in 1910 (see also Harvey, 1982; Harvey & Theodorou, 1986; Arhan et al., 1994). What is it that is being called MOW influence? In detail, the Hill and Mitchelson-Jacob (1993) observation is of a salinity inflection in the temperature-salinity relation leading to a maximum salinity departure of about 0.05 near 7°C from Harvey's (1982) ENAW standard curve. But as can been seen on our reproduction of their 59°N section (Fig. 10(c)) this is not a dramatic aspect of Rockall Trough cross-sections, being perceptible only through the 35.2 isohaline crossing isotherms near 1000m between their onshore station A800 and station AS1. Ellett, Kruseman, Prangsma, Pollard, van Aken, Edwards et al. (1983) noted a similar amplitude salinity inflection on temperature-salinity diagrams near 6.5°C and attributed it to "the core of the remaining influence of the Gulf of Gibraltar Water". What is it that causes this deflection from the regional average water mass relation?

On DS isopycnals the principal fresh influence at these more northern latitudes is the Subarctic Intermediate Water (SAIW; Bubnov, 1968; Arhan, 1990), on the subpolar side of the NAC, while MOW is the principal saline influence, on the subtropical side of the NAC. As shown on various salinity maps (R79, Fig. 2(b); see also Tsuchiya, 1989, his Fig. 2, R94, its Fig. 12(b) for two other DS isopycnals) and our own maps (Fig. 26), the broad-scale gradient between SAIW and MOW dominates the salinity distribution between 35°N and 55°N. On our DS isopycnal layer salinity maps in Fig. 26, the MOW is the region of diagonal salinity contours in the southeastern corner of the maps, while the SAIW is an intrusion of waters $<$35.0 that enters from the west between 47°N and 56°N. ENAW was defined by Harvey (1982) as the average properties of a band of water aligned with the NAC in the northeastern North Atlantic, where the NAC branch is wheeling northward towards the Rockall Plateau complex, with SAIW to its northwest and MOW to its southeast. His ENAW definition spanned 4° to 12°C (Fig. 25(a)) and thus includes that part of the thermocline corresponding to the DS isopycnals. On the $\sigma_1 = 32.0$ surface of Fig. 26(a) the ENAW salinity is 35.19, and this climatological field shows that there is no "pool" of uniform ENAW on a given DS isopycnal. Instead, the defined ENAW is a narrow width curve on a density surface, since there are substantial lateral gradients of salinity on density surfaces, e.g., Fig. 26. Harvey (1982) illustrated this with a map of salinity on the 8°C surface, where a ±0.05 departure from his defined ENAW value of 35.225 (for 8°C) defined a band along the NAC of typical width 50 km, which was usually less than the station spacing along sections! Even on the smoothed climatological fields of Fig. 26, to the southwest of Porcupine Bank a ±0.05 swath is only about 100–200 km width. In Fig. 20 the synoptic pair of stations indicated by circles are separated by 231 km along 20°W (near 50°N and 48°N, respectively) and show a DS isopycnal salinity range of 0.1–0.15. Paillet, Arhan and McCartney (1988) used a slight alteration of Harvey's (1982) ENAW relationship to define salinity anomalies and to show a number of sections, which

also emphasize the gradients of the anomaly across the NAC, and the relatively small area with anomaly magnitudes <0.05.

With these considerations in mind, we emphasize that the 0.05 amplitude of salinity anomaly relative to ENAW on the DS isopycnals in the Rockall Trough characterized as "Gulf of Gibraltar Water" is very small. Along the coast of Portugal, the MOW anomaly can be as large as +0.8 (Daniault, Maze & Arhan, 1994). According to Harvey's (1982) study, in the northern Bay of Biscay the MOW was still a +0.45 anomaly relative to ENAW. Near 49°N the anomalies had declined to just above 0.3, but near 53.5°N at Porcupine Bank they just exceeded 0.1. Clearly, if the eastern boundary current penetrates to and past Porcupine Bank and is the source of the DS isopycnal waters in Rockall Trough near 1000 m, the MOW has to undergo substantial dilution in the process. Under the deep source hypothesis that is indeed what is required, and the magnitude of this dilution is apparent on the R79 map of salinity on a DS isopycnal near 1200 m in Rockall Trough (Fig. 2(b)), on our own maps of climatological average salinity distributions on three DS isopycnals (Fig. 26), and in the eastern boundary section, Fig. 3. Under the shallow source hypothesis it is the deep flow of the NAC (Fig. 26(e)) that advects weak positive salinity anomalies to the Rockall Trough, which are augmented with inputs from the Wyville-Thomson Overflow plume and by diapycnal exchanges with the overlying warm pool waters.

At issue is the origin of the weak positive salinity anomalies that are observed on the DS isopycnals at depth in the Rockall Trough. The resolution of this issue is not as simple as equating positive salinity anomalies (relative to ENAW) to a MOW component, for there are two other sources for the additional salinity for the deep thermocline isopycnals, the footprint of the convective transformation of thermocline waters, and the Wyville-Thomson Overflow water. Furthermore, there are two alternative pathways by which a MOW component could reach the Trough, either via a subpolar continuation of the eastern boundary undercurrent, or by a northward wheeling branch of the NAC; the latter is our conjectured pathway

The NAC indisputably carries MOW at deep thermocline depths (Fig. 26). MOW is one of several constituents whose lateral mixing, augmented with vertical diffusive fluxes, determines the distribution of salinity on deep thermocline isopycnals including the deep source hypothesis isopycnals of R79 and R94. Indeed, the definition of ENAW is based on the supposition that it is a blend of SAIW and MOW (e.g. Harvey, 1982, Harvey & Arhan, 1988). Arhan and King (1995) have undertaken an analysis of the mesoscale processes effecting mixing between MOW and SAIW in the deep thermocline ENAW across the NAC, and also between the deeper MOW and the Labrador Sea Water (LSW). So we accept as given that the DS isopycnals of both the eastern boundary undercurrent and the NAC include MOW contributions in their composition, and move onto considerations of other sources that may contribute to the regional water mass. We first examine the potential roles of vertical mixing and of the Wyville-Thomson Overflow waters on determining DS isopycnal characteristics in the Rockall Trough.

5.5.1. Transformation beneath the density of winter convection

The impact of the SPMW on the NAC water mass is not restricted to the PV minimum core layer at and above the density of local convection, it reaches to deeper/denser levels as a "footprint" of downgradient diapycnal mixing, perhaps enhanced in the thermocline immediately beneath the base of the convecting layer. This is to be expected, for a "pure" convection process would create an SPMW with temperature and salinity steps at the base of the convecting layer (Fig. 25(b)). In general such steps are not observed, but they may indeed occur at the time of convection, although they are evidently mixed away after active convection shuts down. Instead, the observed transition from the SPMW to the underlying thermocline is a rounded shoulder in property-depth profiles. Rather than a PV = 0 layer, there is an inflection point in the density profile giving a minimum in the PV profile defining the core of the eroded influence of winter convection. Shay and Gregg (1986) and Gregg (1987) have described the entrainment zone beneath deepening convection as having a thickness of about 20% of the convective layer. In that entrainment zone the measured turbulent dissipation decays from the very high levels of the buoyancy-forced convective layer

to the background values of the permanent thermocline. They additionally noted that the entrainment fluxes into the mixed layer are critical in determining the evolution of the mixed layer, being of the same order as the air-sea fluxes, a measurement in agreement with the inferences of Marshall et al. (1993) and Qiu and Huang (1995). It makes sense, then, that the entrainment fluxes at the base of the SPMW convection would result in significant changes in water mass characteristics in a footprint beneath the actual convection depth.

Also contributing to the footprint may be the spatial variability of the winter convection. If there is a small-scale lateral variability of the density of convection, then the footprint could be what evolves in time after the end of winter overturning through the action of lateral advection and stirring. There will have been patches of convection that reached density surfaces somewhat denser than the mean regional density of convection. So the footprint could reflect the decay from essentially 100% convective contact or penetration over the geographic area of the PV minimum at densities somewhat lighter than the mean regional density of convection, to 0% contact at an isopycnal somewhat denser than that mean where there is no convective contact at all.

This footprint of convective influence is evident in all the properties shown in Fig. 23, typically in the depth range 400–800 m upstream of the Rockall Trough, but reaching to 800–1200 m in the Trough where winter convection is so much deeper (McCartney & Talley, 1982; Meincke, 1986). Beneath the SPMW, the PV maximum, which is the high gradient core of the main thermocline, progressively weakens downstream in the NAC (Fig. 23(f)). This is a vertical mixing imprint of the low stratification of the convective mixed layer eroding the higher stratification of the main thermocline beneath, and is the most dramatic evidence for the footprint of convection. The PV minimum core of the warm pool in the Rockall Trough has a density around σ_1 = 31.8–31.9. In the NAC south and west of Porcupine Bank (Fig. 23), stations 1–41, and along the eastern boundary section (Fig. 3), stations 1–12, this density falls at the high PV ridge of the main thermocline. The convection-driven transformation has chewed through most of the ridge of strong stratification. In the Trough the remnant of the high PV ridge is centered on the DS isopycnal layer at σ_1 = 32, with lower PV than found in that layer in the NAC. Note the ~30% increase of spacing of the 32.0, 32.1, and 32.2 contours (Fig. 23) where they are immediately below the warm pool in the Trough, compared to their spacing in the mid-basin NAC, indicative of the weakening of stratification in the DS isopycnal layer. The oxygen minimum layer beneath the warm pool is eroded from above by mixing with the saturated oxygen water in the convective mixed layer (Fig. 23(d)). The silicate of the deeper waters is similarly reduced by mixing with mixed layer water stripped of silicate (Fig. 23(e)), while the deeper salinities are enhanced by mixing with the higher salinity waters of the winter mixed layer (Fig. 23(c)). All these influences are consistent with the notion of a diapycnal down-gradient influence from the PV minimum layer into the layers denser than that reached by direct convection at a given location.

Farther downstream a given density surface, already modified by this footprint process, itself is reached by convection. So in that sense, the footprint is a pre-conditioning step achieving some of the conversion from NACW characteristics to the SPMW of a particular density, with actual convection to that density being the final step. Beneath a given SPMW low-PV core, the footprint represents a salinification that contributes to the positive salinity anomalies relative to NACW, both the ENAW itself being more saline than NACW, and positive anomalies relative to ENAW. In Rockall Trough, beneath the densest convection along this NAC pathway, one interpretation is that these diapycnal fluxes have altered the characteristics of DS isopycnal waters delivered to the area by lower thermocline flow of the NAC, accounting for salinification, the increase in oxygen in the oxygen minimum layer, and reductions in silicate and vertical stratification. However, unlike farther upstream in the NAC, this preconditioning is not followed by direct convective contact farther downstream, because the warm pool waters of Rockall Trough are skimmed across the Wyville-Thomson Ridge, leaving behind the DS isopycnal layer waters in the Trough, with their characteristics altered by the vertical fluxes from those of the approaching deep NAC flow. Convection to the DS isopycnal layer occurs only on NAC pathways passing west of Rockall Plateau, in the area south

of Iceland (Fig. 21), and in the Norwegian Current where the continued evolution of the warm pool waters through air sea fluxes and diapycnal exchanges with NSDW eventually transforms the warm pool remnant to $\sigma_1 > 32.0$.

5.5.2. The influence of the Wyville-Thomson overflow on the DS isopycnal layer in Rockall Trough

One of the primary differences in circulation between the shallow source and deep source hypotheses is the sign of the net flow through Rockall Trough beneath the sill depth of the Wyville-Thomson Ridge. Under the deep source hypothesis that net flow is northward, representing the delivery of DS isopycnal waters northward below sill depth to supply the rising flow up and over the Wyville-Thomson Ridge. But in Section 3 we have demonstrated that, while there is an area over the western Ridge where the DS isopycnal layer is continuous, the flow there, far from rising, is a vigorously descending plume. The spillover is a source for DS isopycnal waters at the northern end of Rockall Trough, through some combination of direct spillover of waters from the Faroese Channels in the density range of the DS isopycnal layer, and spillover of denser waters entraining warm pool waters and lightening to the density range of the DS isopycnal layer.

There are limited possibilities for DS isopycnal layer waters to escape westwards from the northern Rockall Trough to the Iceland Basin. According to the high-resolution bathymetric database used to construct Fig. 4, both the narrow passage between Bill Bailey's Bank and Lousy Bank and the wider one between Lousy Bank and George Bligh Bank have sills at depths slightly shallower than 1100 m. No evidence for spillover waters is visible on a synoptic section observed in 1991 stretching from Hatton Bank eastward across George Bligh Bank and thence northeast to Lousy Bank (data from van Aken, personal communication, 1999).

Unless there is westward flow through these passages substantial enough to remove all the Wyville-Thomson Ridge spillover transport into the DS isopycnal layer in the northern Trough, there will be a net southward flow through the Trough in the layer, which is opposite to what is implied under the deep source hypothesis. We do find property influences of the spillover plume at the westernmost stations of the section in Fig. 7, most notably the lowered silicate (Fig. 7(e)), phosphate and nitrate (not shown). These indicate that some of the spillover waters are indeed flowing southwards along the eastern slope of Rockall Bank. We infer that there is a degree of an overturning cell structure to the flow in Rockall Trough. There is a net northward flow of warm pool water to supply both the Inflow and the entrainment into the spillover, and net southward flow in the DS isopycnal layer representing the cold dense overflow diluted and volumetrically enhanced by the entrained warm pool water and any direct spillover from the Faroese Channels in that density range.

We will not attempt in this paper to resolve the question of the sign of recirculating flow (gyre components) in the DS isopycnal layer within Rockall Trough, but include a few remarks concerning the literature on the subject. Such recirculation will enable spillover waters from the north to blend with the subtropical waters flowing northward past Porcupine Bank. Such blending is presumably the agent of the evolution of the along-trough (Fig. 23) gradients in oxygen and silicate: the lack of any corresponding along-trough gradient of salinity reflects the relatively small contrasts between the salinities of the northern and southern originating waters, e.g. Fig. 18, compared to their distinct contrasts in oxygen and silicate (see the corresponding panels of Figs. 7 and 12). Ellett and Martin (1973) used 10 repeated sections near 56–57°N to indicate the participation of the DS isopycnal layer in the anticyclonic gyre of warm pool waters that occurs to the west of the Rockall Slope Current, in the western and central Trough. This gyre has a western limb of substantial northward flow (we estimate ~8 Sv from their published mean geostrophic velocity section) on the Rockall Bank side of the Trough, as opposed to a less substantial southward flow (~ 4 Sv) over the eastern side of the Trough, that is offshore of the substantial northward flow of the Rockall Slope Current over the upper continental slope. For the DS isopycnal layer the anticyclonic gyre element is ~ 1 Sv in their mean section. It is the tendency of the DS isopycnal to be bowl-shaped in their

sections that is responsible for most of the shear they convert to anticyclonic flow with an 1800 m level of no motion; there is little shear above 800 m because of the homogeneity of the SPMW. This bowl was not particularly apparent in our Fig. 7 cross-section from fall 1996, but was very pronounced when the section was re-occupied in fall 1997 (not shown). The bowl is very prominent in the along trough segment of the section illustrated in Fig. 23, stations 41–59 of which are a synoptic section that Arhan et al. (1994) described as indicating an anticyclonic gyre in the warm pool, transitioning within the DS isopycnal layer to cyclonic flow, with the gyres' centers being defined by the maximum bowl depth near 56.3°N. It is along the southern side of that bowl that the signature of westward flow across the mouth of the Rockall Trough occurs, that was described in Section 5.3.

Recent work by Holliday et al. (2000) analyzes long-term measurements in Rockall Trough near 57°N, and includes a reanalysis of the earlier subset from Ellett and Martin (1973). It supports the concept of a transition from shallow anticyclonic to deep cyclonic circulation, which is particularly supported by a pair of moorings west and east of the Trough axis. Using Ellett's mooring M from 1978–1984 at the base of the continental slope (offshore of the Rockall Slope Current) they estimate warm pool velocities at 150 and 600m to be 3.1 and 3.0 cm/s slightly west of southward; these decline to 1.1 cm/s in a SSW direction at 1100 m, parallel to the continental slope, and at a temperature near 7°C indicating flow in the DS isopycnal layer is directed away from the Wyville-Thomson Ridge towards the eastern Trough. At Ellett's mooring F farther west at the lower part of the slope of Rockall Bank, warm pool velocities of 1.1 and 1.3 cm/s and somewhat north of east at 100 and 500 m were measured, which veered to 1.1 cm/s just east of north at 1000 m; the latter instrument was in the DS isopycnal layer. All these flows were very weak. We have included the 3.1 cm/s mooring M velocity at 150 m and the mooring F velocity at 100 m in Fig. 24 with other warm pool measurements. With the scaling used the mooring M vector is barely discernable as a small reverse flow offshore of the strong poleward flow of the Rockall Slope Current, and the mooring F vector flow is even smaller. Unfortunately we have not located any moorings measuring the flow conditions on the eastern flank of Rockall Bank, where Ellett and Martin found a poleward flow concentration above the 600 m isobath.

These mid-Trough moorings indicate there is anticyclonic flow down to below the sampling level of 1000–1100 m. The measured reversal to a cyclonic circulation appears at the next mooring sampling level ~1800 m, where weak cyclonic speeds are recorded amounting to 36% of the anticyclonic speeds at 1000–1100 m. Nonetheless, Holliday et al. (2000) argue for a level of no motion at 1200 db, just below the 1000–1100 m mooring sampling level, a level chosen by requiring zero net transport below that level for the mean of 23 repeated hydrographic sections. With that level selection for the hydrography they tabulate transports of 3.0, −2.6, 4.3, and −0.7 Sv respectively, for the Rockall Slope Current, the southward anticyclone limb, the northward anticyclone limb, and the flow near the flank of Rockall Bank. Very weak anticyclonic flow occurs in the DS isopycnal layer as 1200 db falls in that layer near 5.5°C. Deeper level of no motion choices give net northward deep transport, while shallower choices give net southward transport. While it is conventional to require zero net transport for cul de sac basins beneath the depth of the bounding sill, we have argued above for an overturning circulation in the Rockall Trough. The transport of "raw" NSDW spilling over the Wyville-Thomson Ridge is <1 Sv, but the warming of that plume is by entrainment, which swells the transport to an unknown amount, and lightens the density, although it is still dense enough to descend to and below 1000 m. Holliday et al. (2000) Figure 5 indicates that an isobaric reference level would have to be shallower than 800 db in order to enable net southward deeper transport approaching 1 Sv. But using that shallow a level would have contradicted the two mooring results by making the flow at 1000–1100 m cyclonic. The answer to this puzzle presumably lies in a requirement for a variable level of no motion, or additive barotropic fields. Additionally we note that with the net flow being the difference between two large opposed transport limbs, the net is more sensitive to section details of bottom triangles and station placements than is the amplitude of the gyre. The repeated sections have rather sparse sampling intervals, and the lack of tight station spacing at the flank of the Rockall Bank in

particular may have missed significant shear. In our own section across the Trough in Fig. 7, we occupied seven stations in a 65 km band on that flank, which revealed westward rising isopycnals above, in and beneath the DS isopycnal layer. This shear converted into northward flow above a selected level of no motion, and the oxygen profile at one of these stations showed an intensification of the oxygen minima at 9.5°C and 7°C, both indicative of a stronger influence of NAC waters at that station. The upper minimum reflected the absence of SPMW convection at that temperature at that station compared to the adjacent stations, while the deeper minimum indicated there was more direct advection of the strong oxygen minimum layer of the NAC lower thermocline at that station. Both observations were consistent with the level of no motion being deeper than the DS isopycnal layer at the time of the observation. We repeated this section a year later, and once again found a band of isopycnals rising westwards and stronger oxygen minima, but the band then spanned the western half of the Trough and looked more like the Ellett and Martin (1973) anticyclonic gyre structure than a narrow current flowing against the slope of Rockall Bank.

The current meter data reported by Holliday et al. (2000) from 1000–1100 m at the two sites in the DS isopycnal layer showed weak northward flow in the western Trough, and weak southward flow in the eastern Trough. These observations can be combined with the northern Trough data in Fig. 16(c), in which the southwestern-most vector defines the eastward flow once the descending plume has exited the gully between Ymir and Wyville-Thomson Ridges. The combination of these three mooring sites suggests that the DS isopycnal layer in Rockall Trough may have an anticyclonic gyre superimposed upon whatever net southward flow the spillover and entrained water provides.

Below the DS isopycnal layer in Rockall Trough, the deep water flow has been described as an inflow from the south past Porcupine Bank along the base of the continental slope. This flows around the Trough and returns southward in the western Trough to flows westward to the south of the Rockall Plateau (Lonsdale & Hollister, 1979). This is a component of the deep northern boundary current system. In addition to water mass characteristics (Lonsdale, 1982; McCartney, 1992) evidence for it includes the patterns and characteristics of bottom sediments, most notably the Feni Drift. McCave and Tucholke (1986) have summarized the Rockall Trough sediment studies, and more detailed treatments are found in Roberts and Kidd (1979), Lonsdale and Hollister (1979) and Lonsdale (1982). Deep current meter data ($>$2000 m) across the mouth of the Rockall Trough are described by Dickson et al. (1986) and Dickson and Kidd (1986) demonstrating cyclonic looping of flow within the deep levels of the Trough, following in a rather detailed fashion the deep bathymetric contours of the Trough in the direction that keeps the shoaling topography to the right in the downstream direction. All the current meter data they reported, though, are well below the depth of the DS isopycnal layer, as is the sediment evidence reported in the studies cited above.

The overturning circulation within Rockall Trough provides another potential source for increasing the salinities of the DS isopycnals in Rockall Trough, in addition to the deep footprint of winter convection of the overlying warm pool waters, for as the overflow plume evolves by entrainment its characteristics describe a positive salinity anomaly (see Fig. 18 and discussion in Section 3.4.4). Comparison between the DS isopycnal layer property distributions along the plume section (Fig. 12), and those for the section across Rockall Trough (Fig. 7) shows that the salinity values are very similar, but the plume shows higher oxygen and but lower silicate concentrations compared to the Trough to the south. Referring to the segment of the section in Fig. 23 that extends along the axis of the Trough (i.e. stations 41–58) the combined action of this northern source for DS isopycnal layer water, and the footprint of convection can been recognized in the along-Trough gradients of oxygen and silicate.

We have identified two processes within Rockall Trough that act to increase salinity in the DS isopycnal layer above that of waters in the DS layer flowing towards the Trough in the NAC. They also both act to increase oxygen and decrease silicate, and indeed, these latter two effects are more pronounced than the salinification in their impacts on the DS isopycnal layer waters in the NAC. The first process involves the vertical (diapycnal) fluxes from the convection of the local mode waters, convection that penetrates to within 200 m of the top of the DS isopycnal layer, and whose enhanced mixing footprint may salinify and

oxygenate that layer while partly stripping out its silicate. The second process is the result of the Wyville-Thomson Ridge Overflow providing a net southward flow of water through the Trough, bringing an admixture of different water mass characteristics into the circulating DS isopycnal layer waters of the Trough. This DS isopycnal layer "northern source" has elevated salinity, higher oxygen and lower silicate than the NAC waters being delivered to Porcupine Bank (Fig. 23(c)–(e)), but lower salinity, higher oxygen and lower silicate relative to the eastern boundary undercurrent waters south of Porcupine Bank. This completes the basis for our third conjecture, that DS isopycnal layer waters delivered by the NAC envelop the Rockall Trough and Plateau and, with modifications by diapycnal mixing and by admixture of Wyville-Thomson Overflow set the salinity of the regional DS isopycnal layer

6. Summary

We have examined two alternative hypotheses for the origin of the warm and saline waters flowing into the Nordic Seas, where they undergo transformation into a variety of overflows. We reject the hypothesis (R79) that a northward flow of Mediterranean Outflow Water reaches the Rockall Trough as an eastern boundary undercurrent near 1200 m (Fig. 1(b)) and then rises to flow over the Wyville-Thomson Ridge thereby supplying the Nordic Seas Inflow (Fig. 1(a)). We find the silicate argument for this hypothesis relies on spurious data. A steeply rising flow of deep water from the depths of the northern Rockall Trough into the Faroe-Shetland Channel does not occur; indeed, this is a place where the Wyville-Thomson Ridge overflow brings dense water out of the Faroe Bank Channel to descend to the deep Rockall Trough! Where the deep source isopycnals are continuous across the Ridge, current meters have measured southward descending flow, not northward rising flow. Long southward meridional excursions of North Atlantic Current Waters are required under the deep source hypothesis, with the accompanying large rise and fall of salinity values, but these do not occur.

We adapt the old hypothesis first proposed by Nansen (1912), and elaborated on by Helland-Hansen and Nansen (1926) that warm and saline upper waters of the North Atlantic Current branch northwards in the eastern Atlantic and supply the Nordic Seas Inflow (Fig. 1(c)). Our shallow source hypothesis combines this dominance of the North Atlantic Current advection with the recognition that the advected waters undergo progressive evolution, the subpolar mode water transformation of North Atlantic Central Water. The Nordic Seas Inflow's warmth and elevated salinity represents an advective memory of upper ocean subtropical origins rather than an advective memory of Mediterranean Outflow Water rising from depth. While the transformation of upper waters represents a cooling and freshening, when viewed on density surfaces the process is one of salinification. When a given density horizon is contacted by convection at some downstream location along the North Atlantic Current, its salinity is modestly increased over that observed at that density upstream.

It is conjectured that the eastern boundary undercurrent diminishes northward, and finally vanishes near Porcupine Bank, (Fig. 1(d)). Both the Nordic Seas Inflow (Fig. 1(c)) and the Deep Northern Boundary Current (Fig. 1(d)) are supplied by the North Atlantic Current's branch into the subpolar gyre, with modifications to water mass characteristics brought about by diapycnal mixing from the convective layer immediately above, and by admixture of the Wyville-Thomson Ridge Overflow waters in Rockall Trough. The northward diminution of the eastern boundary undercurrent is not merely the dilution of its water mass, but is also an expulsion of its mass transport of MOW into the interior of the subtropical gyre. Within and to the south of the Rockall Trough, and over the southern flank of the Rockall Plateau, waters of the density classes corresponding to the eastern boundary undercurrent are delivered by the lower thermocline flow of the North Atlantic Current wheeling northward. The water mass characteristics of these waters are

subsequently modified by diapycnal fluxes from the immediately-overlying subpolar mode water, and by southward flow of Wyville-Thompson Ridge spillover waters

Acknowledgements

MSM wishes to acknowledge the late Val Worthington for inspiring his 25-year study of the topic of warm water transformations in the northern North Atlantic, and thanks Bill Schmitz for his help in bringing things into focus. Jerome Paillet and Xavier Carton of the Service Hydrographique et Océanographique de la Marine, Brest, France, are thanked for their hospitality to MSM in June 1997, while this paper was drafted. MSM has been funded by the National Science Foundation and the National Oceanographic and Atmospheric Administration, most recently grants OCE 95-29606 and GC97-019, respectively. CM acknowledges the support of grant SHOM 12/27 from the Service Hydrographique et Océanographique de la Marine, as well as The James S. Cole and Cecily C. Selby Endowed Fund and The Penzance Endowed Fund in Support of Assistant Scientists. The authors are particularly grateful to Harry Dooley of ICES for making available data from his three Wyville-Thomson Ridge moorings, to Lesley Rickards of BODC for tracking down current meters from the experiments in the Ridge area by Jim Crease, Dave Ellett and John Gould, to Deb West-Mack for the rapid processing of all those current meter records, and to Pascal Morin for tracking down nutrient data near the Iberian Peninsula. This is contribution number 10177 of the Woods Hole Oceanographic Institution, and World Ocean Circulation Experiment contribution number 613.

References

Arhan, M. (1990). The North Atlantic current and subarctic intermediate water. *Journal of Marine Research*, *48*, 109–144.

Arhan, M., Colin de Verdiere, A., & Memery, L. (1994). The eastern boundary of the subtropical North Atlantic. *Journal of Physical Oceanography*, *24*, 1295–1316.

Arhan, M., & King, B. (1995). Lateral mixing of the Mediterranean Water in the eastern North Atlantic. *Journal of Marine Research*, *53*, 865–895.

Baringer, M. O., & Price, J. F. (1997). Momentum and energy balance of the Mediterranean outflow. *Journal of Physical Oceanography*, *27*, 1678–1692.

Booth, D. A., & Ellett, D. J. (1983). The Scottish slope current. *Continental Shelf Research*, *2*, 127–146.

Booth, D. A., & Meldrum, D. T. (1984). *Drifting buoys in the northeast Atlantic and Norwegian Sea*. ICES CM 1984/C:27, 9 pp.

Booth, D. A., & Meldrum, D. T. (1987). Drifting buoys in the northeast Atlantic. *International pour l'Exploration de Journal du Conseil la Mer*, *43*, 261–267.

Bower, A. S., Richardson, P. L., Hunt, H. D., Rossby, T., Prater, M. D., Zhang, H.-M., Anderson-Fontana, S., Perez-Brunius, P., & Lazarevich, P. (2000). Warm-water pathways in the Subpolar North Atlantic: An overview of the ACCE RAFOS float programme. *International WOCE Newsletter*, *38*, 14–16 & 23.

Bubnov, V. A. (1968). Intermediate subarctic waters in the northern part of the Atlantic Ocean. *Okeanologia*, 19, 1126–153. [English translation (NOO Trans 545), U. S. Naval Oceanographic Office, Washington, DC 1973].

Coachman, L. K., & Aagaard, K. (1988). Transports through Bering Strait: annual and interannual variability. *Journal of Geophysical Research*, *93*, 15535–15539.

Cunningham, S. A., & Haine, T. W. N. (1995). Labrador Sea Water in the eastern North Atlantic. Part 1: A synoptic circulation inferred from a minimum in potential vorticity. *Journal of Physical Oceanography*, *25*, 649–655.

Currie, R. I., Edwards, A., & Ellett, D. J. (1974). *R.R.S. Challenger* cruise 10/1973 cruise report and data list. *Dunstaffnage Marine Research Laboratory, Cruise Report Series*, *1*, 23.

Cushman-Roisin, B. (1987). Subduction. In: P. Muller & D. Henderson (Eds.), *Dynamics of the oceanic surface mixed layer, Proceedings, "Aha Huliko"a, Hawaiian Winter Workshop, Univ. Hawaii at Manoa*, January 14–16, 1987, Hawaii Institute of Geophysics Special Publications, pp. 181–196.

Daniault, N., Maze, J. P., & Arhan, M. (1994). Circulation and mixing of Mediterranean water west of the Iberian Peninsula. *Deep-Sea Research, I, 41*, 1685–1714.

Dickson, R., & Brown, J. (1994). The production of North Atlantic deep water: Sources, rates and pathways. *Journal of Geophysical Research, 99*(12), 319–12341.

Dickson, R. R., Gould, W. J., Griffiths, C., Medler, K. J., & Gmitrowicz, E. M. (1986). Seasonality in currents of the Rockall Channel. *Proceedings of the Royal Society of Edinburgh, 88B*, 103–125.

Dickson, R. R., & Kidd, R. B. (1986). Deep circulation in the southern Rockall Trough — the oceanographic setting of Site 610. In: W. F. Ruddiman, R. B. Kidd, E. Thomas et al. (Eds.), *Initial reports of the deep sea drilling project* (Vol. XCIV), 1994, pp. 1061–1074.

Dooley, H. D., Martin, J. H. A., & Payne, R. (1976). Flow across the continental slope off northern Scotland. *Deep–Sea Research, 23*, 875–880.

Dooley, H. D., & Henderson, E. W. (1980). *Low-frequency currents north of Rockall Bank*. ICES CM 1980/C:25, 11 pp.

Dooley, H. D., & Meincke, J. (1981). Circulation and water masses in the Faroese Channels during Overflow '73. *Deutsche Hydrographische Zeitschrift, 34*, 41–54.

Ellett, D. J., & Martin, J. H. A. (1973). The physical and chemical oceanography of the Rockall Channel. *Deep-Sea Research, 20*, 585–625.

Ellett, D. J., & Roberts, D. G. (1973). The overflow of Norwegian Sea Deep Water across the Wyville-Thomson Ridge. *Deep-Sea Research, 20*, 819–835.

Ellett, D. J. (1978). Subsurface temperatures at the Scottish Continental Slope, Dunstaffnage Marine Research Laboratory, Marine Physics Group Report, 2, 19.

Ellett, D. J., & Edwards, A. (1978). *A volume transport estimate for Norwegian Sea overflow across the Wyville-Thomson Ridge*. ICES CM 1978/C:19, 12 pp.

Ellett, D. J., Kruseman, P., Prangsma, G. J., Pollard, R. T., van Aken, H. M., Edwards, A., Dooley, H. D., & Gould, W. J. (1983). Water masses and mesoscale circulation of North Rockall Trough waters during JASIN 1978. *Philosophical Transactions of the Royal Society of London, 308*, 231–252.

Ellett, D. J., Edwards, A., & Bowers, R. (1986). The hydrography of the Rockall Channel — an overview. *Proceedings of the Royal Society of Edinburgh, 88B*, 61–81.

Ellett, D. J. (1991). *Norwegian Sea Deep Water overflow across the Wyville-Thomson Ridge during 1987–1988*. ICES CM1991/C:41, 11 pp.

Fuglister, F. C. (1960). Atlantic Ocean atlas of temperature and salinity profiles and data from the international geophysical year of 1957–1958. *Woods Hole Oceanographic Institution Atlas Series, 1*, 209.

Ganachaud, A. S. (1999). *Large-scale, oceanic circulation and fluxes of freshwater, heat, nutrients, and oxygen*. Ph.D. thesis, Massachusetts Institute of Technology/Woods Hole Oceanographic Institution Joint Program, Cambridge, Massachusetts, 266 pp.

Gordon, L. I., Jennings, J. C., Ross, A. A., & Krest, J. M. (1993). *A suggested protocol for continuous flow automated analysis of seawater nutrients (phosphate, nitrate, nitrite, and silicic acid) in the WOCE Hydrographic Program and the Joint Global Ocean Fluxes Study*. OSU College of Oceanography, Descriptive Chemical Oceanography Group Technical Report 93–1, 55 pp. WOCE Hydrographic Program Office, Methods Manual WHPO 91–1 (available from http://whpo.ucsd.edu/manuals.html).

Gould, W. J., Loynes, J., & Backhaus, J. (1985). *Seasonality in slope current transports NW of Shetland*. ICES CM 1985/C:7.

Gregg, M. C. (1987). Structures and fluxes in a deep convecting mixed layer. In P. Muller and D. Henderson, (Eds.), *Dynamics of the oceanic surface mixed layer, Proceedings, "Aha Huliko"a, Hawaiian Winter Workshop*, Univ. Hawaii at Manoa, January 14–16, 1987, Hawaii Institute of Geophysics Special Publications, pp. 1–23.

Hansen, B., Larsen, K. M. H., Østerhus, S., Turrell, W., & Jónsson, S. (1999). The Atlantic Water inflow to the Nordic Seas. *International WOCE Newsletter, 35*, 33–35.

Hansen, B., & Østerhus, S. (2000). North Atlantic-Nordic Seas exchanges. *Progress in Oceanography, 45*, 109–208.

Harvey, J. (1982). Theta-S relationships and water masses in the eastern North Atlantic. *Deep-Sea Research, 29*, 1021–1033.

Harvey, J. G., & Theodorou, A. (1986). The circulation of Norwegian Sea overflow water in the eastern North Atlantic. *Oceanologica Acta, 9*, 393–402.

Harvey, J., & Arhan, M. (1988). The water masses of the central North Atlantic in 1983–84. *Journal of Physical Oceanography, 18*, 1855–1875.

Heath, G. R. (1974). Dissolved silica and deep-sea sediments. In W. H. Hay, (Ed.). *Studies in paleo-oceanography*. Society of Economic Paleontologists and Mineralogists, *20*, 77–93.

Helland-Hansen, B. & Nansen, F. (1909). *The Norwegian Sea*. Report on Norwegian Fishery and Marine Investigations 2, Kristiana, 390 pp.

Helland-Hansen, B., & Nansen, F. (1926). The Eastern North Atlantic. *Geofysiske Publikas-joner, 4*, 76.

Hill, A. E., & Mitchelson-Jacob, E. G. (1993). Observations of a poleward-flowing saline core on the continental slope west of Scotland. *Deep-Sea Research, I, 40*, 1521–1527.

Holliday, N. P., Pollard, R. T., Read, J. F., & Leach, H. (2000). Water mass properties and fluxes in the Rockall Trough, 1975–1998. *Deep-Sea Research I*, *47*, 1303–1332.

Huthnance, J. M. (1986). The Rockall Slope Current and shelf-edge processes. *Proceedings of the Royal Society of Edinburgh*, *88B*, 83–101.

Huthnance, J. M., & Gould, W. J. (1989). On the Northeast Atlantic Slope Current. In S. J. Neshyba, C. N. K. Mooers, R. L. Smith and R. T. Barber (Eds.), *Poleward flows along eastern ocean boundaries*. Coastal and Estuarine Studies, *34*, 76–81.

Iorga, M. C., & Lozier, M. S. (1999a). Signatures of the Mediterranean outflow from a North Atlantic climatology, Salinity and density fields. *Journal of Geophysical Research*, *104*(25), 985–26009.

Iorga, M. C., & Lozier, M. S. (1999b). Signatures of the Mediterranean outflow from a North Atlantic climatology, diagnostic velocity fields. *Journal of Geophysical Research*, *104*, 26011–26029.

Isayev, G., & Levitus, S. (1995). A diagnosis of the North Atlantic horizontal and vertical circulation with error estimates. *Journal of Geophysical Research*, *100*, 6795–6815.

Iselin, C. O'D. (1936). A study of the circulation of the western North Atlantic. *Papers in Physical Oceanography and Meteorology*, *4*, 101.

Jacobsen, J. P. (1929). Contribution to the hydrography of the North Atlantic. In *The Danish "Dana" Expeditions 1920–22*. Carlsberg Foundation, Copenhagen, 1, pp. 98.

Jia, Y. (2000). Formation of an Azores Current due to Mediterranean Overflow in a modeling study of the North Atlantic. *Journal of Physical Oceanography*, *30*, 2342–2358.

Johnson, G. C., & Sanford, T. B. (1992). Secondary circulation in the Faroe Bank Channel outflow. *Journal of Physical Oceanography*, *22*, 927–933.

Johnson, R. G. (1997a). Climate control requires a dam at the Strait of Gibraltar. *EOS Transactions of the American Geophysical Union*, *78*, 277.

Johnson, R. G. (1997b). Reply to Comment on "Climate control requires a dam at the Strait of Gibraltar". *EOS Transactions of the American Geophysical Union*, *78*, 507.

Johnson, R. G. (1998). Comment on "Influence of Mediterranean outflow on climate". *EOS Transactions of the American Geophysical Union*, *79*, 292.

Käse, R. H., & Krauss, W. (1996). The Gulf Stream, the North Atlantic Current, and the Origin of the Azores Current. In W. Krauss (Ed.), *The warm water sphere of the North Atlantic Ocean*. Gebruder Borntraeger, Borntraeger, Berlin, Stuttgart, pp. 291–337.

Klein, B., & Siedler, G. (1989). On the origin of the Azores current. *Journal of Geophysical Research*, *94*, 6159–6168.

Koltermann, K. P., Sokov, A. V., Tereschenkov, V. P., Dobroliubov, S. A., Lorbacher, K., & Sy, A. (1999). Decadal changes in the thermohaline circulation of the North Atlantic. *Deep-Sea Research II*, *46*, 109–138.

Krauss, W. (1986). The North Atlantic Current. *Journal of Geophysical Research*, *91*, 5061–5074.

Krauss, W. (1995). Currents and mixing in the Irminger Sea and in the Iceland Basin. *Journal of Geophysical Research*, *100*, 10851–10871.

Lonsdale, P. F., & Hollister, C. D. (1979). A near-bottom traverse of Rockall Trough: Hydrographic and geologic inferences. *Oceanologica Acta*, *2*, 91–105.

Lonsdale, P. (1982). Sediment drifts of the northeast Atlantic and their relationship to the observed abyssal currents. *Bulletin de l'Institut Geologie du Bassin d'Aquitaine*, *31*, 141–149.

Lozier, M. S., Owens, W. B., & Curry, R. G. (1995). The climatology of the North Atlantic. *Progress in Oceanography*, *36*, 1–44.

Luyten, J., Stommel, H., & Wunsch, C. (1985). A diagnostic study of the northern Atlantic subpolar gyre. *Journal of Physical Oceanography*, *15*, 1344–1348.

Macdonald, A. M. (1998). The global ocean circulation: A hydrographic estimate and regional analysis. *Progress in Oceanography*, *41*, 281–382.

Marotzke, J., Adcroft, A., & Johnson, R. G. (1997). Comments on "Climate control requires a dam at the Strait of Gibraltar". *EOS Transactions of the American Geophysical Union*, *78*, 507.

Marshall, J. C., Nurser, A. J., & Williams, R. G. (1993). Inferring the subduction rate and period over the North Atlantic. *Journal of Physical Oceanography*, *23*, 1315–1329.

Mauritzen, C. (1996). Production of dense overflow waters feeding the North Atlantic across the Greenland-Scotland Ridge. Part 2: An inverse model. *Deep-Sea Research I*, *43*, 807–835.

Mauritzen, C., Morel, Y., & Paillet, J. (2001). On the influence of Mediterranean Water on the Central waters of the North Atlantic Ocean. *Deep-Sea Research I*, *48*, 347–381.

McCartney, M. S. (1982). The subtropical recirculation of mode waters. *Journal of Marine Research*, *40* (supplement), 427–464.

McCartney, M. S., & Talley, L. D. (1982). The subpolar mode water of the North Atlantic Ocean. *Journal of Physical Oceanography*, *12*, 1169–1188.

McCartney, M. S., & Talley, L. D. (1984). Warm-to-cold water conversion in the northern North Atlantic Ocean. *Journal of Physical Oceanography*, *14*, 922–935.

McCartney, M. S. (1992). Recirculating components to the deep boundary current of the northern North Atlantic. *Progress in Oceanography*, *29*, 283–383.

McCave, I. N., & Tucholke, B. E. (1986). Deep current-controlled sedimentation in the western North Atlantic. In P. R. Vogt, & B. E. Tucholke (Eds.), *The geology of North America, volume M, The western North Atlantic region*. Geological Society of America, Chapter 17, pp. 451–468.

McDowell, S., Rhines, P., & Keffer, T. (1982). North Atlantic potential vorticity and its relation to the general circulation. *Journal of Physical Oceanography*, *12*, 1417–1436.

Meincke, J. (1986). Convection in the oceanic waters west of Britain. *Proceedings of the Royal Society of Edinburgh*, *88B*, 127–139.

Metcalf, W. G. (1969). Dissolved silicate in the deep North Atlantic. *Deep-Sea Research*, *16* (Suppl.), 139–145.

Montgomery, R. B. (1938). Circulation in the upper layers of the southern North Atlantic deduced with the use of isentropic analysis. *Papers in Physical Oceanography and Meteorology*, *VI* (2), 55.

Nansen, F. (1912). Das Bodenwasser und die Abkuhlung des Meeres. *Internationale Revue der Gesamten Hydrobiologie und Hydrographie*, *5*, 1–42.

Nansen, F. (1913). The waters of the northeastern North Atlantic. *Internationale Revue der Gesamten Hydrobiologie und Hydrographie* (Suppl. to Vol. 4).

New, A. L., Barnard, S., Herrmann, P., & Molines, J.-M. (2001). On the origin and pathway of the saline inflow to the Nordic Seas: Insights from models. *Progress in Oceanography*, *48*, 255–287.

Nielsen, J. N. (1907). Contribution to the hydrography of the northeastern part of the Atlantic Ocean. *Medd. f. Komm. f. Havundersog. Serie Hydrografi, Bd*, *I*(9), Köbenhavn.

Østerhus, S., Hansen, B., Kristiansen, R., & Lundberg, P. (1999). The Outflow through the Faroe Bank channel. *International WOCE Newsletter*, *35*, 35–37.

Otto, L., & van Aken, H. M. (1996). Surface circulation in the northeast Atlantic as observed with drifters. *Deep-Sea Research I*, *43*, 467–499.

Özgökmen, T. M., Chassignet, E. P., & Rooth, C. G. H. (2001). On the connection between the Mediterranean Outflow and the Azores Current. *Journal of Physical Oceanography*, *31*, 461–480.

Paillet, J., & Arhan, M. (1996). Shallow pycnoclines and mode water subduction in the eastern North Atlantic. *Journal of Physical Oceanography*, *26*, 96–114.

Paillet, J., & Mercier, H. (1997). An inverse model of the eastern North Atlantic general circulation and thermohaline ventilation. *Deep-Sea Research I*, *44*, 1293–1328.

Paillet, J., Arhan, M., & McCartney, M. S. (1998). Spreading of Labrador Sea Water in the eastern North Atlantic. *Journal of Geophysical Research*, *103*, 10223–10239.

Pingree, R. D., & LeCann, B. (1989). Celtic and Armorican slope and shelf residual currents. *Progress in Oceanography*, *23*, 303–338.

Pingree, R. D., & LeCann, B. (1990). Structure, strength and seasonability of the slope currents in the Bay of Biscay region. *Journal of the Marine Biology Association, U.K.*, *70*, 857–885.

Pingree, R. D. (1993). Flow of surface waters to the west of the British Isles and in the Bay of Biscay. *Deep-Sea Research II*, *40*, 369–388.

Pollard, R. T., Griffiths, M. J., Cunningham, S. A., Read, J. F., Pérez, F. F., & Ríos, A. F. (1996). Vivaldi 1991 — A study of the formation, circulation and ventilation of Eastern North Atlantic Central Water. *Progress in Oceanography*, *37*, 167–192.

Pollard, R. T., & Pu, S. (1985). Structure and circulation of the upper Atlantic Ocean northeast of the Azores. *Progress in Oceanography*, *14*, 443–462.

Qiu, B., & Huang, R. X. (1995). Ventilation of the North Atlantic and North Pacific: Subduction versus obduction. *Journal of Physical Oceanography*, *25*, 2374–2390.

Rahmstorf, S. (1998a). Influence of Mediterranean outflow on climate. *EOS Transactions of the American Geophysical Union*, *79*, 281.

Rahmstorf, S. (1998b). Reply on "Influence of Mediterranean outflow on climate". *EOS Transactions of the American Geophysical Union*, *79*, 292.

Reid, J. L. (1965). Intermediate waters of the Pacific Ocean. *Johns Hopkins Oceanographic Studies*, *2*, 85.

Reid, J. L. (1978). On the mid-depth circulation and salinity field in the North Atlantic Ocean. *Journal of Geophysical Research*, *83*, 5063–5067.

Reid, J. L. (1979). On the contribution of the Mediterranean Sea outflow to the Norwegian-Greenland Sea. *Deep-Sea Research*, *26*, 1199–1223.

Reid, J. L. (1994). On the total geostrophic circulation of the North Atlantic Ocean: Flow patterns, tracers, and transports. *Progress in Oceanography*, *33*, 1–92.

Robbins, P. E., Price, J. F., Owens, W. B., & Jenkins, W. J. (2000). The importance of lateral diffusion for the ventilation of the lower thermocline in the subtropical North Atlantic. *Journal of Physical Oceanography*, *30*, 67–89.

Roberts, D. G., & Kidd, R. B. (1979). Abyssal sediment fields on the Feni Ridge. *Rockall Trough: Long-range sonar studies. Marine Geology*, *33*, 175–191.

Roemmich, D. (1980). Estimation of meridional heat flux in the North Atlantic by inverse methods. *Journal of Physical Oceanography*, *10*, 1972–1983.
Saunders, P. M. (1982). Circulation in the eastern North Atlantic. *Journal of Marine Research*, *40* (Suppl.), 641–657.
Saunders, P. M., & Gould, W. J. (1989). CTD data from RRS Challenger Cruise 15/87 around the Faroe Islands. *Institution Oceanography Science, Deacon Laboratory Report*, *256*, 79.
Saunders, P. M., & Gould, W. J. (1988). Current measurements made around the Faroe Islands in 1986 and 1987. *Institution Oceanography Science, Deacon Laboratory Report*, *261*, 80.
Saunders, P. M. (1990). Cold outflow from the Faroe Bank Channel. *Journal of Physical Oceanography*, *20*, 29–43.
Schmitt, R. W., Bogden, P. S., & Dorman, C. E. (1989). Evaporation minus precipitation and density fluxes for the North Atlantic. *Journal of Physical Oceanography*, *19*, 1208–1221.
Schmitz, W. J., & McCartney, M. S. (1993). On the North Atlantic circulation. *Reviews of Geophysics*, *31*, 29–49.
Schott, F., & Stommel, H. (1978). Beta spirals and absolute velocities in different oceans. *Deep-Sea Research*, *25*, 961–1010.
Shay, T. J., & Gregg, M. C. (1986). Convectively driven turbulent mixing in the upper ocean. *Journal of Physical Oceanography*, *16*, 1777–1798.
Smith, W. H. F., & Sandwell, D. T. (1997). Global seafloor topography from satellite altimetry and ship depth soundings. *Science*, *277*, 1956–1962.
Spall, M. A. (1992). Cooling Spirals and recirculation in the subtropical gyre. *Journal of Physical Oceanography*, *22*, 564–571.
Spall, M. A., & Pickart, R. S. (2001). Where does dense water sink? A subpolar gyre example. *Journal of Physical Oceanography*, *31*, 810–826.
Speer, K., & Tziperman, E. (1992). Rates of water mass formation in the North Atlantic Ocean. *Journal of Physical Oceanography*, *22*, 93–104.
Stommel, H. (1979). Oceanic warming of western Europe. *Proceedings of the National Academy of Science*, *76*, 2518–2521.
Stramma, L. (1984). Geostrophic transport in the warm water sphere of the eastern subtropical North Atlantic. *Journal of Marine Research*, *42*, 537–558.
Sverdrup, H. U., Johnson, M. W. & Fleming, R. H. (1942). *The oceans: Their physics, chemistry and general biology*. Englewood Cliffs, New Jersey: Prentice-Hall.
Swallow, J. C., Gould, W. J., & Saunders, P. M. (1977). Evidence for a poleward eastern boundary current in the North Atlantic Ocean. *International Council for the Exploration of the Sea*. C.M. Paper C: 32 (mimeo).
Sy, A. (1988). Investigation of large-scale circulation patterns in the central North Atlantic: the North Atlantic current, the Azores current, and the Mediterranean water plume in the area of the Mid-Atlantic Ridge. *Deep-Sea Research*, *35*, 383–413.
Sy, A., Schauer, U., & Meincke, J. (1992). The North Atlantic current and its associated hydrographic structures above and eastwards of the Mid-Atlantic ridge. *Deep-Sea Research*, *39*, 825–853.
Sy, A., Rhein, M., Lazier, J. R. N., Koltermann, K. P., Meincke, J., Putzka, A., & Bersch, M. (1997). Surprisingly rapid spreading of newly formed intermediate waters across the North Atlantic Ocean. *Nature, London*, *386*, 675–679.
Tait, J. B. (1957). Hydrography of the Faroe-Shetland Channel, 1927–1952. *Scottish Home Department Marine Research*, *2*, 309.
Talley, L. D., & McCartney, M. S. (1982). Distribution and circulation of Labrador Sea water. *Journal of Physical Oceanography*, *12*, 1189–1205.
Tsuchiya, M. (1989). Circulation of the Antarctic Intermediate Water in the North Atlantic Ocean. *Journal of Marine Research*, *47*, 747–755.
Tsuchiya, M., Talley, L. D., & McCartney, M. S. (1992). An eastern Atlantic section from Iceland southward across the equator. *Deep-Sea Research*, *39*, 1885–1917.
Turrell, W. R., Hansen, B., Østerhus, S., Hughes, S., Ewart, K., & Hamilton, J. (1999). *Direct observations of inflow to the Nordic Seas through the Faroe Shetland Channel 1994–1998*. International Council for the Exploration of the Sea. C.M. 1999/L:01, pp. 16.
van Aken, H. M. (1988). Transports of water masses through the Faroese Channels determined by an inverse method. *Deep-Sea Research*, *35*, 595–617.
van Aken, H. M. (1995). Mean currents and current variability in the Iceland Basin. *Netherlands Journal of Sea Research*, *33*, 135–145.
van Aken, H. M., & Becker, G. (1996). Hydrography and throughflow in the northeastern North Atlantic Ocean: The Nansen Project. *Progress in Oceanography*, *38*, 297–346.
van Aken, H. M., & de Boer, C. J. (1995). On the synoptic hydrography of intermediate and deep water masses in the Iceland Basin. *Deep-Sea Research I*, *43*, 165–189.
Warren, B. A. (1972). Insensitivity of subtropical mode water characteristics to meteorological fluctuations. *Deep-Sea Research*, *19*, 1–19.
Wijffels, S. E., Schmitt, R. W., Bryden, H. L., & Stigebrandt, A. (1992). Transport of freshwater by the oceans. *Journal of Physical Oceanography*, *22*, 155–162.
Woods, J. D. (1985). The physics of the thermocline ventilation. In J. C. J. Nihoul (Eds.), *Coupled ocean-atmosphere models*, Elsevier Science Publishers B.V., Amsterdam, 543–590.
Worthington, L. V. (1976). On the North Atlantic circulation. *The Johns Hopkins Oceanographic Studies*, *6*, 110.

Wunsch, C., & Grant, B. (1982). Towards the general circulation of the North Atlantic. *Progress in Oceanography*, *11*, 1–59.
Wunsch, C. (1984). An eclectic Atlantic Ocean circulation model. Part 1: The meridional flux of heat. *Journal of Physical Oceanography*, *14*, 1712–1733.
Wunsch, C., & Roemmich, D. (1985). Is the North Atlantic in Sverdrup balance? *Journal of Physical Oceanography*, *15*, 1876–1880.
Wüst, G. (1935). Schichtung und Zirkulation des Atlantischen Ozeans. Das Bodenwasser und die Stratosphare. *Wissenschaftliche Ergebnisse der Deutschen Atlantischen Expedition "Meteor" 1925–1927*, (Band 6), 1–288.